UNIVERSITY OF LONDON

PLATINUM COMPLEXES AND THEIR RELEVANCE TO CANCER TREATMENT

by

Richard Thompson Riley

A thesis submitted for the Degree of
Doctor of Philosophy

MAY 1985

Department of Chemistry
Imperial College of Science & Technology
London SW7 2AZ

A B S T R A C T

The complex *cis*-diamminedichloroplatinum(II) (*cis*-Pt(II)) is used in many drug combination regimes in the treatment of cancer. Results are presented of a study of the interaction of *cis*-Pt(II) with several component drugs commonly used in such protocols. A mechanism is advanced to account for the synergic effect observed in such systems.

A study has been made of the interaction of some second generation platinum complexes [viz. $Pt(NH_3)_2$(ethylmalonate) and $Pt(NH_3)_2$(cyclobutane-dicarboxylate)] with components of DNA. A significant difference was observed in their initial coordination to such species as opposed to the behaviour of *cis*-Pt(II).

The synthesis of several potential antitumour compounds was undertaken utilizing ligands of known biological activity. Some complexes containing carboxylate groups participating in the Krebs' cycle, and others related to them, were prepared by analogy with the established second generation drugs containing dicarboxylate groups. The structure of the dimeric complex $[Pt(NH_3)_2(glutarate)]_2$ was solved by X-ray crystallography, and this compound was found to contain an unusual 16-membered ring system formed by glutarate bridges connecting pairs of platinum atoms. The, now known to be active, antitumour agent $K[PtCl_3(caffeine)]$ was prepared and similar related alkaloid complexes were also obtained.

C O N T E N T S

		Page
Abstract		I
CHAPTER ONE:	**INTRODUCTION**	1
1.1:	Historical	1
1.2:	Structure/Activity Studies	2
1.3:	Mode of action of *cis*-Pt(II)	3
CHAPTER TWO:	**INTERACTION OF $Pt(NH_3)_2$(ETMAL) and $Pt(NH_3)_2$(CBDCA) WITH DNA CONSTITUENTS**	11
2.1:	Introduction	11
2.2:	Guanosine 5'-monophosphate, GMP	17
2.2i	The interaction between GMP and $Pt(NH_3)_2$(ETMAL), r=1	22
2.2ii	The interaction between GMP and $Pt(NH_3)_2$(ETMAL), r=0.5	26
2.2iii	The interaction between $Pt(NH_3)_2$(CBDCA) and GMP (r=0.5 and r=1)	31
2.3:	Inosine 5'-monophosphate, IMP, and inosine	33
2.3i	The interaction between inosine and $Pt(NH_3)_2$(ETMAL), r=1	36
2.3ii	The interaction between IMP and $Pt(NH_3)_2$(ETMAL)	45
2.3iii	The interaction between $Pt(NH_3)_2$(CBDCA) and inosine	45
2.4:	Adenosine 5'-monophosphate, AMP and adenosine, A	49
2.4i	The interaction of $Pt(NH_3)_2$(ETMAL) with AMP	52
2.4ii	The interaction of $Pt(NH_3)_2$(CBDCA) with AMP	53
2.5	Conclusions	54

Page

CHAPTER THREE: STUDIES OF INTERACTIONS OF cis-Pt(II) WITH DRUGS USED IN COMBINATION CHEMOTHERAPY 55

3.1: Introduction 55
3.2: The Cell Cycle 56
3.3: Cytosine Arabinoside 58
3.4: 5-Fluorouracil 61
3.5: Cyclophosphamide 61
3.6: Bleomycin 62
3.6i Introduction 62
3.6ii The interaction of blenoxane and *cis*-$Pt(II)_{aq.}$ 67
3.6iii The Interaction of $Pt(NH_3)_2$(ETMAL) with blenoxane 90
3.6iv Discussion of sections 3.6ii and 3.6iii 101
3.6v Interaction of K_2PtCl_4 and blenoxane 105
3.7 Conclusion 116

CHAPTER FOUR: THE SYNTHESIS OF POTENTIAL PLATINUM ANTITUMOUR COMPLEXES 117

4.1: Introduction 117
4.2: Caffeine and related alkaloids 117
4.2i *cis*-$[Pt(caffeine)_2Cl_2].0.4H_2O$ 118
4.2ii $K[PtCl_3(caffeine)]$ 119
4.2iii Reactions of $[PtCl_3(caffeine)]^-$ with other ligands 121
4.2iv Analogous alkaloid complexes 122
4.3: Krebs Cycle Acids 123
4.3i Succinic and related acids 123
4.3ii Some reactions of $[Pt(NH_3)_2(glutarate)]_2$ 127

CHAPTER FIVE: EXPERIMENTAL TECHNIQUES 130

5.1: Physical Methods 130
5.2: Ligands 131
5.3: Platinum antitumour agents 132

REFERENCES 134
ACKNOWLEDGEMENTS 140

G L O S S A R Y

cis-Pt(II)	*cis*-diamminedichloroplatinum(II).
cis-$Pt(II)_{aq}$	*cis*-$[Pt(NH_3)_2(H_2O)(OH)]^+$
$Pt(NH_3)_2$(CBDCA)	(Diammine)(1,1-cyclo-butanedicarboxylato) platinum(II)
$Pt(NH_3)_2$(ETMAL)	(Diammine)(ethylmalonato)platinum(II)
G	guanosine
GMP	guanosine 5'-monophosphate
I	inosine
IMP	inosine 5'-monophosphate
A	adenosine
AMP	adenosine 5'-monophosphate
DNA	deoxyribonucleic acid
en	ethylenediamine
dien	diethylenetriamine
DCA	dicarboxylic acid
TMS	tetramethylsilane
TMP	trimethylsilylpropane-sulfonic acid
araC	cytosine arabinoside
5-FU	5-fluorouracil
BLM	bleomycin
BLN/BNX	"Blenoxane"
epr	electron paramagnetic resonance
NMR	nuclear magnetic resonance
δ	all chemical shifts expressed in terms of δ convection. ie.: $\delta 0 \equiv$ TMS
$\Delta\delta$	complexation shift. A positive value indicates a shift to higher field on complexation

IR	infrared
w	weak
m	medium
s	strong
br	broad
v	very
UV	ultraviolet
pD	pH in D_2O-using meter calibrated with H_2O based buffers

TABLES

2.1: ^{1}H and ^{13}C NMR chemical shifts of $Pt(NH_3)_2(CBDCA)$ and $Pt(NH_3)_2(ETMAL)$.

2.2: ^{1}H NMR of $Pt(NH_3)_2(ETMAL)$ in aqueous solution at various pD's.

2.3: Structural parameters of Pt-guanosine complexes.

2.4: Correlation of Pt-N(7) bond length and H(8) chemical shift.

2.5: ^{1}H NMR data of Platinum GMP complexes.

2.6 ^{13}C NMR data of $Pt(NH_3)_2(GMP)_2$ and Na_2 GMP.

2.7: H(8) and H(2) chemical shifts of platinum inosine complexes.

2.8: Structural parameters of platinum complexes of inosine or IMP.

2.9: ^{13}C NMR chemical shifts of inosine and the isolated intermediate $[Pt(NH_3)_2(I)(ETMAL)]^{x+}$.

2.10: H(8) and H(2) chemical shifts of platinum complexes of AMP or A.

3.1: ^{13}C NMR chemical shift data for Blenoxane and BNX/cis-$Pt(II)_{aq}$ (r=1).

4.1: IR and Raman data (600-200cm^{-1}) of dicarboxylic acid complexes.

F I G U R E S

1.1 Second generation platinum drugs.

1.2 Possible modes of *cis*-Pt(II) interaction with N(7)-O(6) of guanine.

1.3 A comparison of the (a) Watson-Crick G-C pair, (b) the platinated G-G pair, and (c) the methylated G-T pair.

2.1 (Diammine)(1,1-cyclobutanedicarboxylato)platinum(II)-$Pt(NH_3)_2$)(CBDCA).

2.2 Typical ^1H NMR spectra of species studies in Chapter Two.

2.3 (Diammine)(ethylmalonato)platinum(II)-$Pt(NH_3)_2$(ETMAL).

2.4 ^1H NMR of $Pt(NH_3)_2$(ETMAL) and Na_2GMP (1:1 in H_2O).

2.5 Probable reaction pathway of $Pt(NH_3)_2$(ETMAL) with GMP.

2.6 250MHz ^1H NMR of $Pt(NH_3)_2$(ETMAL) and Na_2GMP (1:1, 3 days).

2.7 400MHz ^1H NMR of $Pt(NH_3)_2$(ETMAL) and Na_2GMP(1:1, 3 days).

2.8 Reaction sequence of *cis*-$Pt(II)_{aq}$ with inosine.

2.9 ^1H NMR of $Pt(NH_3)_2$(ETMAL) and inosine (1:1 in water).

2.10 Reaction sequence of $Pt(NH_3)_2$(ETMAL) and inosine, r = 1.

2.11 Graph of absorption (290nm) versus fraction no. of Sephadex separation of intermediate species.

2.12 ^1H NMR of $Pt(NH_3)_2$(ETMAL)(Inosine) intermediate.

2.13 ^{1}H NMR of $Pt(NH_3)_2$(ETMAL) and IMP (1:1, day 2).

2.14 ^{1}H NMR of $Pt(NH_3)_2$(CBDCA) and inosine (1:1, day 5).

3.1 The phases of the cell cycle where antitumour drugs exert their lethal effects.

3.2 The epr spectra of Pt-araC blue and 'purified' blue.

3.3 The structure of bleomycin.

3.4 The structure of Cu(II)(P-3A).

3.5 Model for the complex of bleomycin, DNA, Fe^{2+} and O_2.

3.6 Catalytic cycle of Fe-BLM.

3.7 Region 1 (0-30ppm). ^{13}C-NMR spectra of *cis*-$Pt(II)_{aq}$ interaction with blenoxane (r = 0.1, 0.3 and 0.5).

3.8 Region 2 (30-60ppm). ^{13}C-NMR spectra of *cis*-$Pt(II)_{aq}$ interaction with blenoxane (r = 0.1, 0.3 and 0.5).

3.9 Region 3 (60-90ppm). ^{13}C-NMR spectra of *cis*-$Pt(II)_{aq}$ interaction with blenoxane (r = 0.1, 0.3 and 0.5).

3.10 Region 4 (90-130ppm). ^{13}C-NMR spectra of *cis*-$Pt(II)_{aq}$ interaction with blenoxane (r = 0.1, 0.3 and 0.5).

3.11 Region 5 (130-160ppm). ^{13}C-NMR spectra of *cis*-$Pt(II)_{aq}$ interaction with blenoxane (r = 0.1, 0.3 and 0.5).

3.12 Region 6 (160-180ppm). ^{13}C-NMR spectra of *cis*-$Pt(II)_{aq}$ interaction with blenoxane (r = 0.1, 0.3 and 0.5).

3.13 Lost and broadened resonances of BLM on interaction with *cis*-$Pt(II)_{aq}$.

3.14 Regions 1 and 2 (0-60ppm). ^{13}C-NMR spectra of blenoxane and *cis*-$Pt(II)_{aq}$ interaction with blenoxane, r = 1.

3.15 Regions 3 and 4 (60-130ppm). ^{13}C-NMR spectra of blenoxane and *cis*-Pt(II)$_{aq}$ interaction with blenoxane, r = 1.

3.16 Regions 5 and 6 (130-180ppm). ^{13}C-NMR spectra of blenoxane and *cis*-Pt(II)$_{aq}$ interaction with blenoxane, r = 1.

3.17 Split resonances on immediate addition of r = 1, *cis*-Pt(II)$_{aq}$.

3.18 Region 1 (0-30ppm). ^{13}C-NMR spectra of $Pt(NH_3)_2$(ETMAL) interaction with blenoxane (r = 0.1, 0.3 and 0.5).

3.19 Region 2 (30-60ppm). ^{13}C-NMR spectra of $Pt(NH_3)_2$(ETMAL) interaction with blenoxane (r = 0.1, 0.3 and 0.5).

3.20 Region 3 (60-90ppm). ^{13}C-NMR spectra of $Pt(NH_3)_2$(ETMAL) interaction with blenoxane (r = 0.1, 0.3 and 0.5).

3.21 Region 4 (90-130ppm). ^{13}C-NMR spectra of $Pt(NH_3)_2$)(ETMAL) interaction with blenoxane (r = 0.1, 0.3 and 0.5).

3.22 Region 5 (130-160ppm). ^{13}C-NMR spectra of $Pt(NH_3)_2$(ETMAL) interaction with blenoxane (r = 0.1, 0.3 and 0.5).

3.23 Region 6 (160-180ppm). ^{13}C-NMR spectra of $Pt(NH_3)_2$(ETMAL) interaction with blenoxane (r = 0.1, 0.3 and 0.5).

3.24 Region 1 (0-30ppm). ^{13}C-NMR spectra of K_2PtCl_4 interaction with blenoxane (r = 0.1, 0.3, 0.5 and 0.7).

3.25 Region 2 (30-60ppm). ^{13}C-NMR spectra of K_2PtCl_4 interaction with blenoxane (r = 0.1, 0.3, 0.5 and 0.7).

3.26 Region 3 (60-90ppm). ^{13}C-NMR spectra of K_2PtCl_4 interaction with blenoxane (r = 0.1, 0.3, 0.5 and 0.7).

3.27 Region 4 (90-130ppm). ^{13}C-NMR spectra of K_2PtCl_4 interaction with blenoxane (r = 0.1, 0.3, 0.5 and 0.7).

3.28 Region 5 (130-160ppm). ^{13}C-NMR spectra of K_2PtCl_4 interaction with blenoxane (r = 0.1, 0.3, 0.5 and 0.7).

3.29 Region 6 (160-180ppm). ^{13}C-NMR spectra of K_2PtCl_4 interaction with blenoxane (r = 0.1, 0.3, 0.5 and 0.7).

4.1 The structure of $Pt_2(NH_3)_4(glutarate)_2$.

CHAPTER ONE

INTRODUCTION

1:1 Historical

The discovery of the anti-tumour activity of *cis*-dichloro-diammineplatinum(II) now commonly referred to [1] as *cis*-Pt(II), which was first synthesised in 1845 (Peyrone's chloride), is a classical case of serendipity.

In 1965 Rosenberg *et al.* described [2] a surprising effect of passing an alternating electric current, via platinum electrodes, through a growth medium (which contained as one of its constituents ammonium chloride), supporting the gram negative bacteria, E. Coli. With the current on, cell division was inhibited and long filamentous rods resulted. If the current was switched off after several hours normal appearance of the rods was observed. This process could be repeated *ad. infinitum*. After a long period of detective work it was found that, due to electro- and photochemical reactions, *cis*-$Pt(NH_3)_2Cl_4$ and other Pt species had been produced at a concentration of some 10ppm. Solutions of *cis*-$Pt(NH_3)_2Cl_4$ and *cis*-Pt(II) at the 10ppm level produced the same filamentous growth.

The intuitive jump to the hypothesis that these complexes might, by virtue of their action in bacterial cells, also inhibit cell division in rapidly growing cancer cells was then investigated [1]. Encouraging results were obtained and *cis*-Pt(II) was found to be capable of regressing large solid Sarcoma 180 tumours (8 days old) in Swiss white mice [3]. Some mice were completely cured and kept

alive after treatment for six months, during which time they remained free from tumours.

Despite these encouraging results the world of clinical oncology was initially sceptical about the potential usefulness of a drug based on a heavy metal.

However, in December 1978 *cis*-Pt(II) received U.S. Food and Drug Authority approval [4] as an anti-cancer drug for testicular and ovarian cancers. Three months later approval was given in the U.K., where it is marketed under the name of Neoplatin, and applications are either pending or have been granted in many other countries.

1:2 Structure/Activity Studies

The anti-tumour property of *cis*-Pt(II) initiated the synthesis and screening of many analogous complexes. From this work, which has been extensively reviewed [5-7], several structure/activity correlations have been proposed [8]:

(1) These complexes must exchange only some ligands quickly in reactions with biological molecules.

(2) The complexes should be electrically neutral although the active form may be charged after undergoing ligand exchange in the animal.

(3) Two *cis* monodentate (or one bidentate) leaving groups are required. The corresponding trans isomers are inactive.

(4) The rates of exchange of these ligands should fall into a restricted range of lability.

(5) The non-exchanging ligand groups trans to the leaving groups should preferentially be strongly bonded, relatively inert amine systems.

In summary, the desired platinum complex may be represented as *cis*-$Pt(A)_2(X)_2$ where $(A)_2$ is the bis or chelated amine(s) and $(X)_2$ is the bis or chelated, relatively labile, leaving group(s).

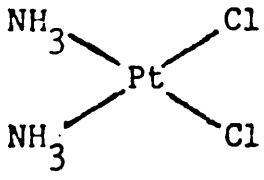
A considerable amount of synthetic work by various research groups has led to the testing of a large range of new *cis*-$Pt(A)_2(X)_2$ compounds. This, in turn, has permitted the selection [9] (Figure 1.1) of several complexes whose properties, e.g. aqueous solubility, therapeutic index, toxic side reactions, etc., are more favourable than *cis*-Pt(II), for use in clinical trials. We may term these complexes the second-generation platinum drugs.

1:3 Mode of Action of *Cis*-Pt(II)

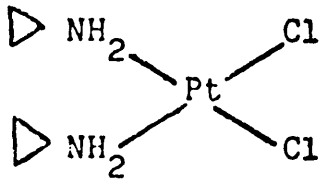
When dissolved in water *cis*-Pt(II) rapidly hydrolyses [10] to produce aquated/hydroxy species which, on standing [11,12], oligomerise to give dimeric and trimeric hydroxy-bridged platinum diammine units. It is now generally accepted [13] that the active form of *cis*-Pt(II) is a hydrolysed species probably *cis*-$[Pt(NH)_2(OH_2)(OH)]^+$, hereafter referred to as *cis*-$Pt(II)_{aq}$ which is the predominant form at physiological pH.

Presumably when *cis*-Pt(II) is injected into the extracellular fluid of an animal the high chloride concentration inhibits any aquation/hydrolysis reactions. Indeed, work by Boreham *et al* [12] supports this hypothesis. The intracellular chloride concentration

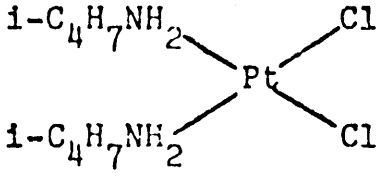
<u>cis</u>-dichlorodiammino Pt(II)



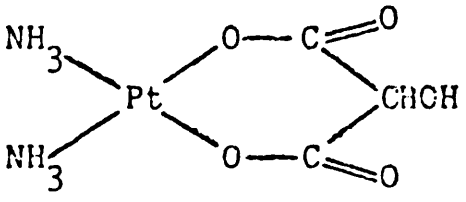
Pt(cyclopropylamine)$_2$ Cl_2



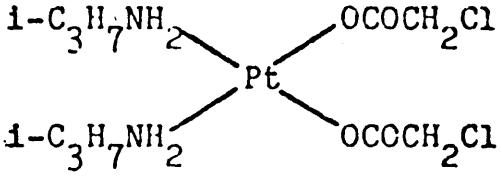
Pt(isobutylamine)$_2Cl_2$



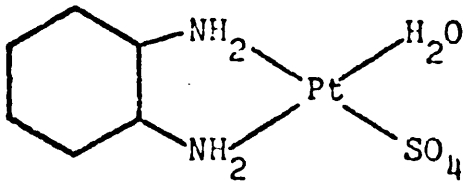
Pt(NH_3)$_2$hydroxy-malonate



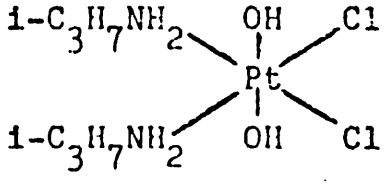
Pt(isopropylamine)$_2$ (chloroacetate)$_2$



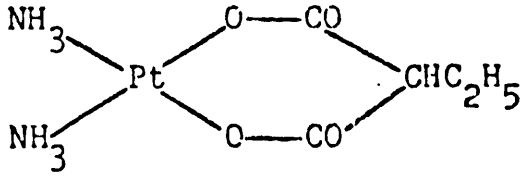
Pt(1,2-diaminocyclo hexane)sulphate



Pt(iso-propylamine)$_2$ $Cl_2(OH)_2$



Pt Ethylmalonate $(NH_3)_2$



Pt(NH_3)$_2$(1,1-cyclo-butyldicarboxylic acid)

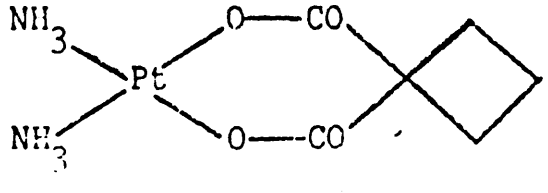


Figure 1.1: Second generation platinum drugs.

of most body cells [11] is very low, so, when *cis*-Pt(II) enters the cell, conditions are right for hydrolysis to occur. There is a wealth of evidence [14] which clearly indicates that DNA is the principal target molecule for *cis*-Pt(II). At the molecular level the initial sites of interaction of *cis*-Pt(II) with DNA are not so clear. For most of the major DNA bases the thermodynamically favoured co-ordination site has been (cf. Chapter 2) clearly determined by X-ray crystallographic studies.

Indeed, the fact that *trans*-Pt(II) (and its analogues) is not an active anti-tumour agent has not been explained by firm chemical evidence.

The original hypothesis of Goodgame *et al* [15] for the attachment of *cis*-$Pt(II)_{aq}$ on double stranded DNA still appears to be the most favoured [13] explanation for the stereoselective dependence of the anti-tumour action.

The N(7) position of guanine in DNA is not involved [16] in Watson-Crick base pairing and is the most open position for attack by a platinum agent. Goodgame *et al.* suggested that *cis*-$Pt(II)_{aq}$ initially formed a bond to only one N(7) position (Figure 1.2a). A hydrogen bond may then be formed between a co-ordinated water (or hydroxy) molecule with the O(6) position. Alternatively, initial Pt binding could involve the elimination of co-ordinated water and the formation of an N(7)-O(6) chelate by guanine (Figure 1.2b). Concurrently Maquet and Theophanides [17] proposed the one step formation of the N(7)-O(6) chelate (Figure 1.2b).

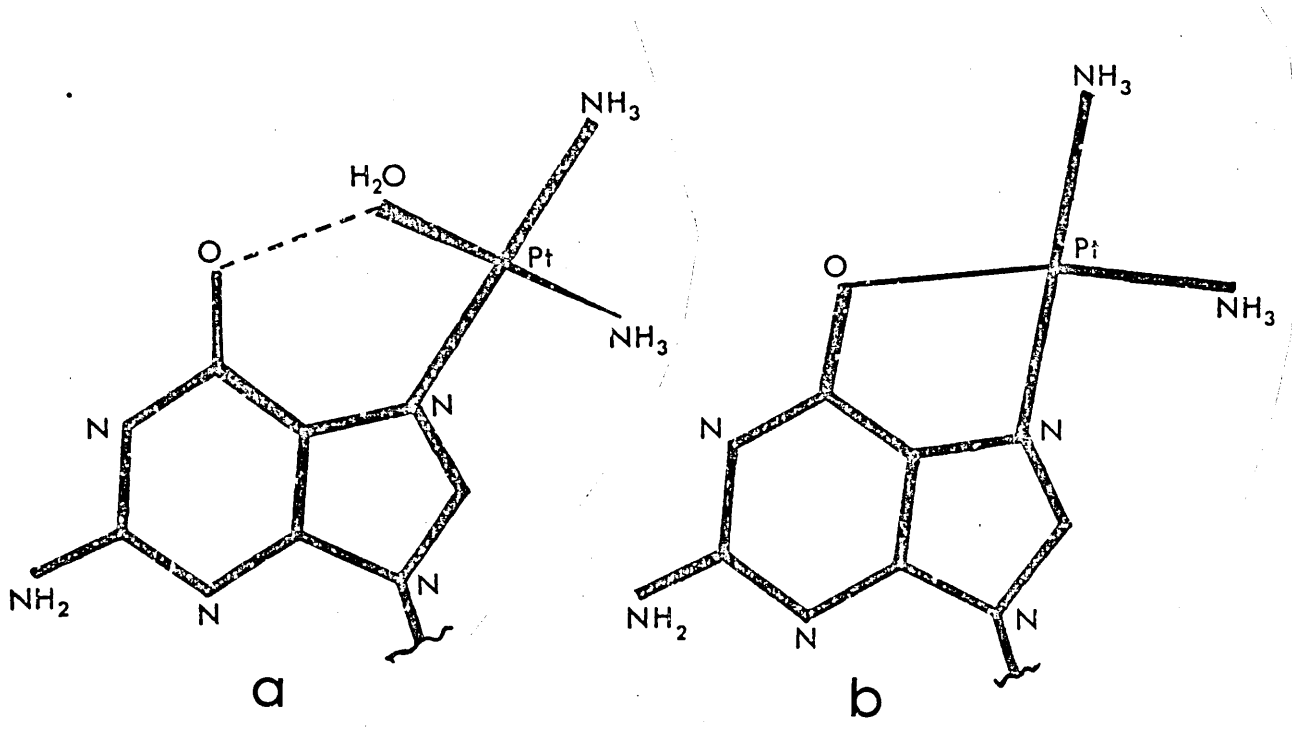


Fig. 1.2 Possible modes of *cis*-Pt(II) interaction with N(7)-O(6) of guanine.

Goodgame *et al* however, went on to propose that as soon as the two strands separate the metal would be free of stereochemical restrictions to replace the labile Pt-O or Pt-OH-O bond by a stronger Pt-N bond to a neighbouring base.

A recent communication from the Dickerson group [18] has reported the primary-binding of *cis*-Pt(II) to a DNA dodecamer. The X-ray structure studies show *cis*-Pt(II) bound at the N(7) of a guanine base, with what is probably an aquo bridge (as in Fig. 1.2a) between Pt and the adjacent O(6) of the same base. Independent work [19] concerning the interaction of *cis*-Pt(II) with t-RNA has corroborated this mode of primary binding. This evidence supports the original hypothesis of Goodgame *et al* describing the initial anchoring of *cis*-Pt(II) to DNA.

Lippard reports [20] that experiments with space filling models show that *cis*-Pt(II) is capable of intrastrand linking to adjacent guanines via N(7) whilst *trans*-Pt(II) is not. Indeed several [21,22,23] ^{1}H NMR studies have demonstrated that *cis*-Pt(II) is capable of intrastrand crosslinking of two adjacent guanines. Indeed the two guanines may be separated by one or more bases [23].

Intrastrand attachment of *cis*-Pt(II) to DNA is now the most favoured explanation of *cis*-activity versus *trans* non-activity. However, workers in the field are not clear if the second guanine base is attached to *cis*-Pt(II) in the double stranded form of DNA. Possibly the stereochemical restrictions have to be lifted first for the second base to be captured by *cis*-Pt(II), for instance, as the strands separate during the replication process.

Elegant work [24] from the Lippard group, reporting the binding of *cis*-Pt(II) to a DNA molecule of known sequence and subsequent degradation by Exonuclease III, showed that the digestion of the enzyme was terminated three bases to the 3' direction of an oligo (dG) - oligo (dC) site. Hence, it was concluded that *cis*-Pt(II) was bound to $(dG)_n$ (dC) sequences, $n \geqslant 2$. The digestion of DNA platinated with either *trans*-Pt(II) or [(dien)PtCl]Cl did not [24] produce the same termination sites of digestion by Exonuclease III and a further communication giving these sites was promised.

Lippert *et al* [25] have determined the crystal structure of [*cis*-$Pt(NH_3)_2$(1-Methylcytidine)(9-Ethylguanine)]$^{X+}$. The bonding in the molecular cation was normal, Pt being attached to N(7) position of 9-EtG and N(3) of 1-MeC. However, co-ordination of

Pt(II) at the N(7) position of 9-EtG significantly shifted the pK of the N(1) position to produce significant amounts of protonated and deprotonated guanine at pH 7. This allowed an intermolecular G-G base pairing as shown in Figure 1.3b which is similar to the Watson-Crick G-C base pair (Figure 1.3a). Lippert [25] suggests that the G-G base pairing would be unlikely to occur in DNA but an alternative mispairing may arise in the DNA structure, namely G-T, by analogy to an N(7) methylated guanosine-thymine pair (Figure 1.3c).

A ^{1}H NMR investigation by Lippert [26] into the effect of N(7) platinum binding on the hydrogen bonding behaviour of 9-ethylguanine essentially showed a loss of selectivity of 9-EtG for cytidine. These results must be treated with caution as the NMR investigation was in DMSO which is an aprotic solvent far removed from the hydrogen bonding capacity of physiological fluid.

To summarise, *cis*-Pt(II) would appear to act as an intrastrand binding agent preferentially bonding at N(7) of guanine which can upset the base pairing hydrogen bonding. Consequent replication of the platinised DNA would result in G mispairing with T. In the next generation of DNA an original G-C pair in one daughter cell is hence substituted by an A-T pair.

An alternative to the hydrogen bonding and consequent base substitution mechanism outlined above is a much simpler concept. If *cis*-Pt(II) captures a second neighbouring base [15] on the single stranded DNA formed during replication the steric changes imposed on the base packing may prevent the formation of daughter double strands from such a damaged template at least in those regions where Pt is bound.

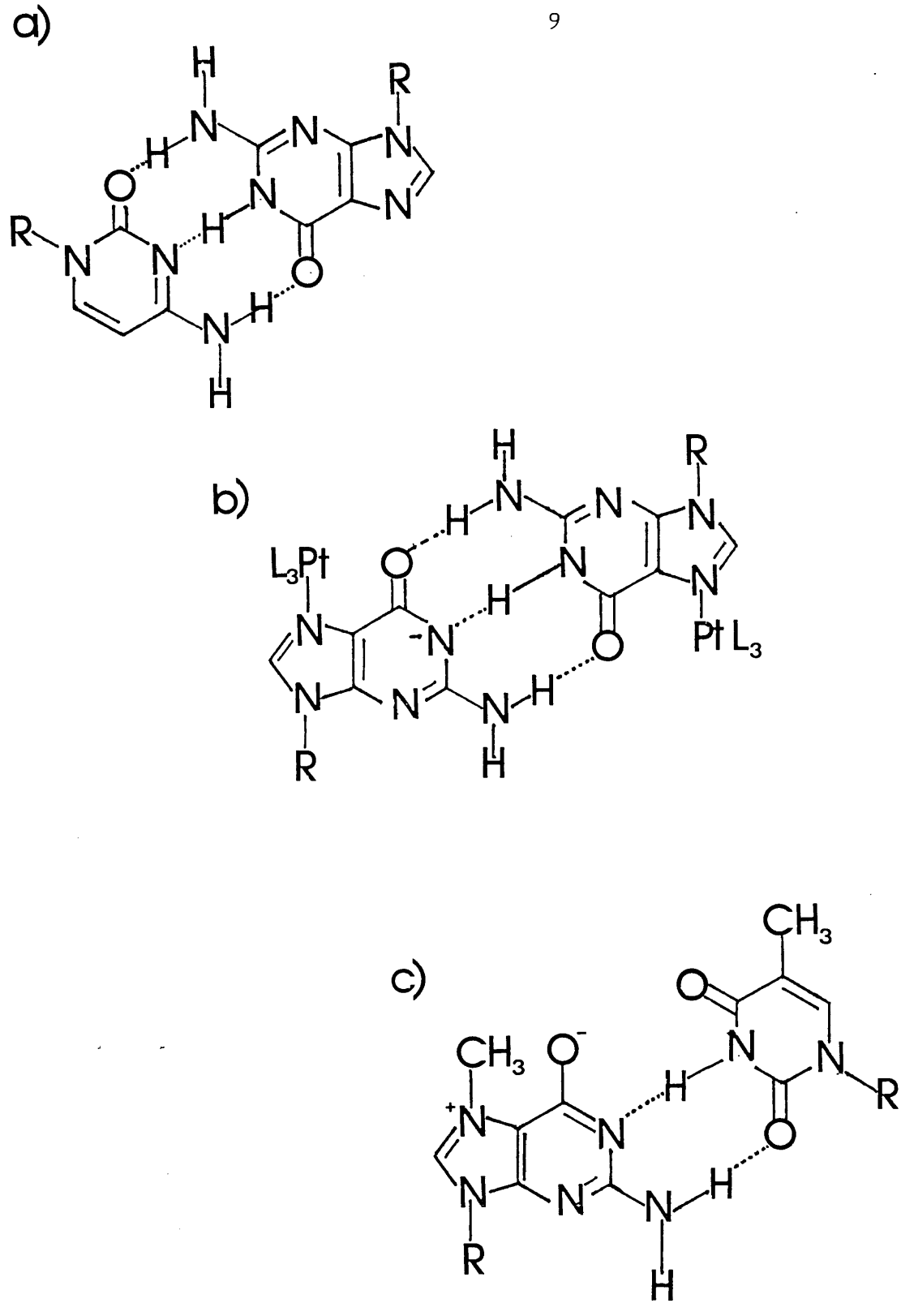


Figure 1.3: A comparison of the (a) Watson-Crick G-C pair, (b) the platinated G-G pair, and (c) the methylated G-T pair.

Cells have the ability to repair DNA lesions either before replication by a process of cutting out and replacing damaged sections of the template or by a postreplication repair mechanism. It has been suggested [8] that in tumour cells the necessary enzymes for the repair mechanisms are deficient. A possible if somewhat naive point of view is that, as tumour cells replicate at a faster rate than normal cells, DNA lesions in a tumour cell cannot be repaired quickly enough to keep pace with replication. Normal cells, however, have enough time to effect complete repair at each stage before the next round of replication. The tumour cell due to the cumulative effect of DNA lesions eventually will be unable to replicate and in the process of attempting to do so will meet with cell death.

There are no other suggestions in the literature to explain the anti-tumour activity opposed to their cytotoxicity of the platinum complexes except for the immunological reactions now considered even by its propagator [8] to be only of a minor component of the resultant activity of the drugs.

Chapter 2 will describe the interaction of two of the most promising second generation complexes, which both contain a dicarboxylate ligand as the leaving group with nucleic acid constituents. This study was undertaken to discover if the sites of reaction were the same as *cis*-Pt(II) and if there were any differences to see if these may be exploited to design and synthesize a more potent platinum anti-cancer agent.

CHAPTER TWO

INTERACTION OF $Pt(NH_3)_2$(ETMAL) AND $Pt(NH_3)_2$ CBDCA WITH DNA CONSTITUENTS

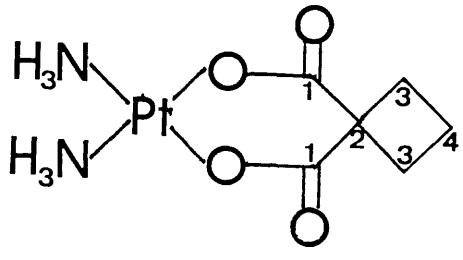
2:1 Introduction

The mode of action of *cis*-Pt(II) is considered to be via aquated and / or hydroxy species. In the pH range involved in intracellular fluid, it is thought that [11] it is mainly *cis*-$[Pt(NH_3)_2(OH_2)(OH)]^+$ which interacts with the target molecule DNA [14]. Studies by ultraviolet spectroscopy and potentiometric measurements on several of the chelated dicarboxylate (DCA) analogs of *cis*-Pt(II) in aqueous and saline solutions have shown that for these complexes there is little or no aquation [6]. Cleare has postulated the activation of such analogs by the removal of chelated dicarboxylic acids by cellular enzymes [4] (e.g. succinate dehydrogenase). Platinum complexes containing chelated dicarboxylic acids have been classified as kinetically inert even though reactions have been observed with thiourea [7].

This chapter will describe the interaction of these so-called kinetically inert species with DNA constituents. By analogy with *cis*-Pt(II), deoxyribonucleic acid is also considered to be their target molecule. The two second generation complexes $Pt(NH_3)_2$(CBDCA) (Fig. 2.1) and $Pt(NH_3)_2$(ETMAL) (Fig. 2.3) were studied and their reactions compared to those of *cis*-Pt(II). The major method of following their interaction with DNA constituents was ^1H NMR, and in some instances ^{13}C NMR, spectroscopy in aqueous solutions. After consideration of the two $Pt(NH_3)_2$ (DCA) complexes,

their interactions with each of the nucleoside and nucleotide species will be discussed. It is also appropriate to survey the situation in the literature regarding the interaction of *cis*-Pt(II) with those DNA constituents, particularly relating the NMR data with the few known crystal structures at each stage.

Fig. 2.1: (Diammine)(1,1-cyclobutanedicarboxylato)platinum(II) $Pt(NH_3)_2(CBCDA)$



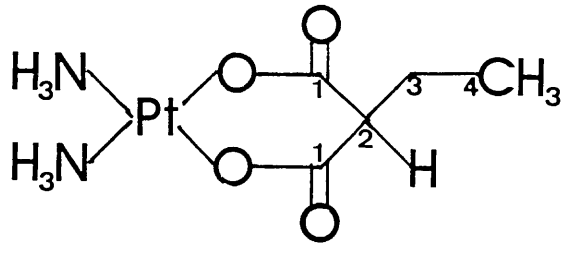
This is a very promising second generation compound which is at present undergoing clinical trials [27] at the Royal Marsden Hospital, London. Animal tests [9] have shown that $Pt(NH_3)_2(CBDCA)$ is less myelo-, and nephro-toxic and less emetic than *cis*-Pt(II) while retaining equal or superior anti-tumour activity.

The structure of $Pt(NH_3)_2(CBDCA)$ was recently determined [28] and related to NMR data. The cyclobutane ring is exactly planar and there are only minor deviations from the expected square-planar geometry around the platinum atom. The platinum-nitrogen bond lengths are 2.010Å which falls in the expected range. Surprisingly the platinum-oxygen carboxylato bond lengths (2.029Å) are only

slightly longer than the platinum-nitrogen distance. Although Pt^{II} has hitherto been regarded as showing a relatively small affinity for oxygen [29] compared to aliphatic amines this conclusion is coming under serious reconsideration in the light of studies now becoming available on a wider range of compounds containing quite strong Pt-O bonds.

The ^{1}H and ^{13}C NMR data for $Pt(NH_3)_2$(CBDCA) and the sodium salt of CBDCA, obtained in this work, are summarised in the Table 2.1 and typical ^{1}H NMR spectra are given in Figure 2.2.

Fig. 2.3: (Diammine)(ethylmalonato)platinum(II), $Pt(NH_3)_2$(ETMAL)



Although, to our knowledge, no clinical trial [27] of $Pt(NH_3)_2$(ETMAL) is planned at present, animal tests have shown it to have similar anti-tumour activity to *cis*-Pt(II) whilst being less nephrotoxic [6].

A very recent structure determination [30] of $Pt(NH_3)_2$(ETMAL) confirmed the expected square planar geometry around the platinum atom. The platinum-nitrogen bond lengths are again very similar to the platinum-oxygen bond lengths at approximately 2.02Å.

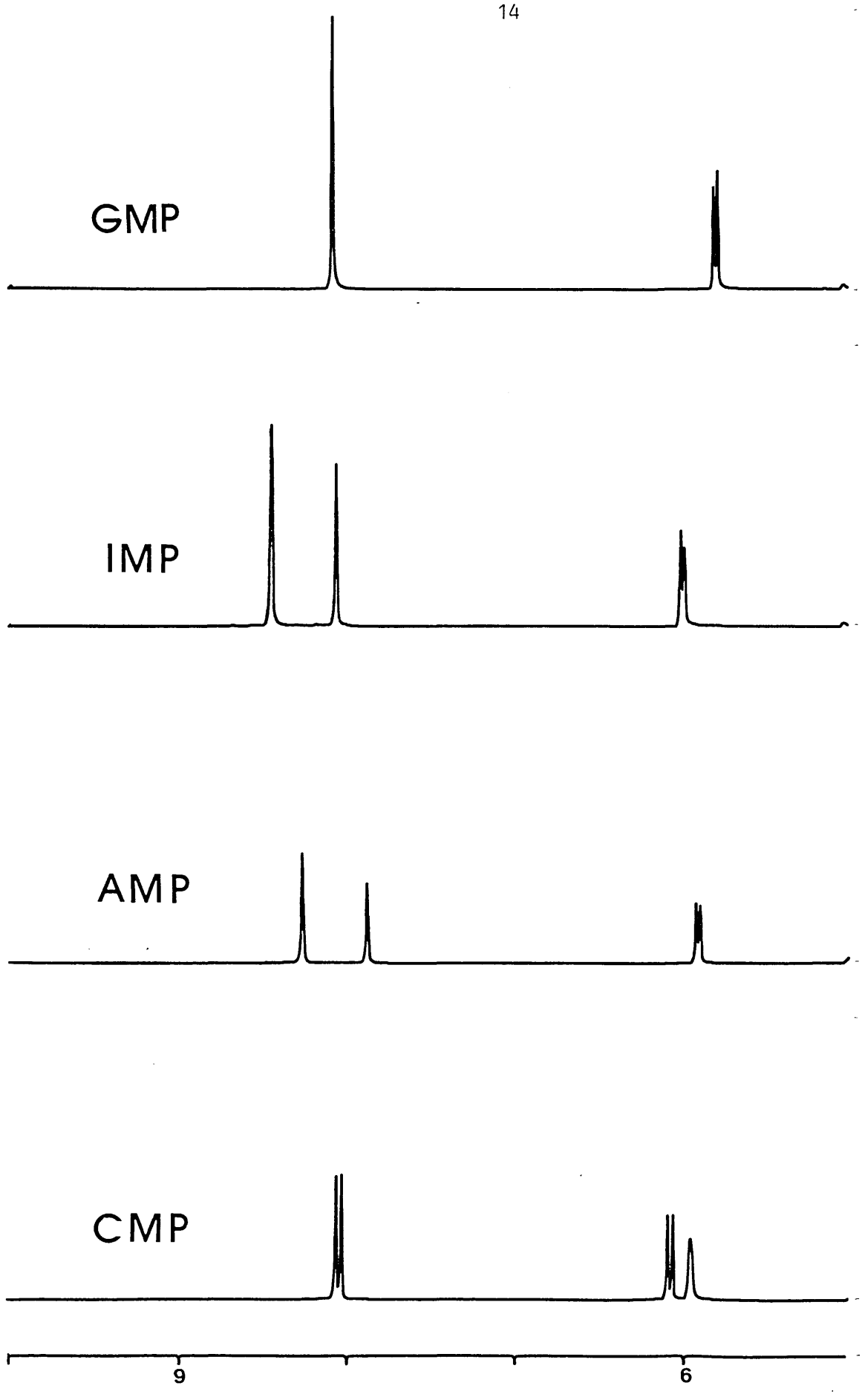


Figure 2.2: Typical ^{1}H NMR spectra of species studies in Chapter Two.

Table 2.1: ^{1}H and ^{13}C NMR chemical shifts

^{1}H NMR[a]	pD	C_2-H	C_3-H[c]	C_4-H
$Pt(NH_3)_2$(CBDCA)	5.02	-	2.86^{t}	1.88^{t}
Na_2CBDCA	7.02	-	2.37^{t}	1.87^{t}
$\Delta\delta$[b]	-	-	-0.49	-0.01
$Pt(NH_3)_2$(ETMAL)	5.70	3.51^{t}	2.54^{q}	1.02^{t}
Na_2ETMAL	6.92	3.05^{t}	1.77^{q}	0.92^{t}
$\Delta\delta$	-	-0.46	-0.77	-0.10

^{13}C NMR[a]	pD	C_1	C_2	C_3	C_4
$Pt(NH_3)_2$(CBDCA)	5.02	180.41	54.36	29.09	13.24
CBDCA		177.61	54.17	29.82	16.57
$\Delta\delta$	-	-2.80	-0.19	+0.73	+3.33
$Pt(NH_3)_2$(ETMAL)	5.70	183.67	62.45	27.37	14.32
Na_2ETMAL	7.32	182.69	63.19	26.29	14.79
$\Delta\delta$	-	-0.98	+0.74	-1.08	+0.47

(a) All chemical shifts are expressed in terms of δ convention i.e. $\delta 0 \equiv$ T.M.S.
(b) $\Delta\delta$ is the complexation shift. A positive value indicates a shift to higher field on complexation.
(c) t = triplet, q = quintet.

The ^{1}H and ^{13}C NMR data obtained during this work for $Pt(NH_3)_2$(ETMAL) and the sodium salt of ETMAL are summarised in Table 2.1 and typical ^{1}H NMR spectra are given in Figure 2.2.

Inspection of the complexation shift values ($\Delta\delta$) shows that for both compounds ^{1}H NMR distinguishes between the free and chelated dicarboxylic acid forms more readily. For both CBDCA and ETMAL the methylene, C_3-H resonances afford the greatest complexation shift differences; -0.49 and -0.77 respectively.

Neidle *et al* [28] obtained similar results for the CBDCA complex (e.g. for the methylene groups, C_3-H$\Delta\delta$ = -0.54), but for the ethylmalonate complex they observed no shift of the methylene resonance on co-ordination (they quote [28] the chemical shift at δ1.69 but at no specified pD value).

A ^{1}H NMR study of $Pt(NH_3)_2$(ETMAL) in D_2O at three initial pD values (Table 2.2) showed that the complex was stable over four days at room temperature (23°C) except at pD 13.5, where some hydrolysis had occurred.

Table 2.2: ^{1}H NMR of *cis*-$Pt(NH_3)_2$(ETMAL) in aqueous solution at various pD's

Solution	Age	pD	C_2-H	C_3-H	C_4-H
A	20 mins	5.00	3.49	2.53	1.01
	4 days	6.80	3.49	2.53	1.01
B	24 hrs	7.15	3.57	2.57	1.02
	4 days	7.09	-[a]	2.60	1.02
C	10 mins	13.5	-	2.54	1.02
	4 days		-	2.55 1.75[b]	1.02

(a) Acidic proton, exchanges with the solvent
(b) Hydrolysis product, possibly free ethylmalonic acid, solution pale blue/green

At pD 7 and above, exchange of the methine, C_2-H proton with the solvent was observed which causes the collapse of the C_3-H quintet. However, C_3-H and C_4-H chemical shifts were found to be essentially independent of pD.

The complexation shift in the ^{1}H NMR of the methylene or methyl resonances has been used as the main probe of the nature of the dicarboxylate acid species present in solution in the following discussion of these two $Pt(NH_3)_2(DCA)$ complexes with DNA constituents.

In the following sections, after a review of the relevant literature results concerning *cis*-Pt(II), the interaction of the two $Pt(NH_3)_2(DCA)$ complexes with various nucleosides or nucleotides will be discussed. The reactions were followed as a function of time at room temperature and in some cases also at body temperature (37°C). Furthermore, to elucidate the products and mechanism of interaction usually two values of r, the initial ratio, of $Pt(NH_3)_2(DCA)$ to nucleic acid component were utilised: r = 1 and r = 0.5.

2:2 Guanosine 5'-monophosphate, GMP

Numerous workers have suggested that guanine is an important site for *cis*-Pt(II) binding to DNA. In particular, Stone *et al* [31] have shown a linear relationship between G-C content of different types of DNA and the amount of *cis*-Pt(II) binding. In a recent publication Wing *et al* [18] have reported the primary binding of *cis*-Pt(II) to the N(7) of a guanine base located in the wide groove

of a complete turn of DNA.

Crystal structures of three platinum guanosine (G) complexes have been determined [32,33,34]. The main structural parameters for these systems are summarized in Table 2.3.

In each case, co-ordination of the platinum is via N(7). For the bis-(G) complexes the dihedral angle between the two guanine planes is very similar and the intermolecular hydrogen bonding between O(6) and the co-ordinated ammine is also similar, though very slightly stronger in the case of the more acidic protons on the ethylenediamine. The greater anti-tumour activity of *cis*-Pt(II) compared with that of $Pt(en)Cl_2$ has been claimed [35] to be due to the greater expected hydrogen bonding ability of ammonia, whereas in fact the opposite is true [32] in the crystal state.

If the intermolecular base stacking persists in solution with the H(8) located in close proximity to a guanine ring then a concentration dependence of the chemical shift of the H(8) resonance may be expected. The more concentrated a solution then the more intermolecular base stacking may be expected, resulting, on average, in a more shielded H(8) resonance. This will provide a shift to higher field i.e. lower δ values.

From the limited data available, the chemical shift of H(8) also appears to depend on the length of the Pt-N(7) bond. The longer the Pt-N(7) bond the larger is the downfield shift of the H(8) resonance (Table 2.4).

Table 2.3: Structural parameters of Pt-guanosine complexes

Complex	Pt-N (ammine)	Pt-N(7)	N(7)-Pt-N(7) angle,deg.	N(7)...N(7) distance A	dihedral angle	Intramolecular N...H...O(6) H bonding Å	Ref.
cis-$Pt(NH_3)_2(G)_2^{2+}$	2.070 2.089	1.992 2.018	88.25	2.79	74	2.943 2.897	32
$Pt(en)(G)_2^{2+}$	2.036	1.967	87.0	2.71	71	2.84	33
$Pt(dien)(G)^{2+}$	1.987 2.023 1.974	2.035	-	-	-	3.18	34

Table 2.4: Correlation of Pt-N(7) bond length and H(8) chemical shift

Complex	Pt-N(7) bond length Å	δ	Δδ	Con-centration
Pt(dien)(G)	2.035[34]	9.08[36a]	-1.23	b
cis-$Pt(NH_3)_2(G)_2$	2.018[32]	8.73[d][37]	-0.88	c
$Pt(en)(G)_2$	1.967[33]	8.60[d][37]	-0.75	c

a H(8) shift for Pt(dien)(GMP)
b not quoted in paper
c in the range 0.05 to 0.1M
d $J(^{195}Pt-^{1}H)$25Hz observed

However, with GMP the same trend in the chemical shift of H(8) in *cis*-$Pt(NH_3)_2$ and $Pt(en)(GMP)_2$ is not observed [38]. Protonation of the phosphate of the nucleotide also affects the position of H(8) chemical shift as well as its dependence on concentration as illustrated in Table 2.5.

The small differences in the chemical shift values of H(8), for example, *cis*-$Pt(NH_3)_2(GMP)_2$ H(8): 8.51 [38] and H(8) : 8.66 [39], may be explained by the different concentrations and small pD variations. However, the H(8) resonance reported by Marcelis *et al* [39] for the intermediate complex *cis*-$Pt(NH_3)_2(GMP)(H_2O)$ differs by 0.5ppm from the value quoted by Chu *et al* [38] for the supposedly analogous complex, even if the degree of protonation of the phosphate is taken into account. The complex reported by Marcelis *et al* is probably better represented as the hydroxy species *cis*-$Pt(NH_3)_2(GMP)(OH)$.

Table 2.5: ^{1}H NMR data of Platinum GMP complexes

Species [a]	pD	H(8)	H(1′)	Δδ	[b] Conc. mM	Ref.
GMP	7.00	8.09	5.86	-	25	[38]
	c	8.17	5.94	-	4	[39]
GMPH	4.5	8.14	5.90	-	25	[38]
cis-$Pt(NH_3)_2(GMP)_2$	8.0	8.51	5.82	-0.42	25	[38]
	c	8.66	5.92	-0.49	4	[39]
$Pt(en)(GMP)_2$	7.0	8.60	5.86	-0.51	25	[38]
$Pt(en)(GMPH)_2$	2.0	8.40	5.87	-0.31	25	[38]
"*cis*-$Pt(NH_3)_2(GMP)(H_2O)$"	c	8.92	6.05	-0.75	4	[39]
cis-$Pt(NH_3)_2(GMPH)(H_2O)$	4.5	8.43	5.84	-0.34	25	[38]

a charges not quoted for clarity
b with respect to total GMP
c pD in the range 6.5 to 6.9

This would follow the concept that the more basic, or better electron donating, are the other ligands in the platinum complex the smaller is the downfield shift of the H(8) resonance. This theory was first proposed by Kong and Theophanides [37] to explain the smaller downfield shift of H(8) for $Pt(en)(G_2)$ compared to *cis*-$Pt(NH_3)_2(G)_2$ as ethylenediamine is a better base (pK_A^1 = 10.71; pK_A^2 = 7.56) than NH_3(pK_A = 9.25). The results for [40] $K[PtCl_3G]$ (H(8) : 8.37, Δδ: -0.52) provide a further example of this effect.

The opposite trend is true for the H(8) chemical shift of *cis*-$Pt(NH_3)_2(GMP)_2$ and $Pt(en)(GMP)_2$ i.e. for the ethylenediamine complex a larger downfield shift of H(8) is observed compared to the bis-ammine (Table 2.5).

The poor correlation between the trends in the H(8) resonances of guanosine on the one hand and the analogous GMP complexes on the other, may perhaps be explained by a large difference in the dihedral angle between the two guanine planes. That large differences in the angle can occur between related complexes involving nucleotides and analogous nucleosides at least in the solid state can be seen from the X-ray results for $Pt(ten)(Me\text{-}5'\text{-}GMP)_2$ (dihedral angle 39.6°)[41] and Pt(en)(guanine) (dihedral angle 71°) [33]. The apparent pulling together of the guanine rings indicated by the closing of the dihedral angle in the nucleotide structure as opposed to the nucleoside structure may be due to the water molecule hydrogen bridge bonding between the phosphate and O(6) of the nucleotide. This would pull around the sugar and thus influence the orientation of the guanine ring.

If the difference in the dihedral angle is not just due to packing in the crystalline state but persists in solution, then, for the nucleotide structure, intramolecular base packing would be more significant than intermolecular base packing, as found for the nucleoside complexes in the solid state.

2:2i The interaction between GMP and $Pt(NH_3)_2(ETMAL)$, r = 1

The interaction between $Pt(NH_3)_2(ETMAL)$ and GMP was initially followed by ^1H NMR in D_2O at 90MHz employing trimethylsilylpropane-

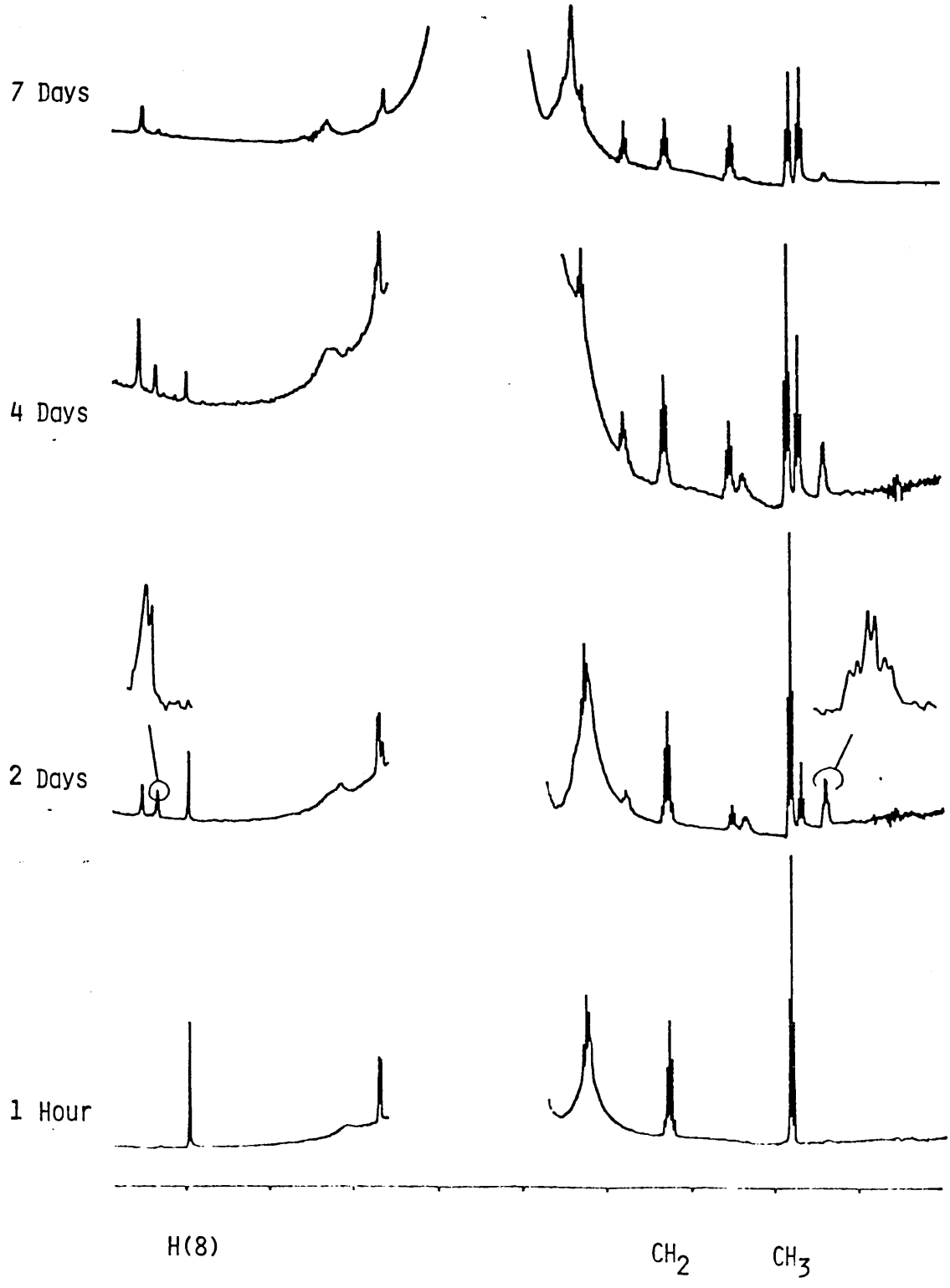


Figure 2.4: ^{1}H NMR of $Pt(NH_3)_2$(ETMAL) and Na_2GMP (1:1 in H_2O).

sulfonic acid (TMP) as an internal reference. During the course of the reaction, exchange of the acidic proton, C_2-H of the ethylmalonate residue with deuterium caused the collapse of the methylene C_3-H quintet. The methyl C_4-H resonances of the free and complexed acid overlapped to a considerable extent and were very close to a subsidiary resonance (from the methylene groups of the acid side chain) of the standard. The system was therefore re-investigated at 250MHz in H_2O using TMP as an external standard reference point. A typical ^1H NMR spectrum of free ethylmalonic acid, the platinum complex and the sodium salt of the GMP are shown, for reference purposes, in Figure 2.2.

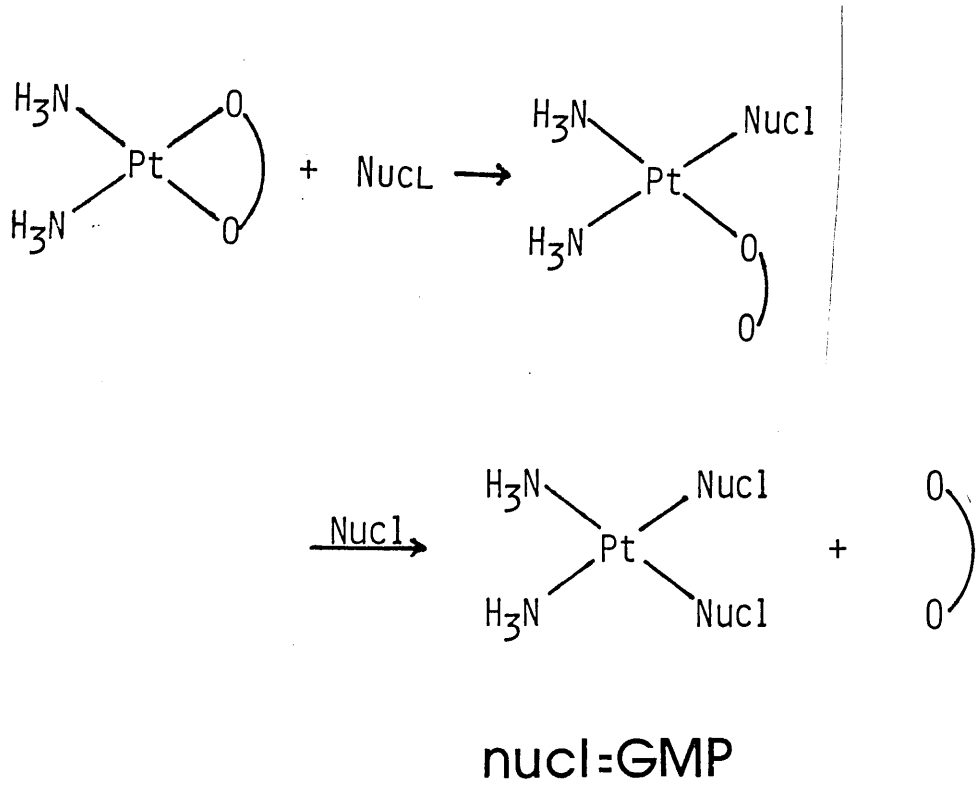
As can be seen in Figure 2.4 the reaction at room temperature was effectively complete after seven days. The only readily followed resonance of the nucleotide is H(8) at δ8.12, the other resonances of the nucleotide being masked by the broad water peak. After seven days H(8) had nearly completely shifted to δ8.65 indicative of the expected reaction product *cis*-$Pt(NH_3)_2(GMP)_2$, c.f. Table 2.5. At days two and four another H(8) resonance was observed at δ8.49 corresponding to neither the reaction product nor free GMP.

After completion of the reaction, the ethylmalonate resonances corresponded to a 1:1 mixture of free acid and $Pt(NH_3)_2$(ETMAL) which supports the conclusion that the final reaction product is *cis*-$Pt(NH_3)_2(GMP)_2$. However, at days two and four additional ethylmalonate resonances were observed at δ1.52 and δ0.52 which do not correspond to free or chelated acid.

Interestingly, the results during the course of the reaction (days two and four) show the presence of significant amounts of an intermediate species, thought to be [*cis*-$Pt(NH_3)_2$(GMP)(ETMAL)]$^{x+}$ in which the ethylmalonate is bound in a monodentate fashion. [The extent of protonation of the nucleotide and/or the ethylmalonate, and hence the formal charge on the intermediate complex cannot be readily determined from the NMR spectra].

Presumably the reaction goes via a two step mechanism (Figure 2.5). Step one involves the displacement of one end of the chelated acid by the first molecule of GMP to produce the intermediate species containing monodentate acid. Step two is the displacement of the monodentate acid by the second molecule of GMP.

Fig. 2.5: Probable reaction pathway of *cis*-$Pt(NH_3)_2$(ETMAL) with GMP



For the intermediate species, doubling of the H(8), methylene (C_3-H), and methyl (C_4-H) was observed (two singlets, very complex splitting pattern and two triplets respectively). This will be discussed in Section 2:4i.

At body temperature (37°C) the reaction at the same concentrations proceeded more quickly than at room temperature and was nearly complete within two days. At this temperature there was a substantial amount of intermediate present after only twelve hours.

2:2ii The interaction between GMP and $Pt(NH_3)_2$(ETMAL), r = 0.5

When the reactants were mixed in a 1:2, Pt:GMP ratio the reaction followed the same route as the r = 1 case (Section 2:2i) and the ^{1}H NMR spectra at the various stages were analogous except for the concentration differences. As expected, on completion of the reaction after seven days at room temperature the species in solution corresponded to *cis*-$Pt(NH_3)_2(GMP)_2$ (H(8), δ8.67) and free ethylmalonic acid only.

The same doubling of the intermediate ^{1}H NMR resonances as found in the r = 1 case was observed. This doubling of the resonances persisted at elevated temperatures even up to 90°C, indicating that conversion between presumably two forms of the intermediate is slow, even at 90°C, with respect to the NMR time scale.

The ^{1}H NMR spectrum of the three day old solution at 250MHz and 400MHz are shown in Figures 2.6 and 2.7 respectively. As can be seen, the intermediate methyl (C_4-H) resonance converges from a double triplet to an apparent quintet but the J value (7.3Hz) is independent of field. This is due to the overlapping of two

Figure 2.6: 250MHz ^{1}H NMR of $Pt(NH_3)_2$(ETMAL) and Na_2GMP (1:1, 3 days).

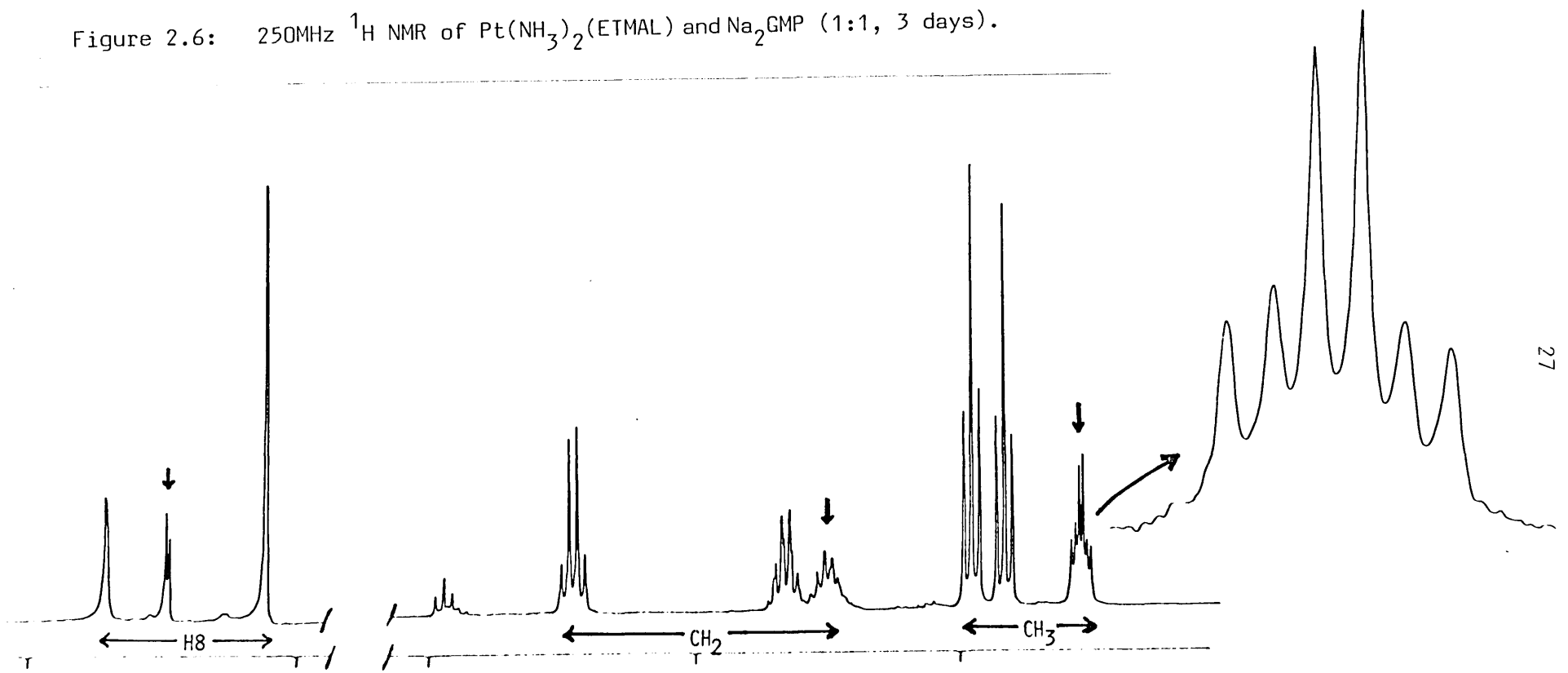
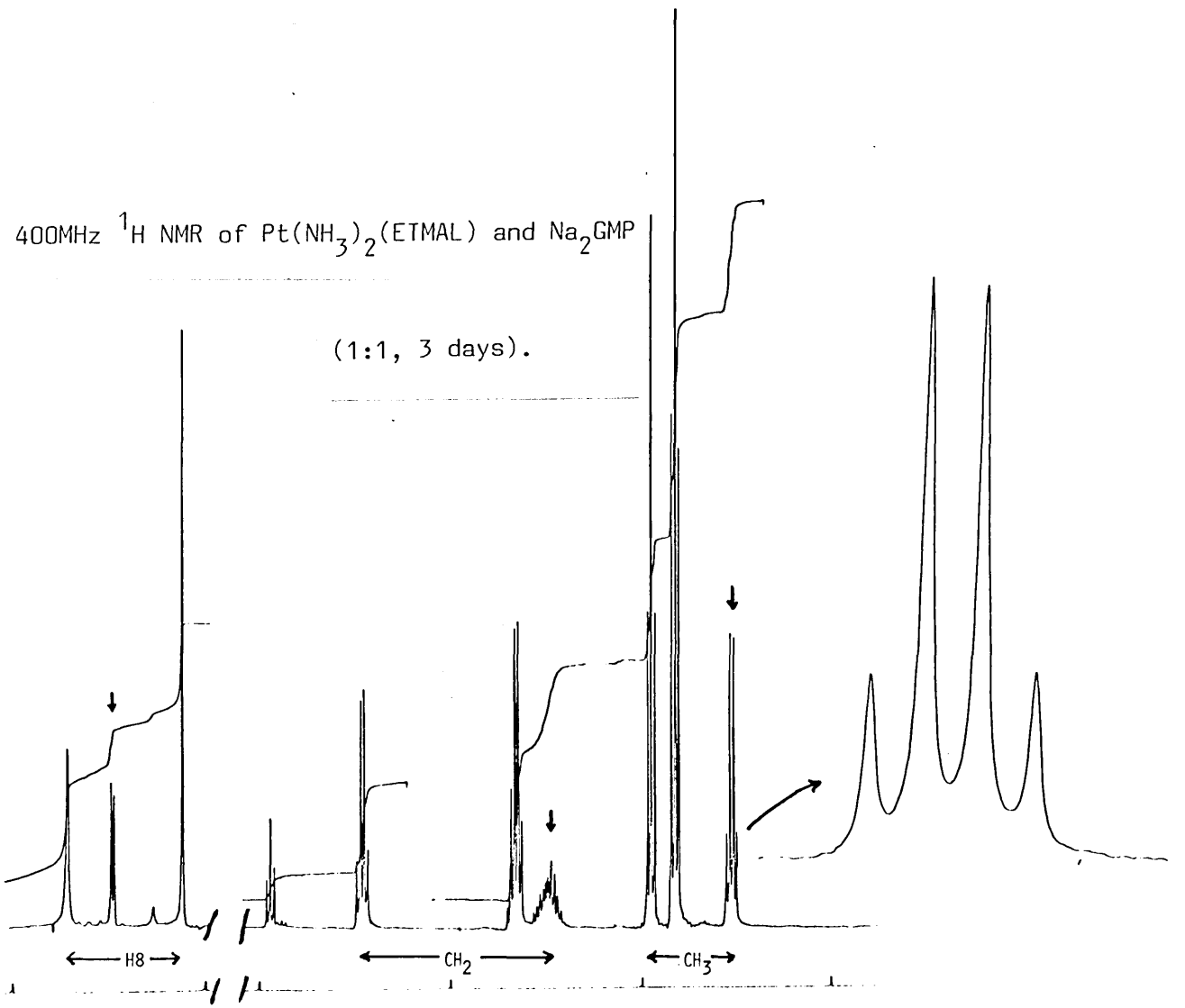


Figure 2.7: 400MHz ^1H NMR of $Pt(NH_3)_2$(ETMAL) and Na_2GMP (1:1, 3 days).



independent triplets to form a quartet when going from 200 to 400MHz. The separation of the two H(8) singlets of the intermediate species is also independent of field. The probable explanation of the existence of two intermediate species will be discussed in Section 2:4i.

A ^{13}C NMR spectrum of *cis*-[$Pt(NH_3)_2(GMP)_2$] in D_2O adjusted to pD 7.25 was compared to one of Na_2GMP, pD 7.12 (Table 2.6). For the guanine ring, C5 and C6 experience complexation shifts of approximately the same magnitude upfield but the C8 shift, also of similar magnitude, is downfield. The largest complexation shift is of C3' ($\Delta\delta$ = +4.7) but the other sugar resonances are not significantly affected.

When solutions of $Pt(NH_3)_2$(ETMAL) and GMP, which by ^1H NMR evidence contained substantial amounts of the intermediate *cis*-$Pt(NH_3)_2$(GMP)(ETMAL), were examined by ^{13}C NMR and their spectra analysed the results were disappointing.

All the resonances associated with the GMP moiety could be attributed to either free GMP or *cis*-$Pt(NH_3)_2(GMP)_2$ except for the sugar C3' and C4' regions which were very complex.

Similarly all the major resonances arising from the ETMAL moiety could be attributed to either free ETMAL or $Pt(NH_3)_2$(ETMAL), except for low intensity resonances at ~ 180.0ppm, 25.8ppm and 14.7ppm assignable to C_1, C_3 and C_4 respectively of the intermediate species. C_2 was observed centred at ~ 62ppm as a broad ill-resolved band, due to C-D coupling.

Table 2.6: ^{13}C NMR data of $Pt(NH_3)_2(GMP)_2$ and Na_2GMP

Species	pD	C2	C4	C5	C6	C8
Na_2GMP	7.25	156.57	154.14	118.97	161.49	140.29
cis-$Pt(NH_3)_2(GMP)_2$	7.12	157.11	152.50	116.15	158.58	142.88
$\Delta\delta$	-	-0.44	+1.64	+2.82	+2.91	-2.59

Species	pD	C1'	C2'	C3'	C4'	C5'
Na_2GMP	7.25	90.04	76.90	73.34	86.98 86.86	66.57
cis-$Pt(NH_3)_2(GMP)_2$	7.12	90.54	77.37	68.64	86.63 86.51	65.69
$\Delta\delta$	-	-0.50	-0.47	+4.70	+0.35	+0.98

2:2iii The interaction between $Pt(NH_3)_2(CBDCA)$ and GMP (with r = 0.5 and r = 1)

In both the cases of $Pt(NH_3)_2(CBDCA)$ to GMP ratios investigated, r = 0.5 and r = 1, a H(8) resonance at δ8.52 was observed after three days of reaction at room temperature. By analogy with the ethylmalonate case (Section 2:2i/ii)this was assigned to the intermediate species *cis*-$[Pt(NH_3)_2(GMP)(CBDCA)]^{x-}$ involving monodentate acid. However, at the same time of observation of the intermediate H(8) resonance, in neither case was there any evident monodentate acid resonance. Even at 250MHz the acid resonances were assignable to chelated and free acid only unless the monodentate acid resonances were coincident with those of either free or bidentate acid. Whereas with $Pt(NH_3)_2(ETMAL)$ the H(8) resonance of the intermediate was doubled, in this case no doubling was observed.

As there was no evidence of any intermediate acid resonances and the H(8) resonance was not doubled, the intermediate in this case may not involve monodentate acid but could be due to a *cis*-$[Pt(NH_3)_2(GMP)(OH)]^{x-}$ or similar species. To check this the following experiments were carried out. Mixing *cis*-$Pt(II)_{aq}$ with GMP in D_2O at ratios of r = 0.5 and r = 1 at room temperature and immediately running their ^1H NMR spectra showed only one H(8) peak at δ8.66 due to *cis*-$Pt(NH_3)_2(GMP)_2$ (Table 2.5).

At 5°C a 10mM solution of GMP was mixed with one equivalent of *cis*-$Pt(II)_{aq}$ to give an initial pD 7.2. Within half an hour at 5°C an appreciable H(8) resonance at δ8.73 was observed. This, over a period of hours, slowly diminished as a new resonance at δ8.62 increased. The latter peak was assigned to be due to the expected

reaction product *cis*-$Pt(NH_3)_2(GMP)_2$. The former peak was attributed to the hydrolysed intermediate *cis*-$[Pt(NH_3)_2(GMP)(OH)]$. The position of the H(8) for such a species found in this work lies in the range between those quoted by other workers [19,20] for similar complexes, H(8) δ8.92[5mM]: H(8) δ8.43[25mM]. This could be rationalised, as the total concentration of GMP[10mM] also lies in the range employed; that is to say that the H(8) resonance of *cis*-$[Pt(NH_3)_2(GMP)(OH)]$ has an unusually high dependence on concentration.

If the intermediate H(8) resonance observed when $Pt(NH_3)_2(CBDCA)$ was reacted with GMP at room temperature was due to a hydrolysed intermediate then it would not be expected to be detectable in the reaction mixture for several days. In fact it may not be detectable at all when the results of *cis*-$Pt(II)_{aq}$ obtained in this work are taken into account. The total GMP concentration was 100mM when r = 0.5 and 50mM when r = 1.0 but the position of the H(8) intermediate derived from $Pt(NH_3)_2$CBDCA was essentially independent of concentration unlike the case for *cis*-$[Pt(NH_3)_2(GMP)(OH)]$ produced from *cis*-$Pt(II)_{aq}$.

These results rule out the intermediate as a hydrolysed species and it may be formulated as *cis*-$[Pt(NH_3)_2(GMP)(CBDCA)]^{x-}$.

In this case the final product of the reaction was isolated. Adjustment of either solution with dilute nitric acid (2M) to give a pH of 2.7 resulted in the formation of fine, filamentous, white needles of $Na_2[Pt(NH_3)_2(GMP)_2].3H_2O$ after five days. [Analysis Calc: C, 22.84; H, 3.45; N, 15.98. Found: C, 23.25; H, 3.49; N, 16.10%]. Unfortunately the needles were not suitable for X-ray structure determination.

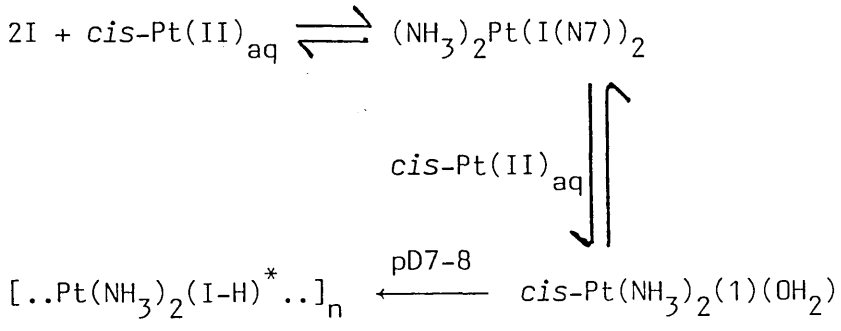
2:3 Inosine 5'-monophosphate, IMP, and inosine

Inosine and inosine 5'-monophosphate will be considered together as their reactions with $Pt(NH_3)_2(DCA)$ are similar.

The effect on the H(8) resonance of inosine and IMP upon complexation to platinum follows a similar trend to that observed for analogous complexes of G and GMP (Table 2.7). However, with I and IMP the situation is further complicated [42] by the possibility of polymer formation involving hypoxanthine rings bridging via N(1)-N(7) after deprotonation of N(1).

Chu and Tobias report [42] the lowering of the pK_A of N(1)-H from ca. 8.8 for I in D_2O to a pK_A of 7.2 ± 0.3 in the presence of an equimolar concentration of *cis*-$Pt(II)_{aq}$. This is supported by work of Sovago and Martin [43] who, for equimolar solutions of $Pd(dien)^{2+}$ and inosine in the pD range 4 to 6, report the N(1)-N(7) binuclear species as the predominant form. At pD 9 inosine [43] binds to $Pd(dien)^{2+}$ almost exclusively at the N(1) deprotonated site. Addition of aliquots of *cis*-$Pt(II)_{aq}$ surprisingly broke down the bis-complex to form the mono inosine aquated complex. At pD 7-8 an N(1)-N(7) polymeric species was produced. The reaction sequence is illustrated in Figure 2.8 and the chemical shifts are given in Table 2.7.

Fig. 2.8: Reaction sequence of *cis*-$Pt(II)_{aq}$ with inosine



* I-H ≡ N(7)-N(1) bridging hypoxanthine ring.

Table 2.7: H(8) and H(2) chemical shifts of platinum inosine complexes

Species	pD	H(8)	H(2)	H(1^1)	conc.	Ref.
Inosine, I	4.5	8.31	8.19	6.05	25mM	[42]
cis-$Pt(NH_3)_2(I)_2^d$	4.5	8.77	8.22	6.04	a	[42]
	b	8.98[c]	8.45	6.2	c	[37]
$Pt(en)(I)_2^d$	b	8.67[c]	8.17	6.0	c	[37]
cis-$Pt(NH_3)_2(I)(OH_2)^d$	4	8.90	8.32	6.15	a	[42]
[Pd(dien)](I-H)[e]	4-6	8.51	8.30	a	30mM	[43]
[Pd(dien)](I-H)[f]	9	8.22	8.22	a	30mM	[43]

a concentration not quoted but believed to be > 25mM
b pD not quoted
c $J^{195}(Pt-^1H)$ 25Hz
d co-ordination via N(7)
e N(7)-N(1) binuclear species
f N(1) dominant co-ordination site

X-ray structural information is available for three compounds involving IMP co-ordinated to Pt, and for one involving inosine. The main structural parameters are summarised in Table 2.8.

Table 2.8: Structural parameters of platinum complexes of inosine or IMP

Compound	Pt-N(Å) (ammine)	Pt-N(7) (Å)	N(7)-Pt -N(7)	N(7)--- N(7)(Å)	dihedral angle between purine planes	Ref.
cis-$Pt(NH_3)_2(IMP)_2$	2.05 2.032	2.02 2.036	89° 90°	2.83 2.88	43° 40.7°	[15] [44]
$Pt(en)(IMP)_2$	a	2.07	a	3.26	31°	[44,45]
$Pt(tn)(IMP)_2$	a	2.08	a	2.96	38°	[46]
Pt(dien)(I)	2.054 2.002 2.001	2.029	-	-	-	[47]

a not quoted

The three platinum IMP structures are essentially non-stoichiometric but are isomorphous with Na_2IMP. In each case the platinum ammine moiety occupies to varying degrees the site of the N(7)---N(7) hydrogen bonded water molecule in the sodium salt. The two independent determinations [15,44] of the structure *cis*-$Pt(NH_3)_2(IMP)_2$ have nearly identical unit cell dimensions but vary slightly in the structural parameters quoted (Table 2.8). This is due to their having different proportions of platinum occupancy

of the water site.

Kistenmacher *et al* [46] have proposed that there is a linear relationship between platinum-ammine site occupancy of the water N(7)---N(7) site in IMP and:

(i) the dihedral angle between the purine planes

and

(ii) the N(7)---N(7) distance.

However, they [44] quote no microanalytical data for their samples of *cis*-$Pt(NH_3)_2(IMP)_2^{2+}$, whereas analytical results given by Goodgame *et al* [15] are in accordance with a 56% Pt occupancy (not the 100% figure quoted in Ref. 46).

The structure of $[Pt(dien)(inosine)]^{2+}$ is similar to that of the analogous guanosine complex. However, the intermolecular ammine ---O(6) hydrogen bonding is, in this case, very weak and the nitrate and water of hydration are more important in stabilising the crystal state.

As in the case of GMP, the following sections will describe the interaction of inosine and IMP with each *cis*-$Pt(NH_3)_2(DCA)$ as a function of time and at two initial ratios of platinum to inosine or IMP, viz. r = 1 and r = 0.5.

2.3i The interaction between inosine and $Pt(NH_3)_2(ETMAL)$, r = 1

The reaction of inosine and $Pt(NH_3)_2(ETMAL)$ was initially followed at 90MHz in D_2O, which revealed high concentrations of the intermediate species involving monodentate ethylmalonate. The system was re-investigated at 250MHz in H_2O and the resulting

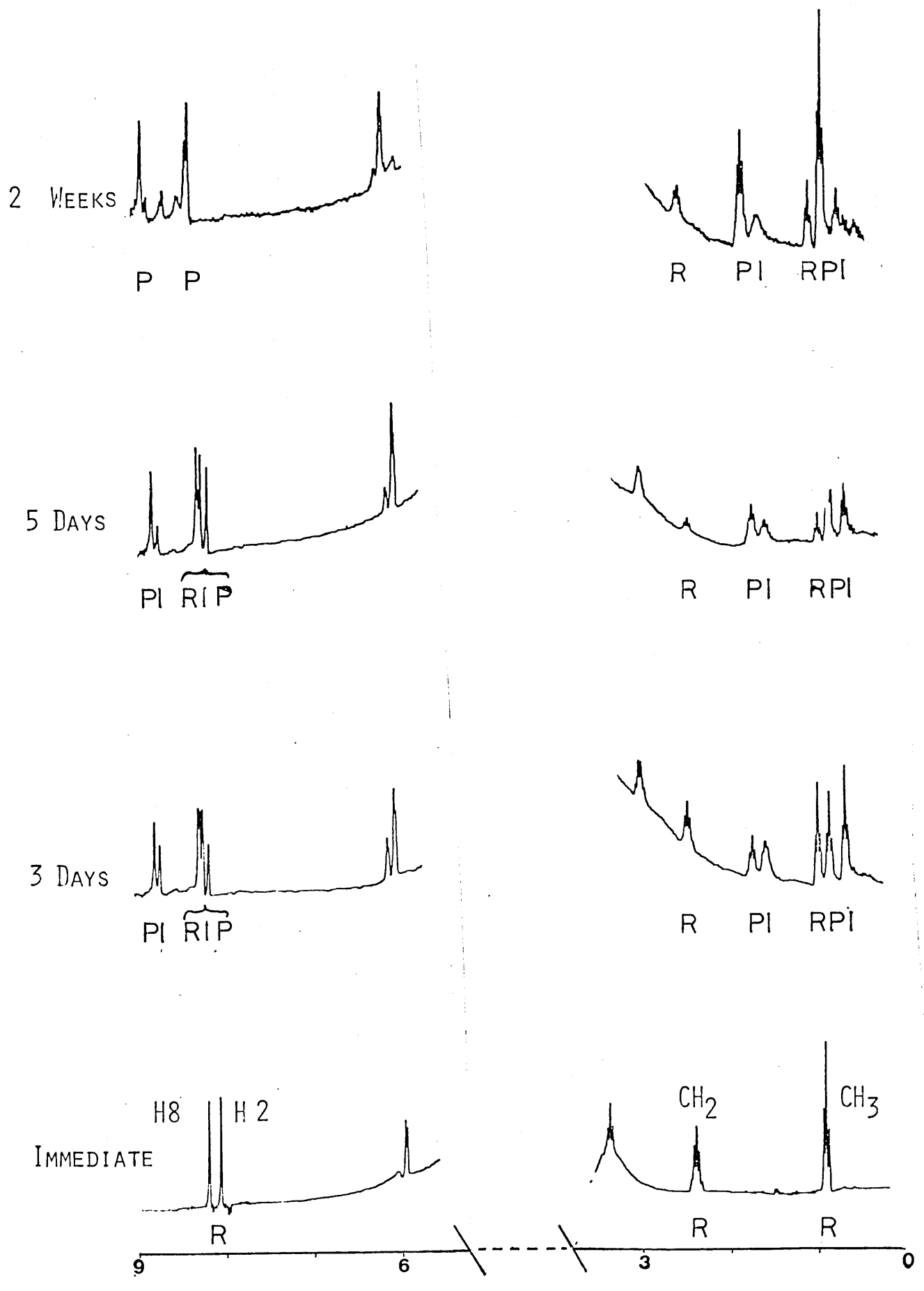


Figure 2.9: ^{1}H NMR of $Pt(NH_3)_2$(ETMAL) and inosine (1:1 in water).

spectra are illustrated in Figure 2.9. After two weeks at room temperature the reaction is complete, as illustrated by the complete shift of the H(8) and H(2) resonances of inosine. The dominant ethylmalonate resonances correspond to those of the free acid.

The highest concentration of intermediate is present after 3 days at room temperature, or after 12 hours at 37°C (body temperature). Inspection of the H(8), H(2) (Figure 2.9) region reveals a third set of resonances (δ8.70, 8.24 respectively) attributable to the intermediate species. Concurrently, resonances due to the methylene C_3-H (δ1.55) and methyl, C_4-H (δ0.64) groups of the ethylmalonate bound in monodentate fashion are observed.

The reaction sequence (Figure 2.10) is similar to that found by Chu and Tobias [42] with *cis*-$Pt(II)_{aq}$ leading to the formation of a monoaquo product *cis*-$[Pt(NH_3)_2(inosine)(H_2O)]^{2+}$.

Fig. 2.10: Reaction sequence of $Pt(NH_3)_2(ETMAL)$ and inosine, r = 1

$$Pt(NH_3)_2(ETMAL) + I \rightleftharpoons Pt(NH_3)_2(I)(ETMAL)$$

pD 5.4

$$[Pt(NH_3)_2(I\text{-}H)]_n^a + ETMAL$$

pD 5.50

(a) H(8): 8.77; H(2): 8.23, H(1'): 6.04 .

Attempts to isolate the intermediate were made as follows. At the day three stage of the reaction 0.5ml of 100mM solution was introduced on to a Sephadex G10 column (20cm long, diameter 2cm) and eluted with pH 6.8 phosphate buffer solution. After collection of the void volume, 3ml aliquots were taken and their absorption at 290nm measured. A typical plot of absorption versus fraction no. is shown in Figure 2.11. Aliquots 6 and 7 were combined and freeze dried (solid X) and aliquots 14 and 15 were similarly treated (solid Y). The ^{1}H NMR spectrum of X, dissolved in D_2O, corresponds to the intermediate species plus a small impurity of ethylmalonic acid (Figure 2.12).

The ^{1}H NMR spectrum of Y corresponds to a mixture of unreacted inosine and *cis*-[$Pt(NH_3)_2$(ETMAL)]. Their elution together was presumably due to an insufficient difference in their molecular weights (268 and 359) for efficient separation. On cooling the solution used to obtain the NMR spectrum of Y, $Pt(NH_3)_2$(ETMAL) crystallised out. The polymeric final product was eluted in the void volume.

The ^{13}C NMR spectrum of the intermediate thus isolated showed only one resonance due to the carboxylic function (183.26ppm) of the ethylmalonate residue, whereas two may be expected for this moiety. However, two ^{13}C resonances of similar intensity corresponding to the methyl group of the acid occur at 13.89 and 13.57ppm downfield from external T.M.P. A comparison of the ^{13}C chemical shifts of inosine and the isolated intermediate is given in Table 2.9.

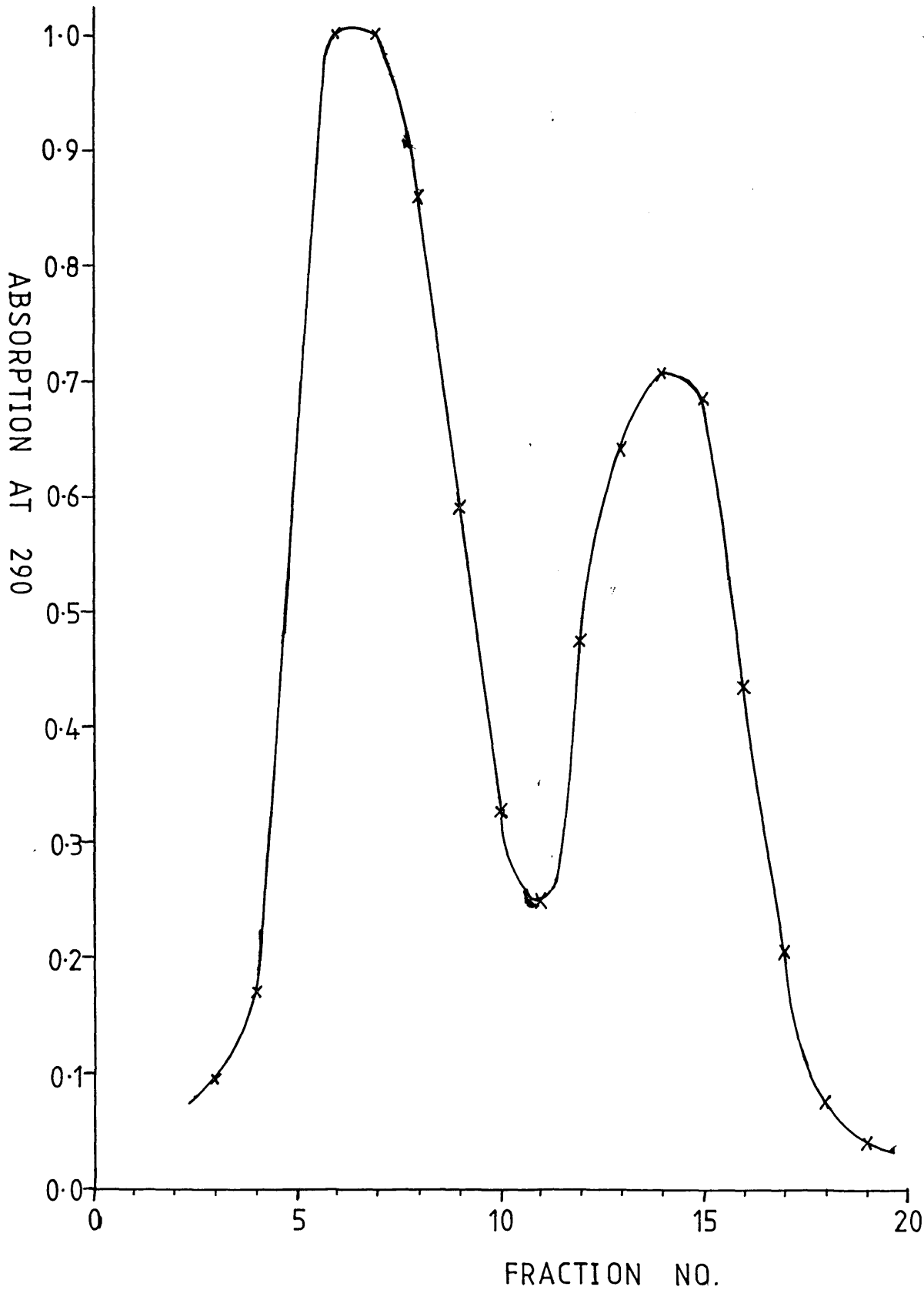
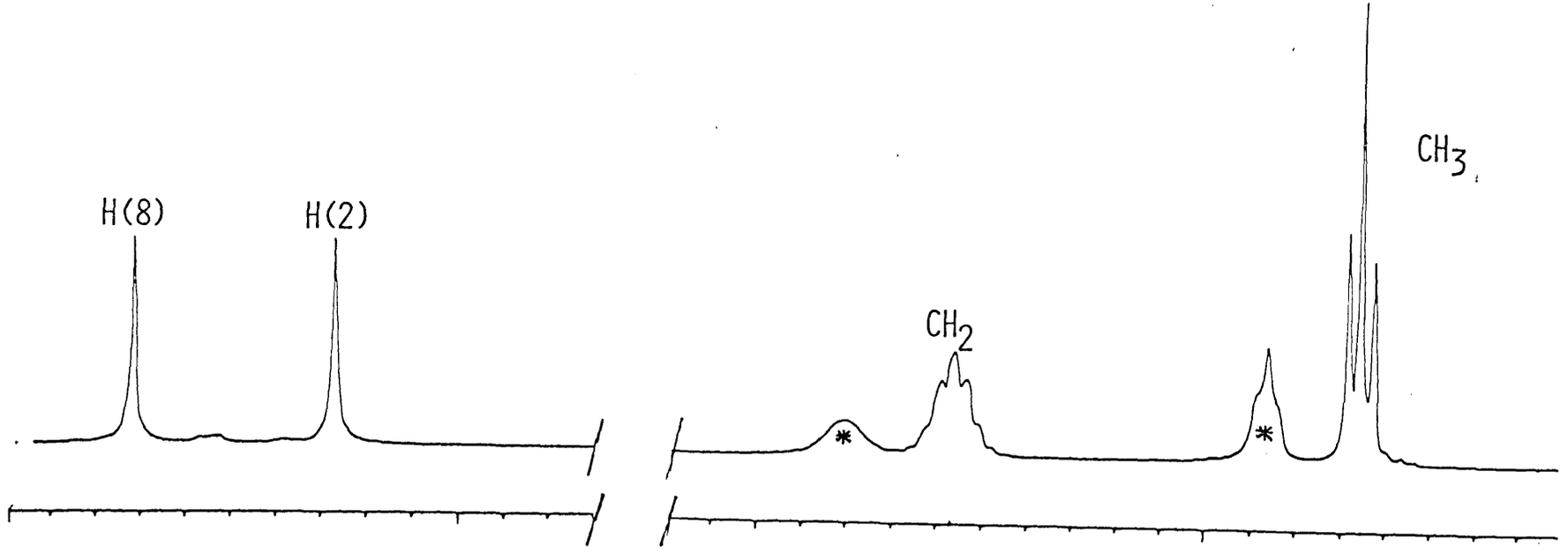

ABSORPTION AT 290
1·0
0·9
0·8
0·7
0·6
0·5
0·4
0·3
0·2
0·1
0·0
0
5
10
15
20
FRACTION NO.

Figure 2.12: ^{1}H NMR of $Pt(NH_3)_2$(ETMAL) (Inosine) intermediate.



(* ETHYLMALONIC ACID IMPURITY)

The sugar ^{13}C resonances are little affected by platinum co-ordination. The complexation shifts of C2, C8 and C6 are similar in magnitude but the former is downfield and the latter upfield.

Presumably the monoaquo product *cis*-$[Pt(NH_3)_2(inosine)(H_2O)]^{2+}$ formed at pD 5.5 when eluted with pH 6.8 phosphate buffer down the Sephadex column reacts on the column to form the N(1)-N(7) polymeric species.

The ^1H NMR shifts of the H(8) and H(2) (δ8.72 and δ8.26 respectively) infer co-ordination of the platinum via N(7) (Table 2.7). If the relationship between molecular weight and elution volume is assumed to be linear in Sephadex chromatography, this would imply a molecular weight for the intermediate of about 620, based on the elution volume and molecular weight of inosine. The molecular weight of *cis*-$Pt(NH_3)_2$(inosine)(ETMALH) is 628.

The ^{13}C NMR C8 complexation shift (Δδ: -2.10) is also in agreement with co-ordination via N7 in the intermediate species (c.f. *cis*-$Pt(NH_3)_2(GMP)_2$, H(8) Δδ: -2.59). However, C2 is also shifted downfield on complexation (Δδ: -1.64, c.f. *cis*-$Pt(NH_3)_2(GMP)_2$, H(2): -0.44) but there is no evidence of a N(7)-N(1) binuclear species.

On standing at room temperature, solutions of the intermediate disproportionate to give free ethylmalonic acid and the reaction product within a few days.

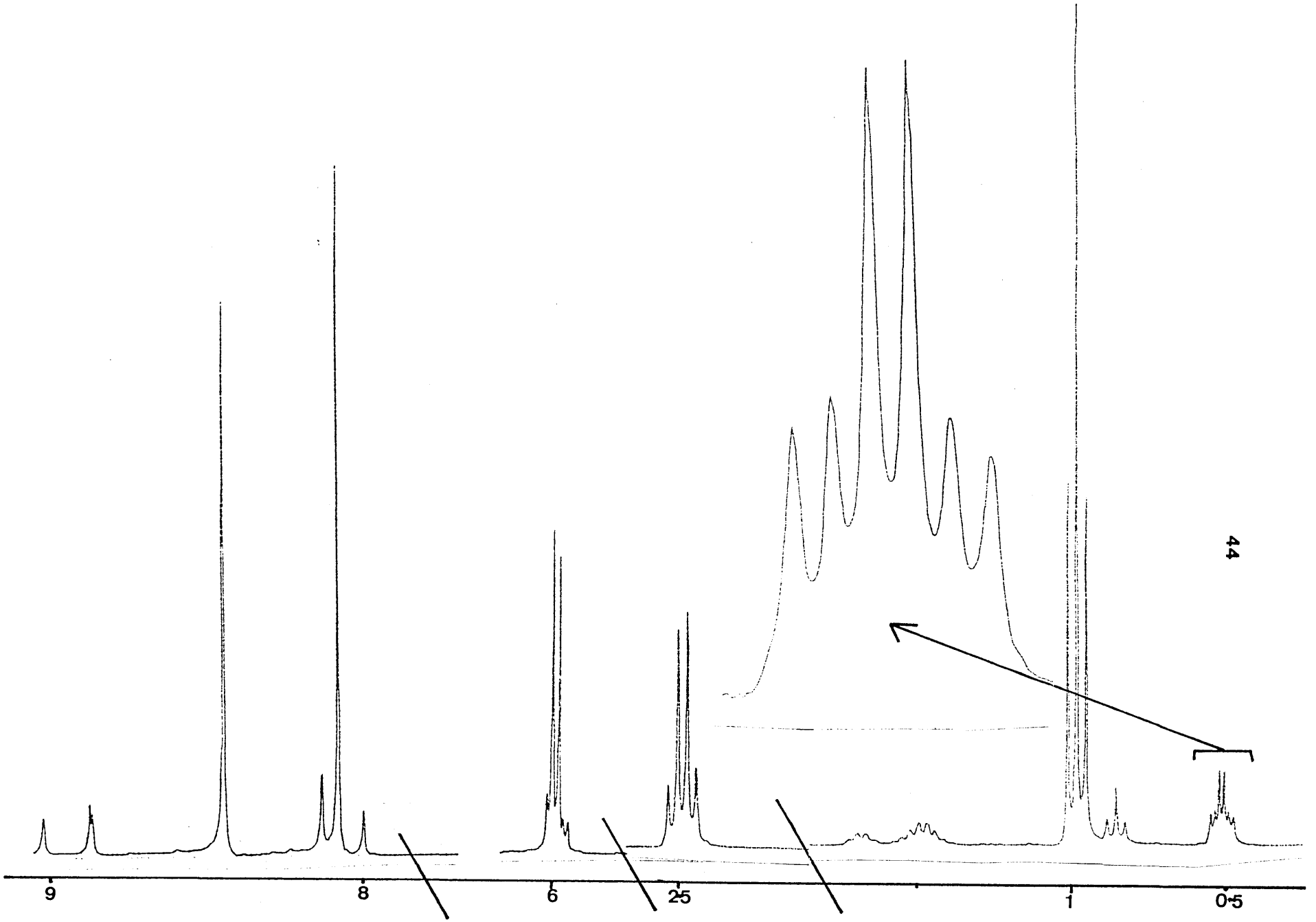


Figure 2.13: ^{1}H NMR of $Pt(NH_3)_2$(ETMAL) and IMP (1:1, day 2).

2:3ii The interaction between IMP and $Pt(NH_3)_2$(ETMAL)

On dissolving IMP and $Pt(NH_3)_2$(ETMAL) in a 1:1 ratio a high field doubled triplet centred at δ0.51 was observed within one hour at room temperature, although it was of low intensity. The ^1H NMR of the two day solution (Figure 2.13) clearly shows doubling of the C_4-H triplet, C_3-H quintet and H(8) singlet of the intermediate species.

After ten days at room temperature, the reaction is complete, with the formation of *cis*-$Pt(NH_3)_2$(IMP), 1:1 species (H(8) δ9.13, H(2) δ8.02) and, in support of this, the ethylmalonate resonances are indicative of free acid only.

At a ratio of r = 0.5,after nine days at room temperature, the proton resonances of the ethylmalonate residues were representative of free acid only. However, two sets of nucleotide H(8) and H(2) resonances of approximately equal intensity were observed. One set, (δ8.51 and δ8.14), is due to unco-ordinated IMP and the other set, (δ9.13 and δ8.06), to a reaction product having a 1:1 Pt : IMP stoichiometry. There is no evidence of N(1) co-ordination, i.e. no significant shift of H(2). Therefore the product is tentatively assigned as the aquo species, *cis*-$[Pt(NH_3)_2(IMP)(H_2O)]^{2+}$.

2:3iii The interaction between $Pt(NH_3)_2$(CBDCA) and inosine

An equimolar solution (r = 1) of $Pt(NH_3)_2$(CBDCA) and inosine, after five days of reaction at room temperature, exhibited a large concentration of the intermediate species, with H(8) and H(2) at δ8.73 and δ8.28 respectively. In this case, resonances due to

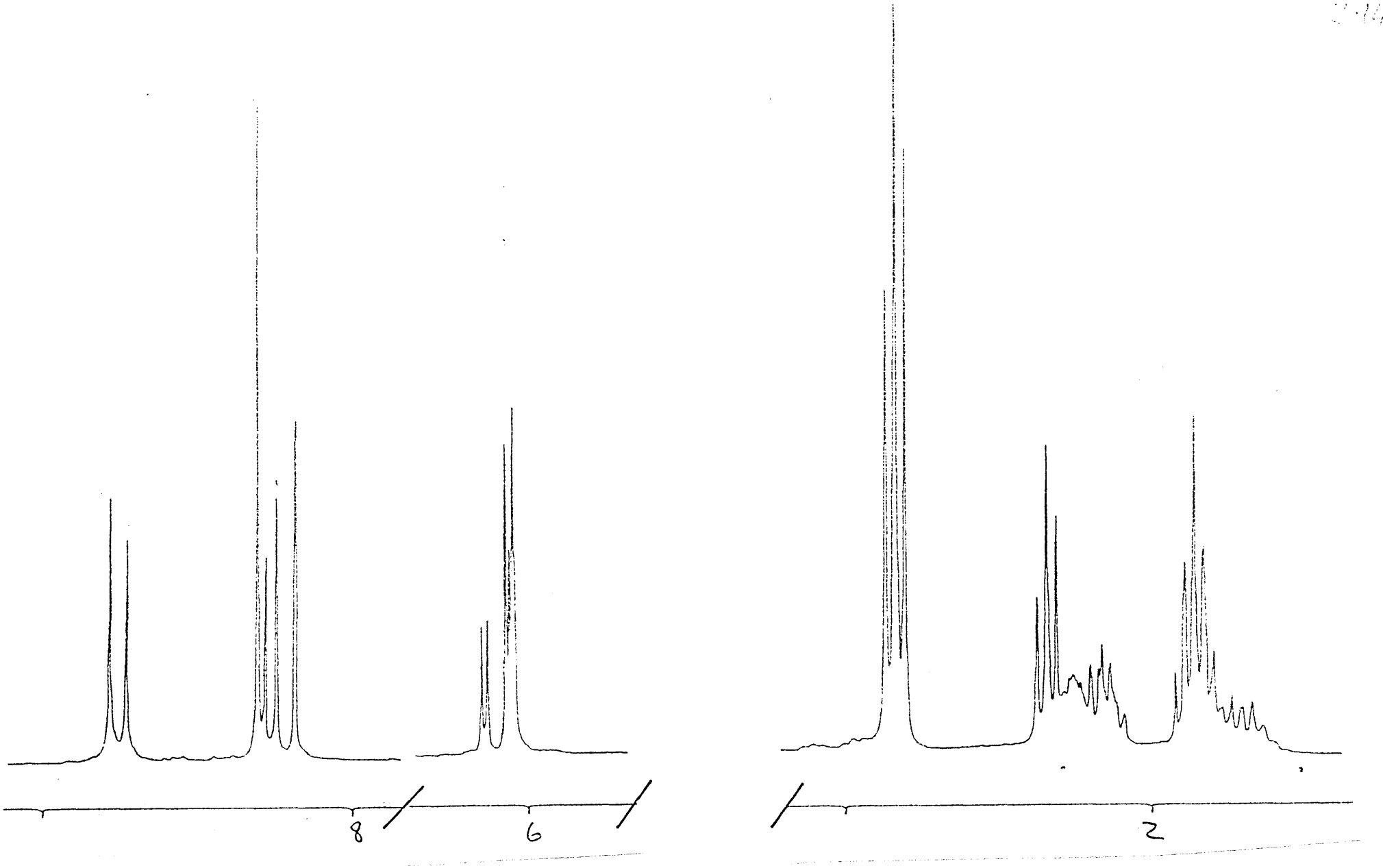


Figure 2.14: ^{1}H NMR of $Pt(NH_3)_2$(CBDCA) and inosine (1:1, day 5).

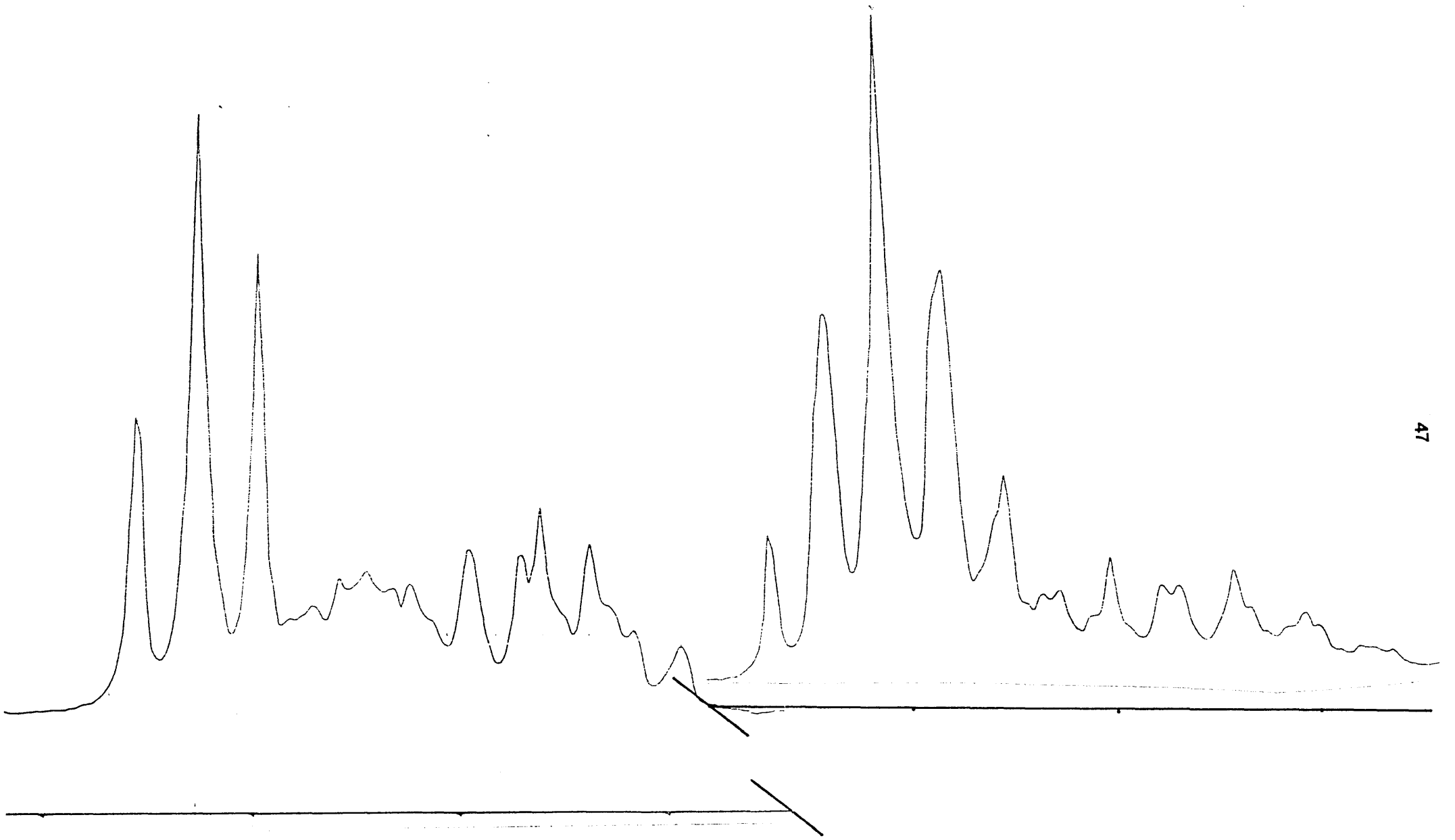


Figure 2.14b: Expansion of alkyl region on figure 2.14 showing intermediate resonance.

the CBDCA moiety which were not due to free or chelated acid were observed (Figure 2.14). The C_3-H resonances are centred at δ2.16 as a complex splitting pattern consisting of at least six peaks. Also, the corresponding C_4-H resonances are detectable on the upfield side of the free/chelated position at δ1.73. Interestingly the H(1') resonances of the ribose sugar unit are centred 0.1ppm downfield from the free/product position.

After twelve days, the reaction mixture had reached an equilibrium position. There were no further changes in the relative intensities of the species present, even after twenty days at room temperature. At the day twelve stage there were two sets of H(8) and H(2) resonances due to the reaction product and inosine in a ratio of 3:1 respectively (δ8.78, δ8.24 and δ8.30, δ8.19). The CBDCA resonances were also in a 3:1 ratio corresponding to free and chelated acid respectively. This implies that the reaction product must contain one inosine per $Pt(NH_3)_2$ unit. A polymeric product involving bridging via N(1)-N(7) can be discounted as there is only a small shift in the H(2) resonance. The product must be a hydrolysed species analogous to the $Pt(NH_3)_2$(ETMAL) case.

Separation of the intermediate by Sephadex chromatography was attempted. However, efficient separation of the intermediate from the reaction product was not achieved.

Investigation at r = 0.5 gave no further information as to the nature of the product. Again an equilibrium position between product, inosine, $Pt(NH_3)_2$(CBDCA) and CBDCA was reached after twelve days of reaction at room temperature. At intermediate times significant resonances due to the intermediate species were observed.

The observation of intermediate resonances associated with CBDCA supports the formulation of the intermediate as a complex involving monodentate acid of the form $[Pt(NH_3)_2(inosine)(CBDCA)]^{x-}$.

2:3iv The interaction between $Pt(NH_3)_2(CBDCA)$ and IMP, r = 1

A solution of $Pt(NH_3)_2(CBDCA)$ and IMP (r = 1), when left at room temperature, followed an analogous reaction course as that involving inosine. However, at no stage was there a comparably high concentration of the intermediate species. On days 2 to 9 it was observed at δ8.98 and δ8.23 corresponding to H(8) and H(2) respectively. Again resonances attributable to monodentate acid were observed.

On day 11 an equilibrium had been reached with resonances due to product : inosine and $Pt(NH_3)_2(CBDCA)$:$CBDCAH_2$ in an intensity ratio of 3:1. The product of the reaction is hence assigned as a hydrolysed species such as $Pt(NH_3)_2(IMP)(H_2O)$.

No further information was obtained using a solution with r = 0.5 apart from substantiation of the results obtained when r = 1.

2:4 Adenosine 5'-monophosphate, AMP and adenosine, A

The only reactions of platinum metal complexes with adenosine 5'-monophosphate, AMP or adenosine, A, that are well documented [36,48] in the literature are those with [Pt(dien)Cl]Cl or its palladium counterpart [Pd(dien)Cl]Cl and their aquated forms.

The pK_A of N(1) [48] of AMP 4.05, and A, 3.89, are orders of magnitude lower than those found for IMP or GMP. Hence, above pH 5 the N(1) site will be deprotonated and is a viable alternative metal co-ordination site to N(7). In DNA the N(1) position is involved in Watson-Crick base pairing with thymine and would not normally be accessible to metal binding. Indeed a ^1H NMR study [49] of the interaction of *cis*-$Pt(II)_{aq}$ with the dinucleotide adenyl-3',5' - adenosine indicated that the main product was co-ordinated to the adenine rings via N(7).

The pioneering work of Kong and Theophanides [36], who studied by ^1H NMR the effect of adding $Pt(dien)^{2+}$ to a solution of AMP, indicated that N(7) was the slightly preferred co-ordination site. The final product on addition of an excess of $Pt(dien)^{2+}$ was an N(1)-N(7) bridging adenine ring between two platinum atoms. The ^1H NMR chemical shifts for the complexes are summarised in Table 2.10.

In an equimolar solution of $Pd(dien)^{2+}$ and AMP at pH 7 Scheller *et al* [48] found that there was an almost equal proportion of N(1) or N(7) complexed AMP accounting for about 70% of the total $Pd(dien)^{2+}$ present.

Only 15% of AMP was co-ordinated at both the N(1) and N(7) positions to form a bridge between two palladium centres.

In a previous communication Lim and Martin [50] reported that $Pt(dien)^{2+}$ is more likely to co-ordinate to the N(7) site rather than the N(1) position of adenosine than is $Pd(dien)^{2+}$.

When a ^1H NMR spectrum of an equimolar solution of $Pd(en)^{2+}$ and AMP at pH 3.5 was compared to one of AMP at pH 5 the H(8) resonance was found [43] to be shifted downfield by 1.06ppm and the H(2) resonance by 0.29ppm. The authors suggested that these

shifts were due to co-ordination at both the N(7) and N(1) sites. At pH 3.5 the N(1) site would be protonated (pK_A = 3.8) and would not be a viable co-ordination site. The shift in H(2) may be explained by protonation of the N(1) site which the authors found [43] caused a downfield shift of some 0.23ppm. The data are consistent with co-ordination at N(7) only. On titration of the solution with one equivalent of base the ^1H NMR showed only weak resonances. The base removed the proton at N(1), not from the phosphate group as claimed, and an N(7)-N(1) bridged polymeric species was formed which is in agreement with the NMR study.

The only reported crystal structure [51] is of trichloro(9-methyladeninium)platinum(II). Platinum is coordinated to the N(7) position and the Pt-N(7) bond length is 2.015Å. The co-ordination geometry around the platinum is a slightly distorted square plane.

Table 2.10: H(8) and H(2) chemical shifts of platinum complexes of AMP or A

Complex	pD	H(8)	H(2)	Ref.
A	a	8.21	8.05	[49]
Pt(dien)-N(7)A	a	8.86	8.27	[49]
Pt(dien)-N(1)A	a	8.35	8.63	[63]
$[Pt(dien)]_2$(N(1),N(7)A)	a	8.94	8.75	[49]
AMP	b	8.56	8.21	
Pd(dien)-N(7)AMP	b	9.25	8.25	[36]
Pd(dien)-N(1)AMP	b	8.59	8.58	[36]
$Pd(dien)_2$-(N(1)N(7)AMP)	b	9.33	8.72	[36]
Pd(en)N(7)AMP N(1)H	b	9.56	8.52	[43]

a pH 5, N(1) deprotonated
b above pH ~ 7, N(1) and phosphate group deprotonated

2:4i The interaction of $Pt(NH_3)_2$(ETMAL) with AMP

The reaction of $Pt(NH_3)_2$(ETMAL) and AMP (r = 1) was followed by ^1H NMR at 250MHz. After six days at room temperature the resonances due to the ethylmalonate moiety were indicative of a mixture of species corresponding to 70% free acid and 30% chelated acid. At the same time, the resonances due to the AMP moiety corresponded to 30% free AMP and 70% complexed AMP. Hence it is considered that the reaction product contains one AMP per $Pt(NH_3)_2$ unit.

The resonances of the product of the reaction are unusual. There are three low field resonances in the H(8)/H(2) region in an integral ratio of 2:1:1. The largest peak occurs at δ8.07 and is assigned to H(2), as it is 0.03ppm upfield from the free AMP position. Typically coordination at N(1) results in a downfield shift of the H(2) resonance of at least 0.5ppm (cf. Table 2.10). Therefore in this case coordination at N(1) can be ruled out. The two resonances of equal intensity, δ9.63 and δ9.49, are both assigned to H(8) of the product. The downfield shifts of the H(8) resonances, Δδ -1.06 and -0.92ppm are consistent with co-ordination of platinum at the N(7) site. Also there are two distinguishable doublets due to H(1') of the sugar. To summarise, there are two forms of the product, which occur in equal intensity, giving rise to separate sets of H(8), H(2) and H(1') resonances. (The H(2) resonances are, by chance, coincident).

In the intermediate species formed with GMP or IMP, doubling of the H(8) resonances was noted. The same explanation for the doubling of the product resonances may also apply in this case.

In these cases two, or more, conformational diastereoisomers may be produced [52,53] with the platinum atom as the chiral centre. Conversion between the conformations is slow, compared to the NMR time scale, and two sets of resonances are therefore resolved. This slow conversion could be due to stereochemical interactions but is more likely due to H-bonding of an intramolecular nature possibly involving the phosphate group of the nucleotide.

At days one and three, resonances due to the intermediate species involving monodentate acid are observed. This is analogous to the situation with GMP, IMP and I. The monodentate acid resonances are centred at δ0.42, (methyl) and δ1.45 (methylene). The corresponding AMP resonances, indicating co-ordination via N(7), are at δ9.24 H(8) and δ8.21 H(2).

2:4ii The interaction of $Pt(NH_3)_2$ (CBDCA) with AMP

An aqueous solution of $Pt(NH_3)_2$(CBDCA) and AMP (r = 1) was allowed to react at room temperature for twelve days. The lowfield resonances were assigned to product only. As in the $Pt(NH_3)_2$(ETMAL) case, the same doubling of all resonances of the product were observed, viz: H(8) δ9.64 and δ9.50; H(2) δ8.13 and δ8.11; H(1') δ6.16 and δ6.07.

On intermediate days, resonances due to the species $[Pt(NH_3)_2(CBDCA)(AMP)]^{x-}$ were observed, viz: H(8) δ9.27 and H(2) δ8.27.

2:5 Conclusions

The $Pt(NH_3)_2(DCA)$ complexes on interaction with purine components of nucleic acids produce significant amounts of an intermediate species containing monodentate acid.

The formation of such intermediate species raises interesting questions regarding the initial anchoring of $Pt(NH_3)_2(DCA)$ to DNA.

In recent literature (cf. Chapter 1) it is now generally accepted that in the case of *cis*-Pt(II) an intrastrand interaction with DNA is responsible for its cytotoxic action.

The initial interaction, or anchoring, of *cis*-$Pt(II)_{aq}$ at N(7) of a guanine base could be stabilised by H-bonding of the water/hydroxy group to O(6). This was first proposed by Goodgame *et al.* During DNA synthesis involving single strands of DNA, the water/hydroxy site would then be replaced to give a bis-guanine intrastrand complex.

The results obtained for the two $Pt(NH_3)_2(DCA)$ complexes studied in this work suggest that both behave in essentially the same way. Unlike *cis*-Pt(II) the DCA complexes are not readily hydrolysed. Hence, it is considered that the $Pt(NH_3)_2(DCA)$ complex is itself interacting with DNA. The initial reaction at N(7) of guanine produces the intermediate species involving monodentate acid. The free end of the acid can then H-bond with the many available sites thereby stabilising the initial anchoring of the platinum complex to DNA. During cell replication the formation of single stranded regions of DNA would permit the replacement of the dicarboxylate group by a neighbouring N(7) to give a bis-guanine intra-strand complex.

CHAPTER THREE

STUDIES OF INTERACTIONS OF CIS-Pt(II) WITH DRUGS USED IN COMBINATION CHEMOTHERAPY

3:1 Introduction

Due to the different spectrum of toxicity of *cis*-Pt(II), particularly its minor toxicity to bone marrow cells - a feature rare in the cytotoxic drugs so far produced for cancer treatment, there have been many drug combinations screened using *cis*-Pt(II) as one of the components. A further condition required by the clinicians for such drug combinations is that the therapeutic benefit must at least be additive. In many cases a synergic effect was observed.

The most potent cytotoxic combinations have been used for the treatment of testicular and ovarian cancers, with very good results [4].

In such drug combinations there is the possibility that *cis*-Pt(II) might react readily with one, or more, of the drugs used in combination with it, and thus alter the amounts of each component available for drug action, or even produce new species with different therapeutic or toxic properties. The interaction bewteen separately injected drugs has, in fact, been demonstrated [54] by the inhibition of the activity of *cis*-Pt(II) by L-methionine or thiourea against leukemia L1210 in mice. Accordingly we have studied the interactions of *cis*-Pt(II) with some of the more commonly used components of these regimes - cytosine arabinoside

(araC), 5-fluorouracil (5-FU), cyclophosphamide and bleomycin (BLM).

Before discussing the results of this work it is desirable to summarize the main features of cell replication.

The molecular level of DNA replication has been very well reviewed in Davidson's book [16] and will not be covered here. However, the cell cycle and the relevance of the phases of the cycle where drugs have their lethal effects will be discussed.

3:2 The Cell Cycle

The cell cycle is the term used to describe the period between one mitosis and the next in one or both daughter cells. It is characterized by a sequence of events that has been grouped into four classic phases:

1. G1, the period between mitosis and the onset of DNA synthesis.
2. S, the period of DNA synthesis.
3. G2, the period between completion of DNA synthesis and mitosis.
4. M, mitosis itself.

Antitumour drugs exert their most lethal effects at particular stages of the cell cycle [55]. Those involving drugs studied in this work are shown in Figure 3.1.

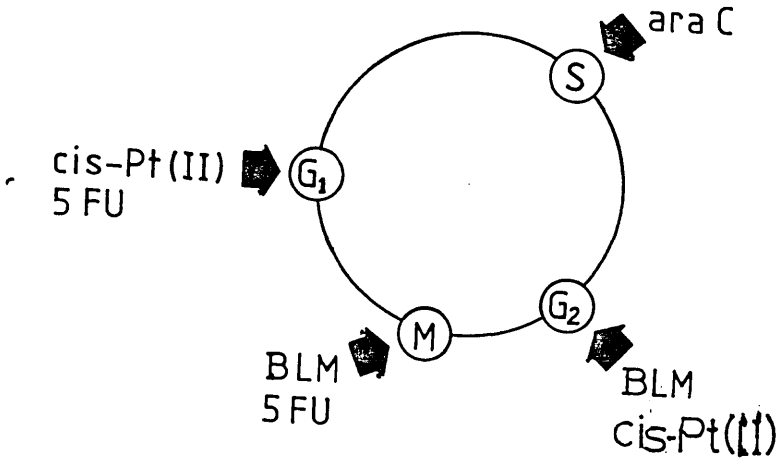


Fig. 3.1: The phases of the cell cycle where anti-tumour drugs exert their lethal effects (from ref.55)(No data available for cyclophosphamide)

Cis-Pt(II) appears to attack in the G1 and G2 phases, which would agree with its modus operandi outlined in Chapter 1. The drugs used in combination with *cis*-Pt(II) have their lethal activity in different cell stages. With 5-fluorouracil and bleomycin, one of their active cycles corresponds to *cis*-Pt(II), but their alternative stage does not.

To obtain a lethal, synergic, cytotoxic combination (that is a drug combination which has a therapeutic benefit greater than the expected additive effect of the components) it may be necessary to use drugs which not only have different toxic side effects but also exhibit their lethal activity at different stages of the cell cycle.

In each of the following sections the interaction of *cis*-Pt(II) with the drugs shown in Figure 3.1 will be discussed.

3:3 Cytosine Arabinoside (araC)

Cytosine arabinoside is a nucleoside antimetabolite with potent antileukaemic and antiviral activity.

Initial studies of the reaction of an aqueous solution of araC with *cis*-$Pt(II)_{aq}$, as followed by ^1H NMR spectroscopy, showed that even after only 30 minutes at room temperature a new species was produced. However after 24 hours at room temperature the initially colourless solution had turned dark blue. The ^1H NMR of the dark blue solution was very poorly resolved. This was attributed to the presence of paramagnetic partially oxidised Pt species forming the blue colour. From this solution a dark blue powder was isolated but this was found not to be of reproducible analytical composition a notorious feature of the platinum blues.

Niedle *et al* [56] have determined the crystal structure of the product of the aqueous reaction of $PtenCl_2$ with araC. In the colourless, long thin needles of the product, [Pt(en)(araC)Cl]Cl coordination of the Pt was found to be via N3 of the cytosine ring.

The limited information available from interpretation of the ^1H NMR of the dark blue solution would be consistent with coordination of the *cis*-$Pt(NH_3)_2^{2+}$ moiety at the N(3) position of cytosine.

In order to obtain further information on the site of coordination and the possibility of forming a new, active platinum antitumour agent the reaction of K_2PtCl_4 with araC was investigated.

The reaction of an equimolar aqueous solution of K_2PtCl_4 and araC was followed by ^1H NMR. Again a dark blue solution was formed. A marked decrease in pH on addition of the K_2PtCl_4 as the dark blue colouration of the solution developed was observed. An analogous reaction of K_2PtCl_4 with cytidine has recently been reported [57].

X-band epr studies on the blue solutions gave spectra similar to those reported by Lippert [58] for a platinum uracil blue.

Chromatographic separation (alumina column) of the components present in the blue solution typically yielded three fractions: (1) yellow, (2) green, and (3) dark blue. The yellow fraction gave no epr signal. The green component was evidently an incompletely converted species as it turned blue on further storage. The epr spectrum of the purified blue fraction was cleaner than the original reaction product and had g_{eff} values of 2.34 and 2.08 (cf. ~ 2.40 and 1.99 for the uracil blue). The epr spectra of the blue and 'purified' blue are shown in Figure 3.2.

Due to the complex polymeric nature of the platinum blues no further study of these araC systems was undertaken. The blues are an antitumour class [59] of their own.

In the case of *cis*-Pt(II)/araC drug combinations it may be the blue complex formed which is reponsible for all, or part, of the effective cytotoxic activity. It would, however, be difficult to obtain firm evidence for the formation of such a species in vivo, though the chemical studies reported here raise it as a possibility.

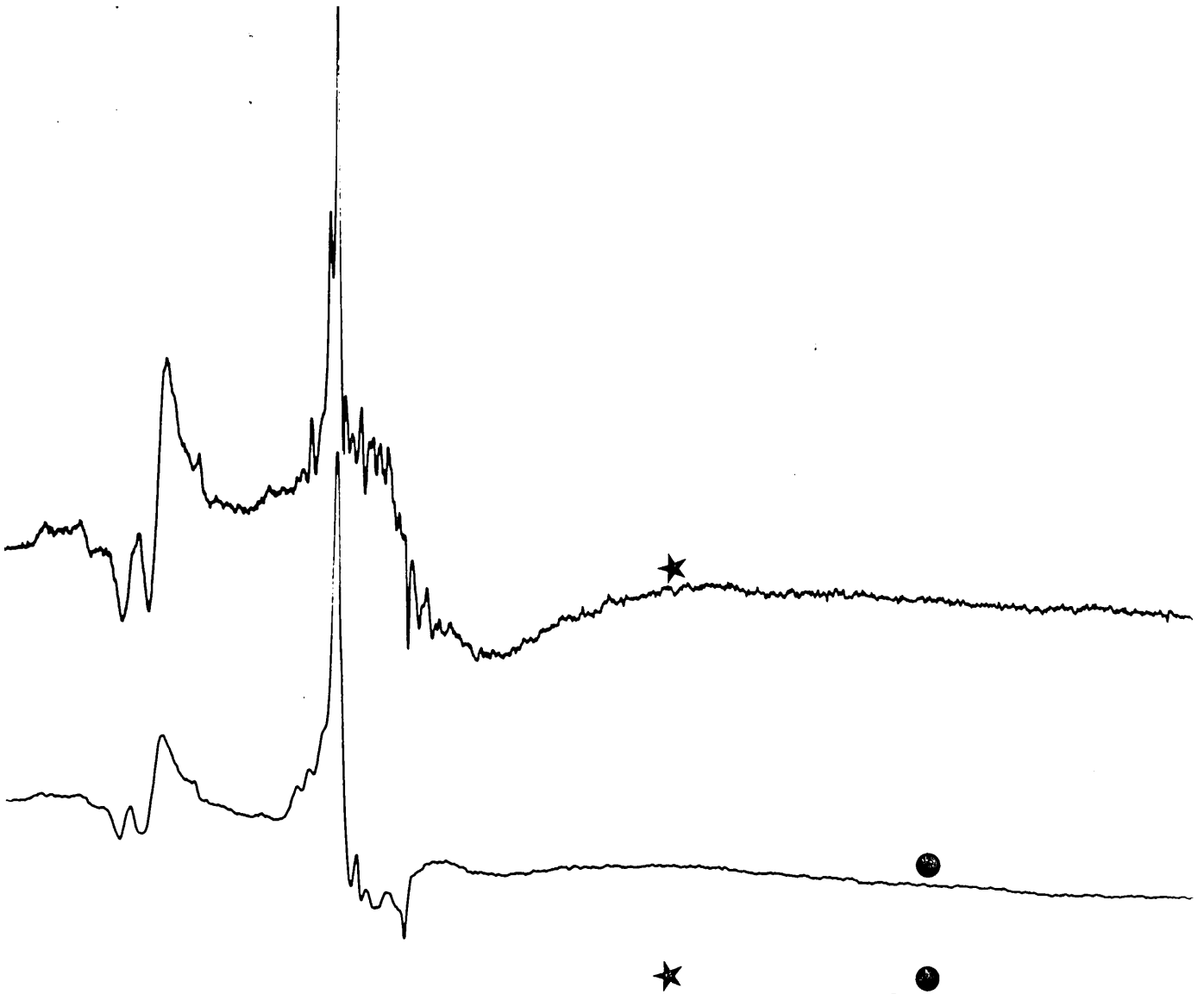


Fig. 3.2: The epr spectra of Pt-araC blue and "purified" blue.

3:4 5-Fluorouracil (5-FU)

5-Fluorouracil is a base antimetabolite.

An equimolar aqueous solution of 5-fluorouracil and *cis*-$Pt(II)_{aq}$, when incubated for two days at 37-40°C in the dark, gave a dark blue solution. A similar reaction has been observed previously by Davidson *et al* [59]. On evaporation of the dark blue solution a blue powder was precipitated. However, analytical results for the blue powders were variable; e.g. Found: C, 12.65; H, 2.26; N, 14.75% and, for a similar preparation, Found: C, 13.05; H, 2.36; N, 15.09%.

The X-band epr spectrum of a frozen aqueous solution of the blue species exhibited g_{eff} values of 2.22 and 2.08 and was similar to that obtained for the cytosine arabinoside blue and the spectrum reported by Lippert [58] for a uracil blue. In the ^1H NMR of the 5-FU-blue solution there were no detectable resonances.

Due to the complex polymeric nature of the blues no further investigation was carried out.

In the combination chemotherapy regimes of *cis*-Pt(II) and 5-fluorouracil the antitumour activity may in part be due to the formation of the 5-FU-blue.

3:5 Cyclophosphamide

Cyclophosphamide is an alkylating agent. Work with this drug was disappointing. ^1H NMR studies showed no evidence for interactions between cyclophosphamide and *cis*-Pt(II), *cis*-$Pt(II)_{aq}$ or K_2PtCl_4 at room temperature or at elevated temperatures.

3:6 Bleomycin

3:6i Introduction

The bleomycins are a family of glycopeptide antibiotics which differ only in their terminal functional groups. They are active against several neoplasia in man. In particular, they have been used in conjunction with *cis*-Pt(II) in the treatment of testicular cancers [60]. When *cis*-Pt(II) is used in combination therapy with bleomycin, in some cases a synergic effect has been observed [61,62].

This section will discuss the interaction of *cis*-Pt(II) with bleomycin (BLM) as followed by ^{13}C NMR spectroscopy. The results of related studies of $Pt(NH_3)_2$(ETMAL) will also be presented.

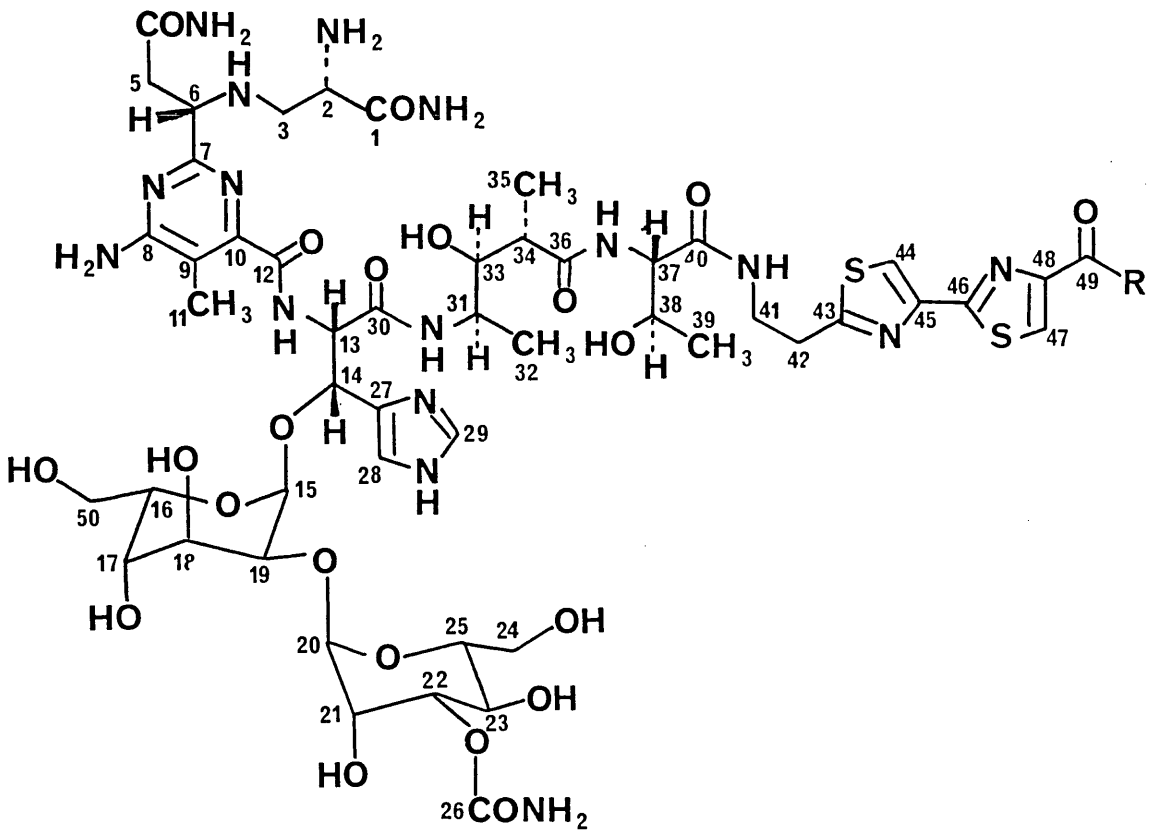
In all cases in this work the commercially available mixture of bleomycin, "Blenoxane" was used. The Bristol-Myers preparation "Blenoxane", now referred to as BLN, contains 55-70% of BLM-A_2 and 25-32% of BLM-B_2 (Figure 3.3).

Separation of the components was not carried out so as to make the studies of the Pt-BLN interactions as close to the clinical conditions as possible.

First the main feature of the co-ordination chemistry of BLM will be discussed, followed by its in vivo mechanism of action and then the data obtained in this work will be analysed.

The co-ordination chemistry of BLM has been the subject of a recent review [63]. Only the more important biological metals, iron and copper, will be discussed. However complexes of BLM with a wide range of transition metals are known [63].

The crystal structure of the biosynthetic intermediate, P-3A cupric complex has been determined [64] (Figure 3.4).



R = $NH(CH_2)_3S^+(CH_3)_2$ Bleomycin A_2, BLM A_2

R = $NH(CH_2)_4NHC(NH)NH_2$ Bleomycin B_2, BLM B_2

Fig. 3.3: The structure of bleomycin

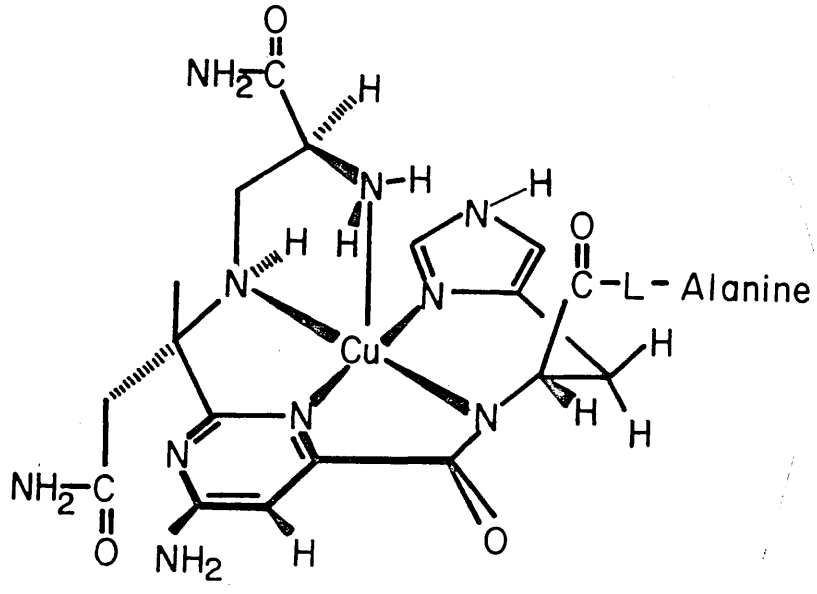


Fig. 3.4: The structure of Cu(II)(P-3A)[64]

Although P-3A differs from bleomycin in having no sugar or bithiazole functions, epr and related studies suggest that this structure is comparable with the suspected copper(II) co-ordination site of bleomycin itself [63].

In the biological function of bleomycin it is thought that the cupric complex is involved in the transportation of BLM in the body [60].

A portion, or all, of the injected bleomycin binds to cupric ion in the blood. After penetration into cells, BLM-Cu(II) complex is reduced by sulfhydryl compounds to the cuprous complex. Then further interaction with a cuprous ion-binding protein leaves the bleomycin in the native metal-free state.

Bleomycin may then intercalate [65] with DNA with the bithiazole rings slotted between the planes of the two base pairs.

However, it is considered that for the necessary activity iron is bound to bleomycin, in the now vacant copper site, in a haemoglobin type structure, with O_2 occupying the free iron co-ordination site (Figure 3.5)

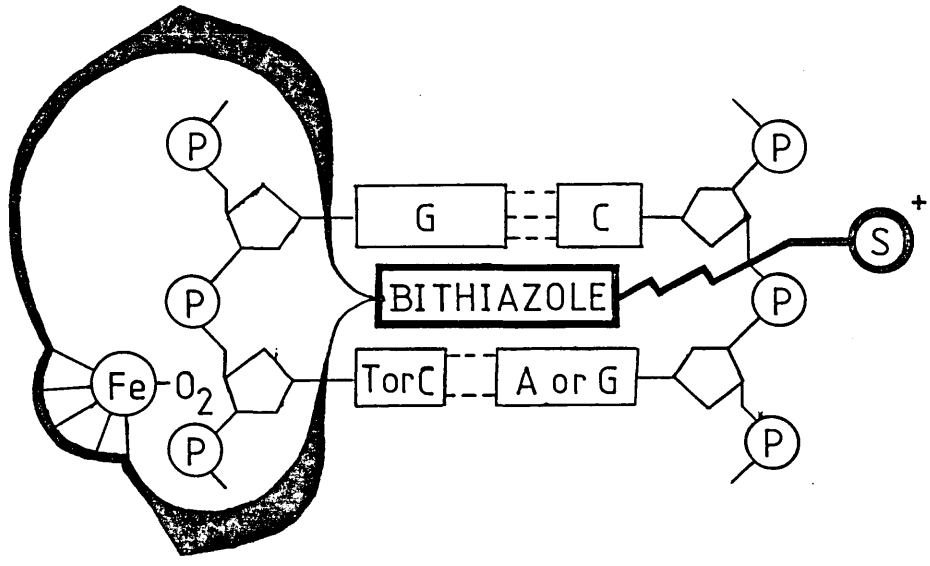


Fig. 3.5: Model for the complex of bleomycin, DNA, Fe^{2+}, and O_2 [65].

A single electron transfer from iron to oxygen occurs to give the Fe(III)BLM-O_2^- species. This exists in two low spin forms and one high spin form, and it is one of the low spin forms which is the active form of BLM [66,67]. This active BLM produces Fe(III)-BLM and $O_2^{\cdot}$ radicals. It is these radicals which cause strand scission of DNA by abstraction of the C'-4 proton of the deoxyribose unit, leading to C_3-C_4 bond cleavage [68]. The Fe(III)-BLM is reduced to Fe(II)-BLM by thiols in the cell, e.g. glutathione, and the cycle continues (Figure 3.6). This explains why only a

small amount of BLM is taken up by the cells [69,70,71].

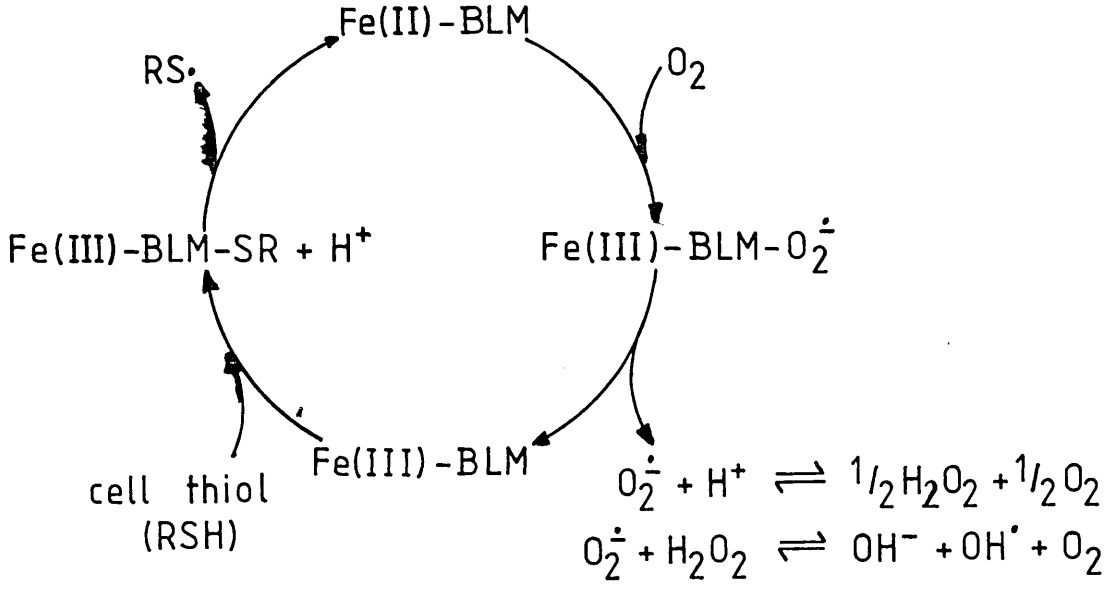


Fig. 3.6: Catalytic cycle of Fe-BLM

Hence the Fe-BLM complex is involved in a redox cycle which generates radicals and degrades DNA molecules. In Fe(II)-BLM and Fe(III)-BLM the iron is thought to occupy a similar site [63] to that of the copper in the crystal structure of the Cu(II)P-3A) compound (Figure 3.4).

As the action of BLM requires the participation of copper and iron, it is relevant to assess the influence platinum may have on the binding sites when BLM and platinum anti-cancer drugs are used in combination. Indeed, Leh and Wolf[72] have used radio-labelled platinum to bind the bleomycin. They observed that the platinated bleomycins localised in tumours and were stable in vivo for up to 48 hours. No details were reported concerning the site

of platinum interaction with BLM.

The following sections will discuss the results found in this work of the interaction of blenoxane with *cis*$Pt(II)_{aq}$, $Pt(NH_3)_2$(ETMAL) and K_2PtCl_4 as followed by ^{13}C NMR spectroscopy.

3:6ii The interaction of blenoxane and *cis*-$Pt(II)_{aq}$

Initially a ^1H NMR study of the system was made. The 90MHz ^1H NMR spectrum of blenoxane was obtained in D_2O. To this colourless solution one equivalent of *cis*-$Pt(II)_{aq}$ was added which caused the solution to become pale yellow. The ^1H NMR spectrum of this yellow solution was obtained as soon as possible after mixing. It was found that the spectra were too complicated for unambiguous analysis. However, it was evident from the spectra and taking into account the production of a yellow solution that an immediate reaction had taken place but the donor sites involved could not be readily identified.

Hence it was decided to investigate the interaction by ^{13}C NMR. The ^{13}C NMR spectrum of blenoxane was obtained as a solution of 0.3mM in 2.5ml of D_2O. The resonance were assigned by reference to results obtained by Dabrowiak *et al* [73]. The same carbon atom numbering system was employed (Figure 3.3). The chemical shift values obtained are listed in Table 3.1, and compared to those reported by Dabrowiak *et al* [73]. In general they are in good agreement. The most significant differences are in the carbon atoms making up the imidazole ring. Carbon atom 27 is 2.21ppm upfield from the value quoted by Dabrowiak *et al*. However they also found

that C27 was significantly shifted from the work on which they based their assignments. The other two carbon atoms of the imidazole ring are also shifted, C28 is 0.52ppm downfield and C29 is 0.79ppm downfield. The differences can probably be explained by the different pH values and concentrations used.

Carbons 15 and 20 gave rise to a degenerate line in this work. Dabrowiak reported separate resonances 0.46ppm upfield and 0.24ppm downfield from the position (100.56ppm) found here. Carbon 24 is 0.45ppm downfield. These three carbons, 15, 20 and 24 are all part of the sugar residue. The differences found may be due to conformational effects due to the different concentrations employed.

Additional resonances were also found. However this is not surprising when comparing the ^{13}C NMR of bleomycin-H_2 with the commercial mixture of bleomycin - "Blenoxane". Two resonances downfield from the degenerate 54/55 peak at 28.10ppm and 28.48ppm were observed. Resonances close to C44, C48, C26 and C43 at 127.29ppm, 151.71ppm, 159.47ppm, 165.20ppm and 165.58ppm were also observed. All these resonances are of a lower intensity than the assigned BLM-A_2 peaks. They are due to the other constituents of Blenoxane which differ only in the side chain R (Figure 3.3).

To this solution of blenoxane in D_2O was added successive amounts of *cis*-$Pt(II)_{aq}$ and at each stage of addition the ^{13}C NMR spectrum was measured and analysed. This strategy was employed to facilitate analysis of the resulting spectra by looking for the growth of new resonances as the additions progressed. Because of the complexity of the spectra the results will be analysed region by region and then they will be discussed in terms of regions of the structure of bleomycin.

Region 1: 0-30ppm

There are six main resonances in this region (Figure 3.7) attributable to carbons 11, 32, 35, 39, 52 and a degenerate line due to 54 and 55. There is also a low intensity doublet due to one of the other constituents of blenoxane apart from BLM-A_2. At the *cis*-$Pt(II)_{aq}$ to BLN ratios, r = 0.3 and 0.5 resonances due to carbons 54, 55, 52 and 39 were not affected. Resonance 35 was broadened and shifted downfield by about 0.2ppm at the r = 0.3 stage. On further addition of *cis*-$Pt(II)_{aq}$, when r = 0.5, peak 35 was further broadened and shifted downfield by 0.3ppm.

When r = 0.1, 0.3, and 0.5, a new resonance, assigned to carbon 11 of Pt-BLN complex, was observed at 10.8ppm, a shift upfield of some 2.6ppm compared to the position of C11 of free BLN.

At the r = 0.5 stage, resonance 32 was shifted upfield by some 0.8ppm and considerably broadened.

The doublet at the low field side of resonance 54/55 was not affected by addition of *cis*-$Pt(II)_{aq}$.

Region 2: 30-60ppm

In this region (Figure 3.8), there are ten separate resonances each assigned to a single carbon.

The spectrum with r = 0.1 was the same as BLN itself, apart from one low intensity resonance at 32.82ppm, which was not observed when r = 0.3 and 4 = 0.5.

Resonances 42, 53, 41 and 51 were not affected by addition of *cis*-$Pt(II)_{aq}$. Resonances 5 and 6 were lost by the r = 0.5 stage

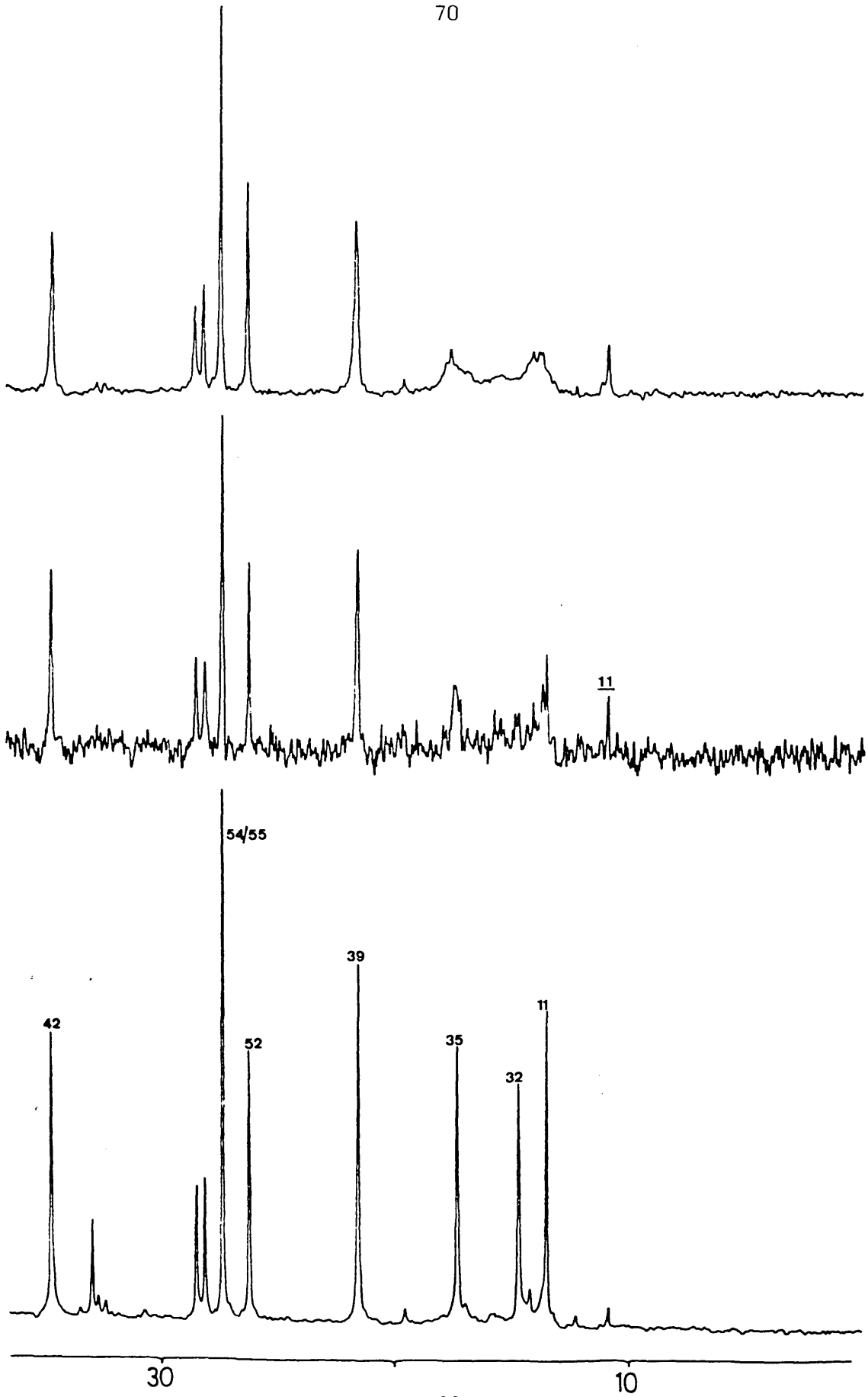


Fig. 3.7: Region 1 (0-30 ppm). ^{13}C-NMR spectra of cis Pt(II)aq interaction with blenoxane (r = 0.1, 0.3 and 0.5)

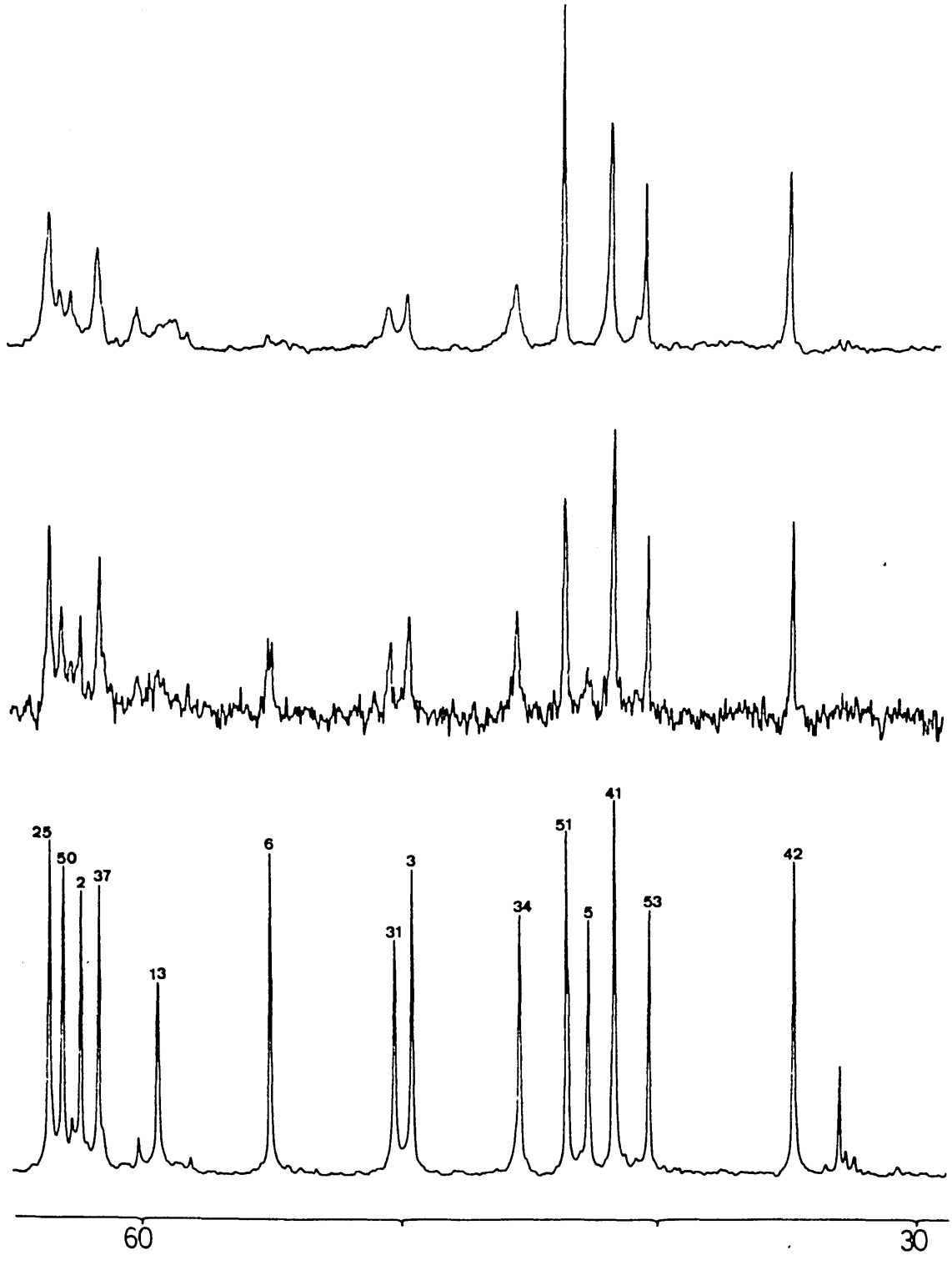


Fig. 3.8: Region 2 (30-60 ppm). ^{13}C-NMR spectra of cis Pt(II)aq. interaction with blenoxane (r = 0.1, 0.3 and 0.5).

but just detectable when r = 0.3. Resonances 3 and 31 were broadened and resonance 13 was so broad as to be nearly classified as "lost".

Region 3: 60-90ppm

In this region there are thirteen close resonances (Figure 3.9) with two assigned to two pairs of degenerate carbon atoms, 16/38 and 22/33. When r = 0.1 the spectrum was very similar to free BLN, apart from one of the degenerate lines 22/33 which was just split by 0.12ppm. There was also an additional resonance upfield from 14 at 70.05ppm.

Resonances 14, 18 and 24 appeared to be lost at the r = 0.5 stage. The remaining resonances 37, 2, 50, 25, 23, 16, 38, 21, 17, 19, 22 and 33 were all broadened, though to varying degrees, and they were not significantly shifted.

Region 4: 90-130ppm

In region four there are five resonances (Figure 3.10) assigned to six carbon atoms and a subsidiary resonance upfield from carbon 44 at 127.29ppm, due to one of the components of BLN apart from BLM-A_2. At the r = 0.1 stage the spectrum was similar to BLN apart from resonances 15/20 which were no longer degenerate.

Resonances 44 and 47 were not affected on addition of *cis*-$Pt(II)_{aq}$. Resonances 28, 15 and 20 were very strongly broadened, whilst resonance 9 was initially shifted by 2.9ppm upfield at the r = 0.3 stage and was then lost when r = 0.5.

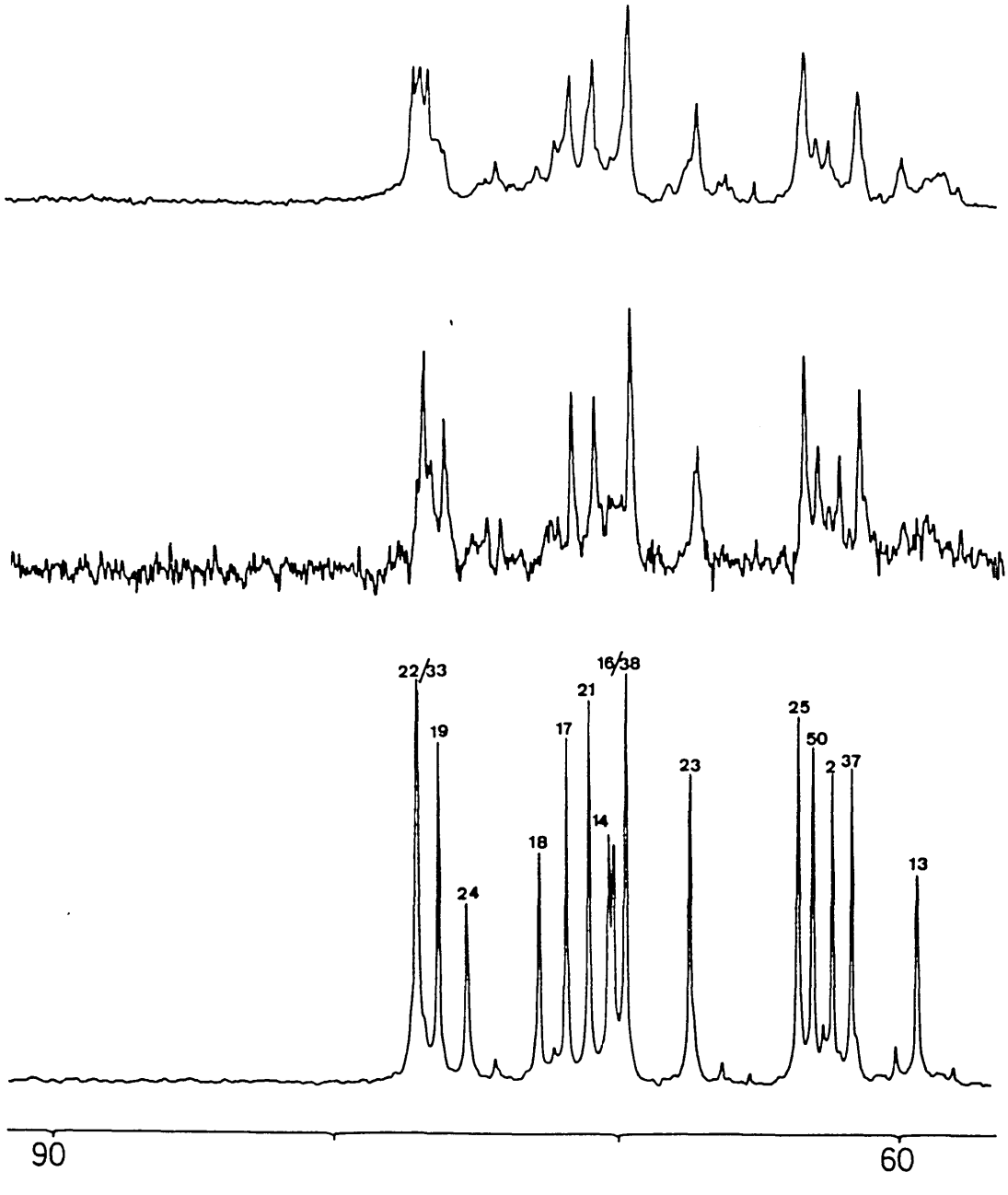


Fig. 3.9: Region 3 (60-90 ppm). ^{13}C-NMR spectra of cis Pt(II)aq interaction with blenoxane (r = 0.1, 0.3 and 0.5).

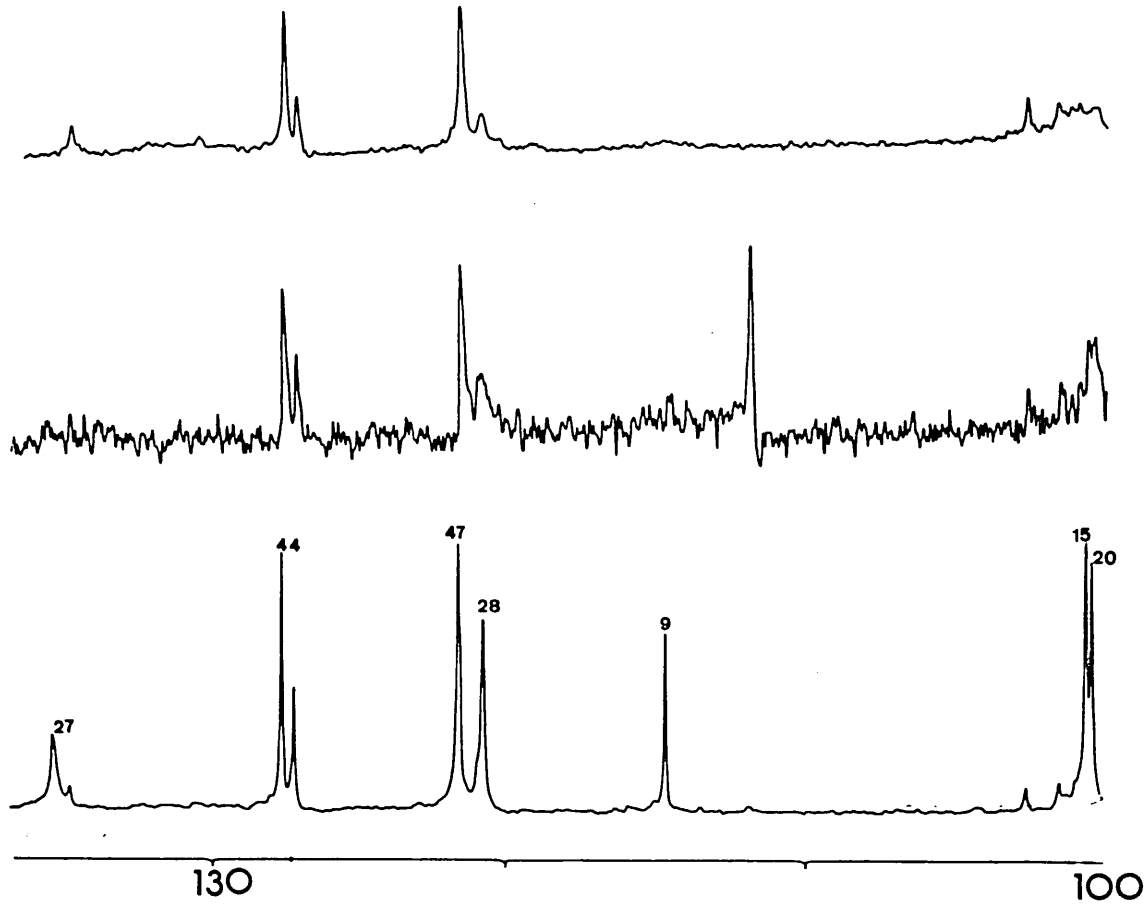


Fig. 3.10: Region 4 (90-130 ppm). ^{13}C-NMR spectra of cis Pt(II)aq interaction with blenoxane (r = 0.1, 0.3 and 0.5).

Region 5: 130-160ppm

In region five there are six resonances assigned to six carbon atoms (Figure 3.11). There are also two subsidiary resonances close to carbons 26 and 48 neither of which was affected by addition of *cis*-Pt(II)$_{aq}$. Resonances 45 and 48 were not effected. 27, 29 and 10 were lost and resonance 26 was considerably broadened.

Region 6: 160-180ppm

In region six (Figure 3.12) there are eleven closely spaced resonances. At the r = 0.1 stage the spectrum was very similar to BLN. However, addition of further *cis*-Pt(II)$_{aq}$ produced significant changes. Resonances 36, 40, 49, 46 and 43 were not significantly affected although they were slightly broadened to varying degrees. Resonances 30 and 12 were very broadened, nearly to the extent of being classified as "lost", whilst resonances 8, 7, 1 and 4 were, in fact, lost.

In view of the number of different factors that control ^{13}C NMR shifts it is difficult to assess unequivocally the precise site of metal binding in a drug of such complexity. Moreover, there is the possibility that Pt occupies more than one site. In Figure 3.13 are shown the lost resonances and the broadened resonances on bleomycin. It is immediately apparent that the bithiazole rings are not the site of platinum co-ordination. This is surprising due to the good sulphur donors present and the

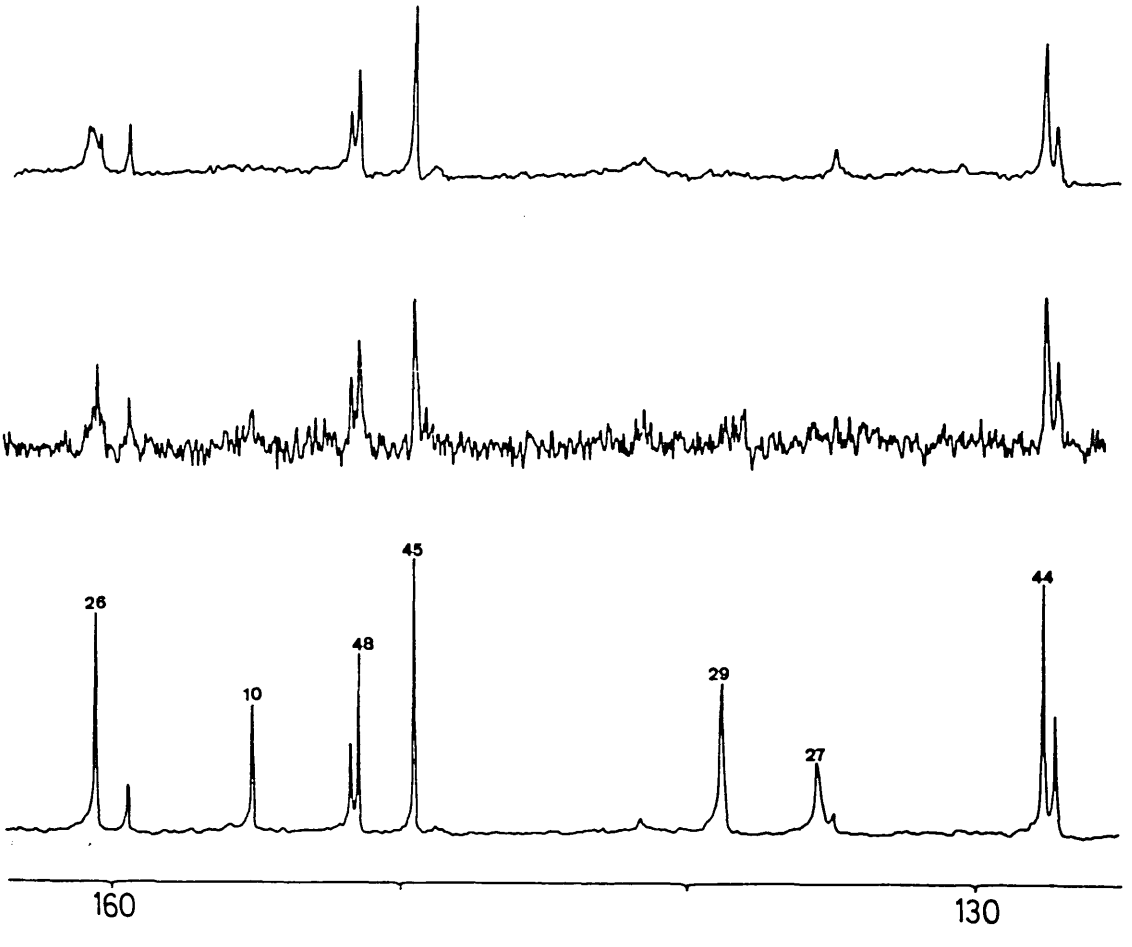


Fig. 3.11: Region 5 (130-160 ppm). ^{13}C-NMR spectra of cis Pt(II)aq interaction with blenoxane (r = 0.1, 0.3 and 0.5).

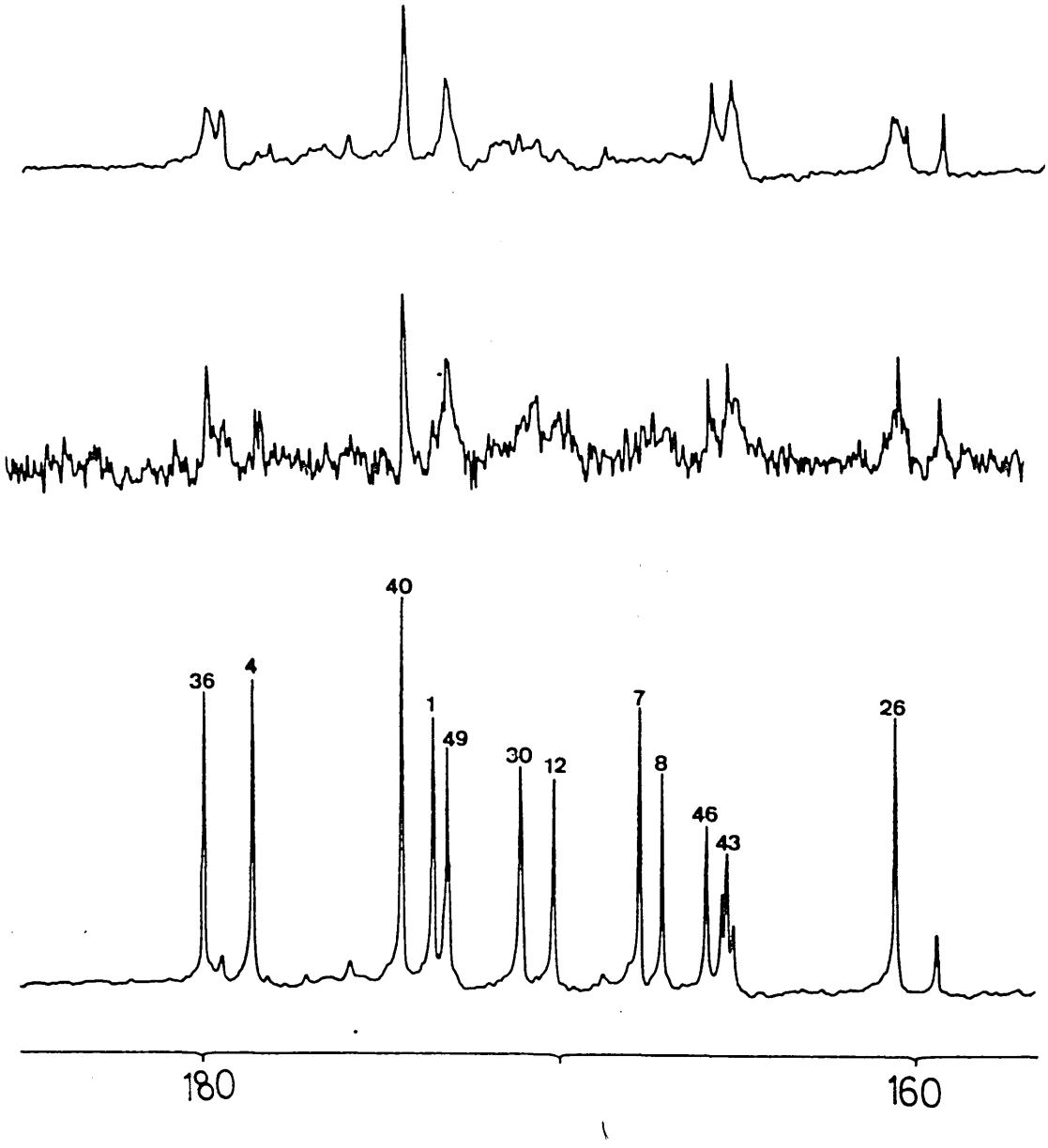


Fig. 3.12: Region 6 (160-180 ppm). ^{13}C-NMR spectra of cis Pt(II)aq interaction with blenoxane (r = 0.1, 0.3 and 0.5).

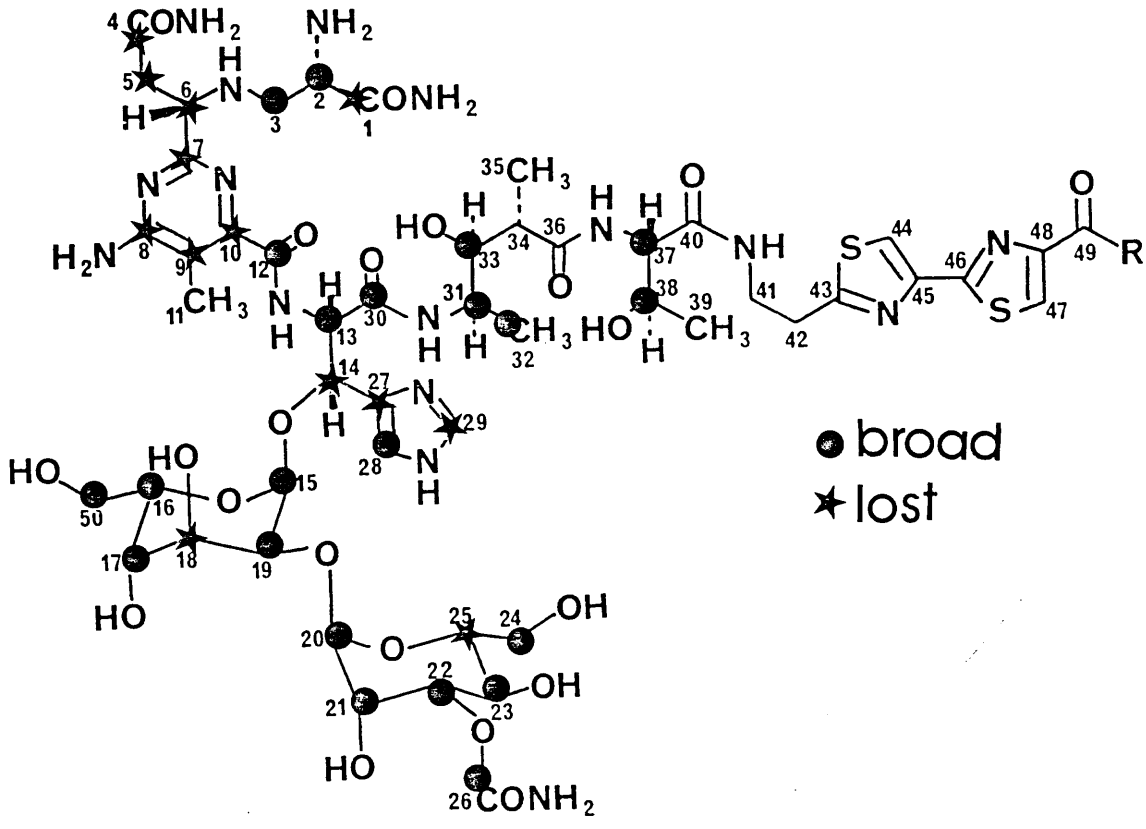


Fig. 3.13: Lost and broadened resonances on interaction with *cis*-Pt(II)$_{aq}$.

and the strong tendency of Pt to bind to sulphur ligands. In vivo the bithiazole rings intercalate between a pair of bases on DNA, so if Pt were binding to BNX after it had interacted with DNA, the bithiazole rings would be effectively screened from any attack by Pt. Conversely, the lack of Pt binding to the bithiazole means that Pt will not interfere with intercalation by that unit.

One of the prime sites for Pt binding appears to be the imidazole ring. Resonances due to carbons 27 and 29 were lost and resonance 28 was considerably broadened. The resonance of carbon 14, immediately adjacent to the ring was also lost. Another prime site for Pt binding appears to be the pyrimidine ring. Resonances due to C7, 8, 9 and 10 were lost completely, (even on addition of r = 0.3 of *cis*-$Pt(II)_{aq}$). Resonance 9 was shifted at r = 0.3 stage and then lost on further addition of Pt. Carbon atoms forming the peptide backbone i.e. C12, 13, 30, 31 and 32, in the vicinity of the imidazole and pyrimidine rings, were considerably broadened. All of the carbon atoms of the sugar resonances were also affected but to varying degrees. In fact C18 and 24 are classified as lost. Presumably the peptide backbone and sugar carbons are affected due to conformational changes, as opposed to actual co-ordination effects. A further possible site is the amide group adjacent to C1 and similarly C4. C1 is lost and the resonances due to the adjacent carbons, C2 and C3, were broadened while in the corresponding group in BNX C4, C5 and C6 are all lost.

To summarise from the data presented so far, the site(s) of *cis*-$Pt(II)_{aq}$ co-ordination on BNX are the pyrimidine ring nitrogen , the imidazole unit, both of the amide groups and possibly nitrogens forming the backbone of the drug.

On first consideration it is difficult to understand why some of the resonances are lost or broadened on addition of Pt. Results of this nature would be expected on introducing a paramagnetic metal. A possible explanation in this case, having ruled out a stray paramagnetic species based on NMR work presented in an early

chapter, is slow exchange. When r = 0.3 and r = 0.5 there are two or possibly more species of BNX present, metal free BNX and platinated BNX. These species are in slow exchange compared to the NMR time scale. This results in a broad or lost resonance on observation of the NMR spectrum. The rate of exchange between the species is dependent on such factors as pH and temperature.

At a much later date (due to machine malfunctions and other user demands) a ^{13}C NMR spectrum of a freshly prepared de-oxygenated solution at r = 1 was obtained. This is shown in Figures 3.14, 3.15 and 3.16, compared to that for BNX itself. In this case, sharp resonances were obtained with none of the broadening or lost effects previously found. The shifts found will be presented region by region as before and then discussed with reference to the r = 0.1 to 0.5 results.

Region 1: 0-30ppm

In region 1 (Figure 3.14) the only affected resonance is due to C35 which was split into two peaks of similar intensity with complexation shift values, $\Delta\delta$ of +0.21 and -0.56ppm. The other resonances in this region due to C11, 32, 35, 39, 52 and 54/55 all had $\Delta\delta$ values of 0.1ppm or less.

Region 2: 30-60ppm

In region 2 (Figure 3.14) only four of the ten resonances had a $\Delta\delta$ of 0.1ppm or less: they are C42, 53, 41 and 34. Resonances due to C3, 31 and 6 had $\Delta\delta$ values of 0.66, 2.94 and 1.40ppm

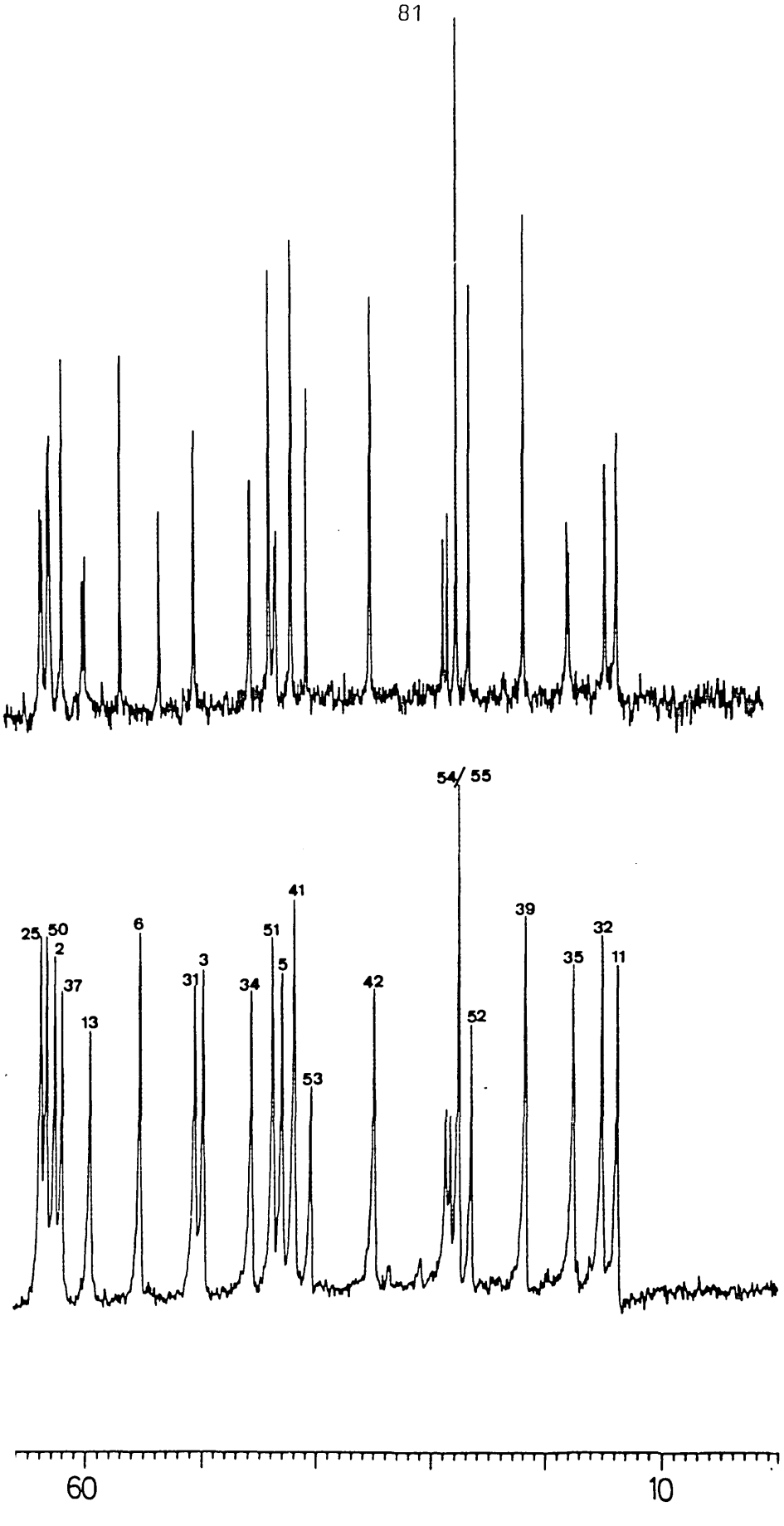


Fig. 3.14: Regions 1 and 2 (0-60 ppm). ^{13}C-NMR spectra of blenoxane and cis- Pt(II)aq. interaction with blenoxane, r = 1.

respectively. Resonances C5, 51 and 13 were split into two lines of about equal intensity with Δδ values of 0.31/0.45ppm, 0.03/0.13ppm and 0.41/0.69ppm respectively.

Region 3: 60-90ppm

In this region (Figure 3.15) the resonances are very close together and hence difficult to assign with absolute certainty. Of the fourteen carbon atoms, in the r = 1 case C37 and 25 had a Δδ value of less than 0.1ppm. C2 was split into two lines of about equal intensity with Δδ of 0.50 and 0.62 ppm. C50 was shifted upfield by 0.43ppm on complexation. Carbons 23, 16/38, 14, 17 and 24 had Δδ values of -0.17, 0.22, 0.41, 0.66 and 0.28ppm respectively. Carbon resonance 19 was split into two with Δδ +0.00 and -0.10ppm. The degenerate resonance 22/33 was split into two with the high field peak possessing about one quarter the intensity of the lowfield one, with Δδ +0.25 and -0.09ppm. Carbon 18 was split into two: Δδ 0.91 and 0.82ppm. Close to the C18 peaks were two resonances at δ72.67 and 73.14ppm which are not assigned. However it must be stressed that in region 3 unambiguous assignment is not possible due to the close proximity of the lines.

Region 4: 90-130ppm

In region 4 (Figure 3.15) there were no resonances which were not affected. C28, 47, 44 and 44* (* refers to resonances associated with BLM-B_2) had Δδ values of +0.22, -0.13, -0.13, and

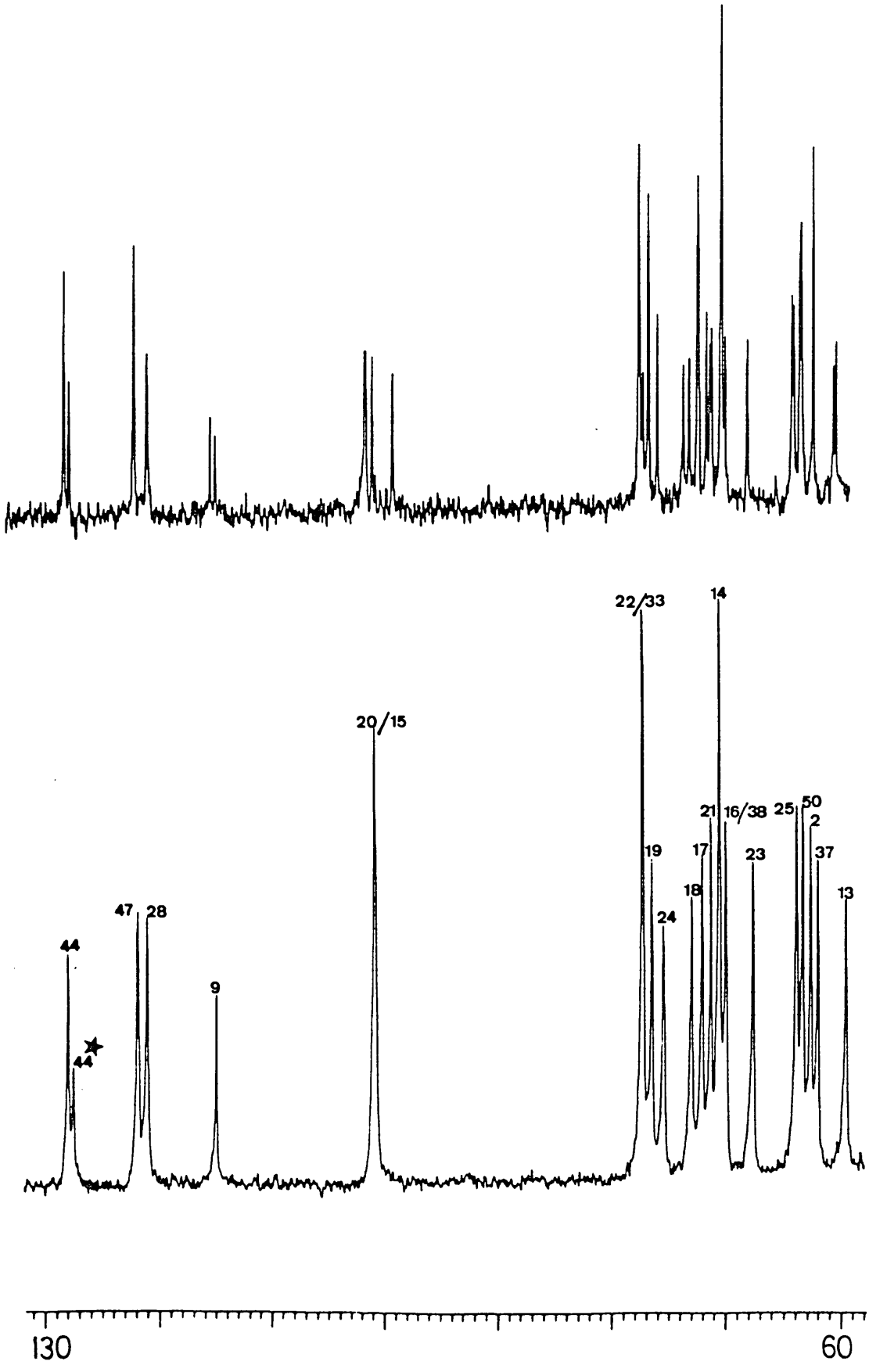


Fig. 3.15: Regions 3 and 4 (60-130 ppm). ^{13}C-NMR spectra of blenoxane and cis- Pt(II)aq interaction with blenoxane, r = 1.

-0.13 respectively. The degenerate resonance 15/20 was split into four peaks with Δδ values of 1.74, 0.12, -0.44 and -0.60ppm. C9 was split into two with Δδ 0.28 and -0.13ppm.

Region 5: 130-160ppm

In region five (Figure 3.16) there were no resonances which were not affected, although C45, C48, C48* and C26* had low Δδ values of -0.13, -0.13, -0.16 and -0.12 respectively. C27 was significantly shifted to lowfield and split into two, with Δδ values of -2.54 and -2.75ppm. C29 was shifted to lowfield by Δδ of -0.91ppm. Both C26 and C10 were split into two with Δδ values of -0.09/-0.16 and -0.03/-0.57ppm.

Region 6: 160-130ppm

In region six (Figure 3.16) there were no resonances which were not affected although C43, 46, 12 and 49 had low Δδ values of -0.25, -0.13, -0.10 and -0.15ppm respectively. C8, 7 and 30 were split,with Δδ of 0.03/-0.10, -0.69/-0.78 and -0.78/-0.87. C1, 40, 4 and 36 were all shifted downfield significantly, with Δδ values of -1.00, -4.32, -2.50 and -1.38ppm.

The assignments are also given in Table 3.1 and Δδ values quoted for reference purposes. It is difficult to reconcile (see later after analysis of $Pt(NH_3)_2$(ETMAL), 3.6iv) the r = 0.1 to 0.5 results where line broadening and complete loss of resonances is found with the observations made when r = 1. The split resonances

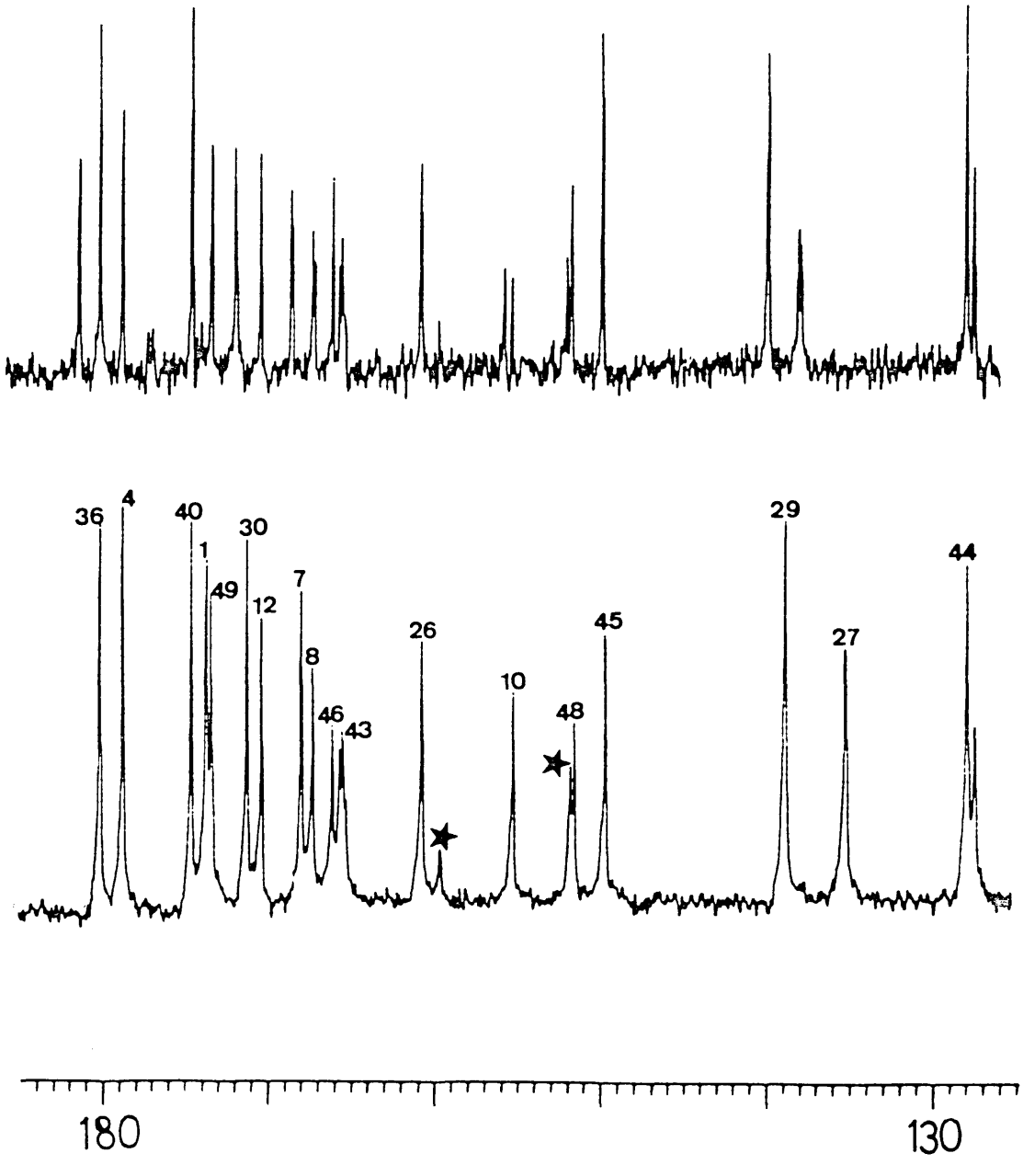


Fig. 3.16: Regions 5 and 6 (130-180 ppm). ^{13}C-NMR spectra of blenoxane and cis- Pt(II)aq. interaction with blenoxane, r = 1.

TABLE 3.1 ^{13}C NMR chemical shift data for Blenoxane and BNX/cis-$Pt(II)_{aq}$ (r=1).

Assignment	Blenoxane	$Pt(NH_3)_2^{2+}$ + BNX, r=1	Δδ
11	13.48	13.45	+0.03
32	14.80	14.48	+0.32
35	17.24	17.55	+0.21
		17.80	-0.56
39	21.50	21.59	-0.09
52	26.22	26.32	-0.10
54/55	27.35	27.44	-0.09
	28.10	28.16	-0.06
	28.48	28.56	-0.06
42	34.64	34.74	-0.10
53	40.27	40.37	-0.10
41	41.68	41.75	-0.08
5	42.71	43.03	-0.31
		43.16	-0.45
51	43.56	43.59	-0.03
		43.69	-0.13
34	45.41	45.31	-0.10
3	49.54	50.20	-0.66
31	50.26	53.20	-2.94
6	55.02	56.22	-1.40
13	59.31	59.72	-0.41
		60.00	-0.69
37	61.72	61.75	-0.03
2	62.38	62.88	-0.50
		63.00	-0.62
50	63.10	63.53	-0.43
25	63.60	63.99	-0.09
23	67.40	67.57	-0.17
16/38	69.70	69.48	+0.22

TABLE 3.1 (Contd)

Assignment	Blenoxane	$Pt(NH_3)_2^{2+}$ + BNX, r=1	Δδ
14	70.20	69.79	+0.41
21	71.01	70.64	+0.37
		70.80	+0.21
17	71.80	71.14	+0.66
18	72.71	71.80	+0.91
		71.89	+0.82
		72.64	?
		73.14	?
24	75.15	75.43	-0.28
19	76.21	76.21	0
		76.31	-0.10
22/33	77.03	76.78	+0.25
		77.12	-0.09
15/20	100.56	98.62	+1.74
		100.44	+0.12
		101.00	-0.44
		101.16	-0.60
9	114.68	114.40	+0.28
		114.81	-0.13
28	120.82	120.60	+ .22
47	121.66	121.79	-0.13
-	127.29	127.42	-0.13
44	127.73	127.86	-0.13
27	135.09	137.63	-2.54
		137.84	-2.75
29	138.72	139.63	-0.91
45	149.58	149.71	-0.13
48	151.46	151.59	-0.13
-	151.71	151.87	-0.16
10	155.12	155.15	-0.03
		155.69	-0.57

TABLE 3.1 (Contd)

Assignment	Blenoxane	$Pt(NH_3)_2^{2+}$ + BNX, r=1	Δδ
-	159.47	159.59	-0.12
26	160.60	160.69	-0.09
		160.76	-0.16
43	165.20	165.55	-0.35
	165.39	165.75	-0.36
	165.58		
46	165.98	166.11	-0.13
8	167.17	167.14	+0.03
		167.27	-0.10
7	167.80	168.49	-0.69
		168.58	-0.78
12	170.24	170.43	-0.19
30	170.09	171.87	-0.78
		171.96	-0.87
49	173.28	173.43	-0.15
1	173.59	174.59	-1.00
40	174.50	178.82	-4.32
4	178.66	180.16	-2.50
36	180.04	181.42	-1.38

and significantly shifted resonances (i.e. those with a $\Delta\delta$ value of > ±0.5ppm) are diagrammatically illustrated on the skeletal framework of BLM (Figure 3.17). It is immediately apparent

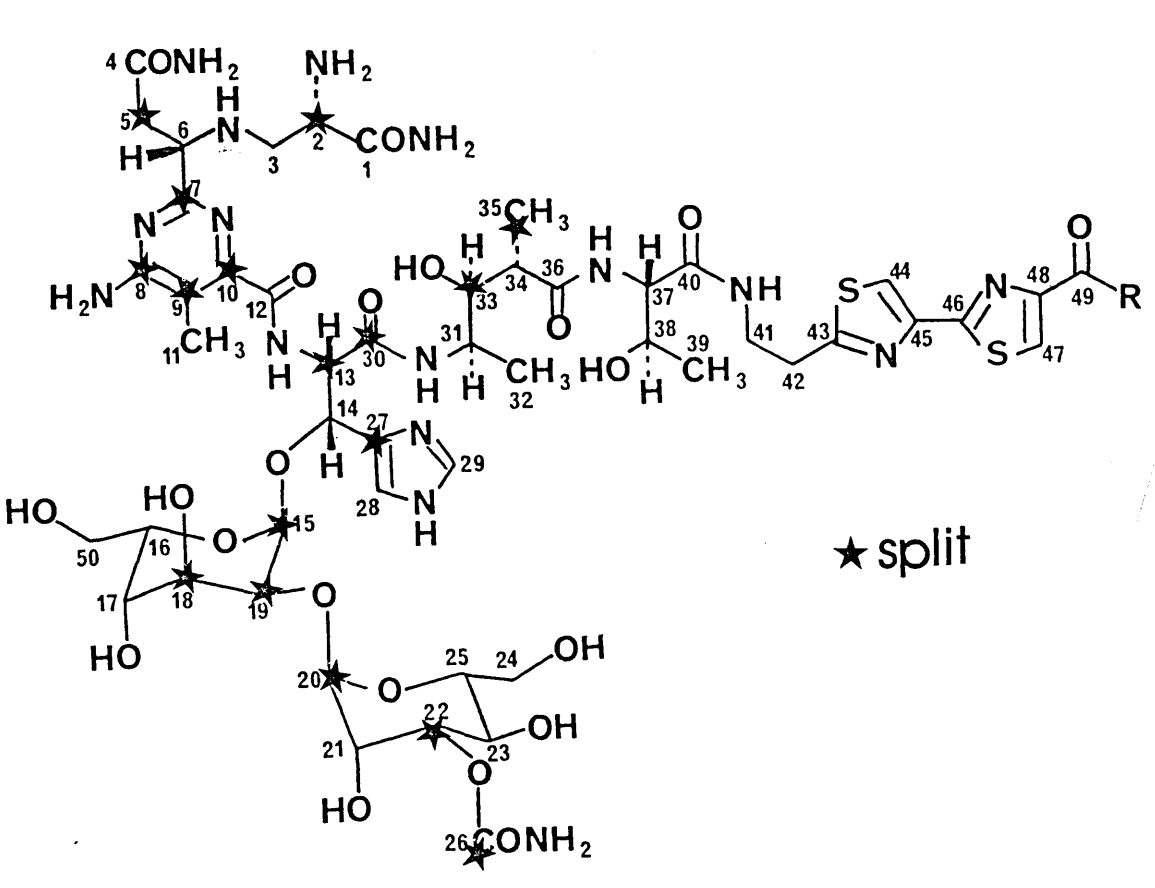


Fig. 3.17: Split resonances with immediate addition of r = 1 *cis*-$Pt(II)_{aq}$

when comparing Figure 3.17 with the similar presentation of results for the r = 0.1 to 0.5 case (Figure 3.13) that there is a very similar pattern. To obtain a completely "platinated" BLM a higher ratio

than r = 1 would have to be utilised. In the r = 1 case the spectrum obtained represents a mixture of free BLM and complexed BLM, or possibly two platinated forms of BLM, as there is potentially more than one site for *cis*-$Pt(II)_{aq}$ co-ordination. However again it is apparent that the bithiazole rings are not involved in complexation of platinum. The pyrimidine ring would appear to be a prime site of co-ordination, as all four carbon resonances were split. The imidazole ring is also a prime site of co-ordination with C27 being split and C29 being shifted by some 0.91ppm. Again the amides adjacent to C1 and C4 would appear to be reasonable sites. The splits in the sugar resonances and skeletal backbone of the nucleoside are probably due to conformational effects on Pt binding.

To identify the specific sites of co-ordination further work is required. Due to the limited amount of machine time available and of supplies of blenoxane it was not possible to carry out this work at this time.

3:6iii The interaction of $Pt(NH_3)_2$(ETMAL) with blenoxane

A similar initial study of the interaction of a second generation complex $Pt(NH_3)_2$(ETMAL) with blenoxane was carried out. Although there are apparently no reports in the literature of combination therapy of a second generation Pt complex with an established anti-tumour drug it is considered that this development will only be matter of time. The same protocol as that used with *cis*-$Pt(II)_{aq}$ was employed : small amounts of $Pt(NH_3)_2$(ETMAL) were successively added and the effects on the ^{13}C NMR spectrum of blenoxane were

monitored. The results will be discussed in the same format as before and compared to the analogous *cis*-Pt(II) spectra.

Region 1: 0-30ppm

In the 0-30ppm range (Figure 3.18) at the r = 0.1 stage the spectrum was very similar to the *cis*-Pt(II) case with six main resonances due to seven carbon atoms and a subsidiary pair of resonances to the lowfield of the degenerate 54/55 peak. Indeed, the chemical shift values are within 0.03ppm of those found with *cis*-Pt(II). However there are additional small resonances adjacent to C11 and C52 resonances at 13.36 and 25.96ppm. These are assigned to C_4 (methyl) and C_3 (methylene) of free ethylmalonic acid. Values previously found (14.79 and 26.29ppm respectively) compare reasonably well for this assumption. As expected, at the r = 0.3 stage these ethylmalonate resonances were more prominent, with the $-CH_2$ (methylene) resonance at 25.96ppm. However there were two distinct methyl peaks at 13.86 and 14.11ppm. On comparison with the same stage as *cis*-Pt(II) it would appear that the reaction has not proceeded as far in this case (the same length of time between the r = 0.1 and r = 0.3 stages had expired). On increasing the concentration of $Pt(NH_3)_2$ETMAL to r = 0.5 there were two predominant resonances at 14.30 and 26.67ppm assigned to the methylene and methyl groups of free ethylmalonic acid. The fact that there are two resonances for the methyl group at the r = 0.3 stage is due to the forms of the acid i.e. bidentate, monodentate and non-coordianted acid. At the r = 0.5 stage, if the two peaks due to the acid were to be subtracted the remaining spectrum would be virtually identical to the analogous *cis*-Pt(II) one (Figure 3.14). This is also

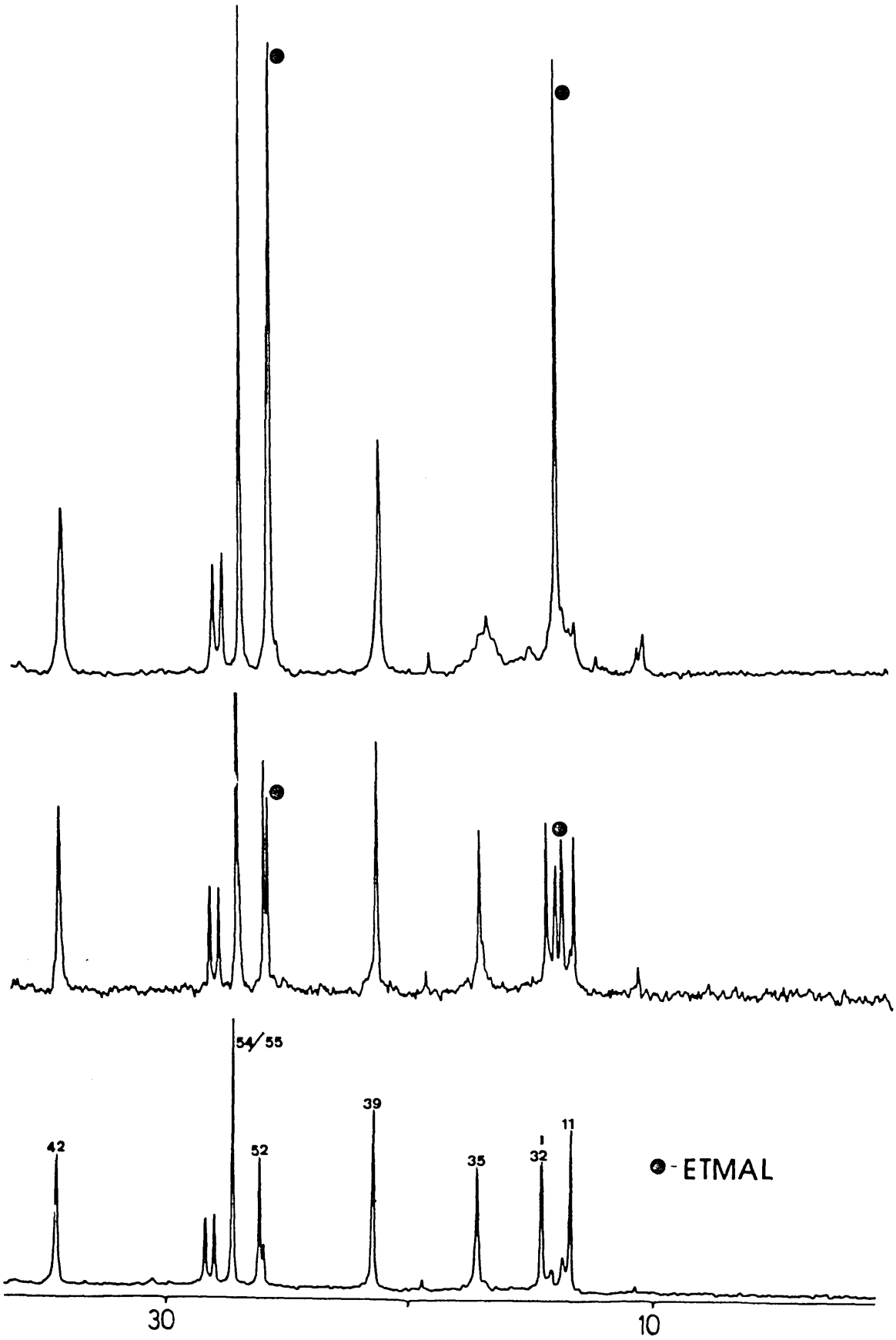


Fig. 3.18 : Region 1 (0-30 ppm). ^{13}C-NMR spectra of $Pt(NH_3)_2$ (ETMAL) interaction with blenoxane (r = 0.1, 0.3 and 0.5).

true at the 0.3 stage. Hence, regarding the bleomycin resonances, the same observations apply. Resonances 54/55, 52 and 39 were not affected, 35 and 32 were considerably broadened, and resonance 11 was shifted upfield by some 3.59ppm.

Region 2: 30-60ppm

In this region (Figure 3.19) the sequence of events is very similar and at the r = 0.3 stage the reaction was not as far advanced. Resonances 42, 53, 41 and 51 were not affected by addition of $Pt(NH_3)_2$ETMAL. Resonances 3, 31 and 34 at the r = 0.3 level were broadened and diminished in intensity, and when r = 0.5 this was further pronounced. The resonance due to C6 was not affected at the 0.3 level and only just detectable at the 0.5 stage. Resonance 13 was sharp when r = 0.3, but represented by a broad band at the 0.5 stage. Resonance 5 was completely lost at the 0.5 stage.

Region 3: 60-90ppm

In this region (Figure 3.20) the results are again very similar to the *cis*-Pt(II) case. A resonance due to C_2, methine carbon, of the ethylmalonate would be expected in the region of 62.45ppm (coordinated ethylmalonate) and 63.19ppm (free acid). At the r = 0.1 stage there was no such detectable resonance. However, at r = 0.3 and 4 = 0.5 there was such a peak at 62.5ppm, but at much lower intensity than expected. In the ^{13}C NMR spectra of $Pt(NH_3)_2$ETMAL and the acid, as its sodium salt, it is of similar intensity to the methyl and methylene peaks. However at high pH due to replacement of the hydrogen with deuterium a broad line

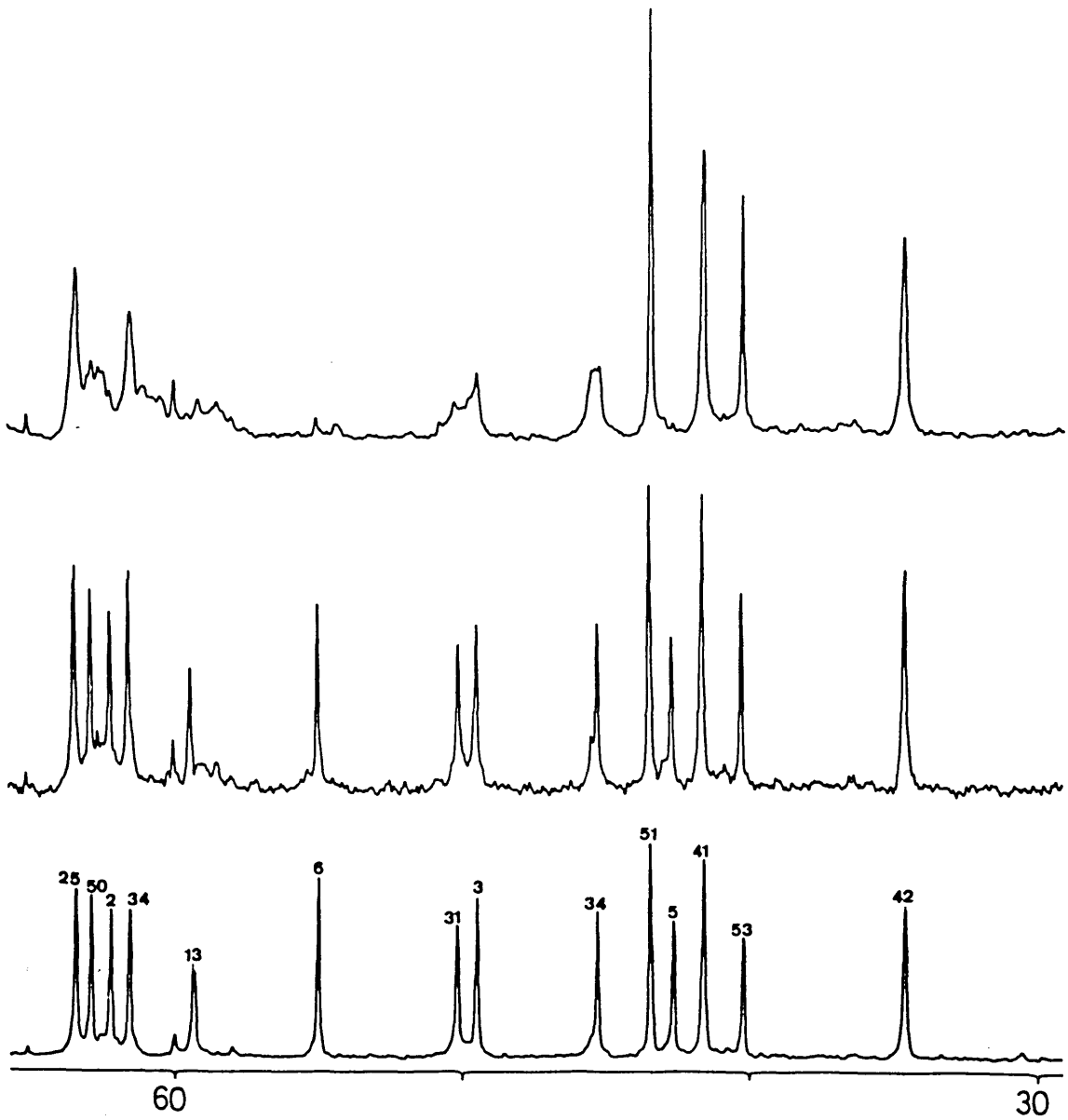


Fig. 3.19: Region 2 (30-60 ppm). ^{13}C-NMR spectra of $Pt(NH_3)_2$ (ETMAL) interaction with blenoxane (r = 0.1, 0.3 and 0.5).

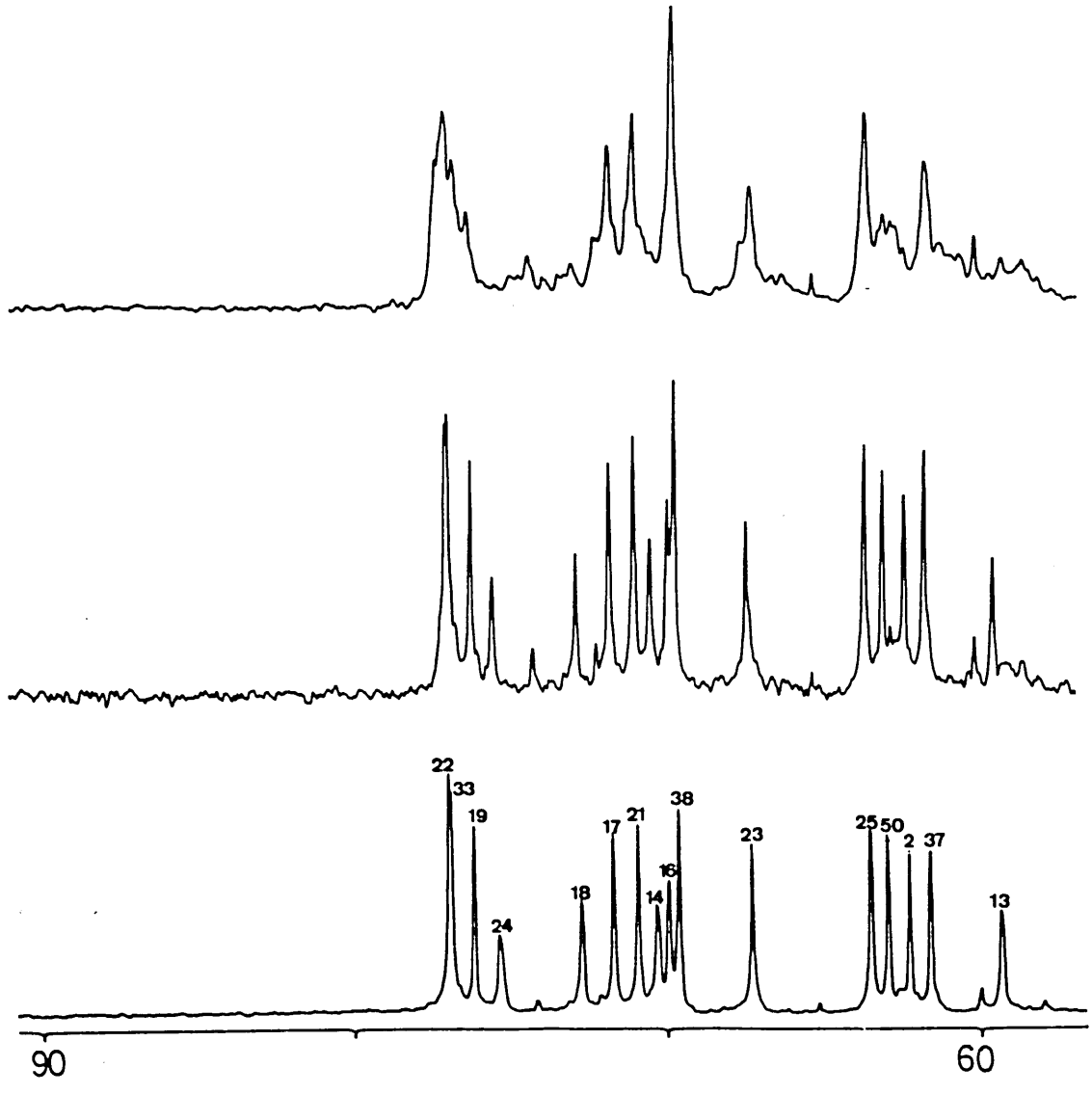


Fig. 3.20: Region 3 (60-90 ppm). ^{13}C-NMR spectra of $Pt(NH_3)_2$ (ETMAL) interaction with blenoxane (r = 0.1, 0.3 and 0.5).

results due to C-D coupling. This explains why a sharp line was not observed here.

The spectra when r = 0.5 and r = 0.1 were very similar to the analogous *cis*-$Pt(II)_{aq}$ ones. However when r = 0.3 there were differences which are explained by a lower rate of reaction. Carbons 22/33, 19, 24, 27, 21, 38, 23, 25 and 37 were broadened and essentially not shifted. Resonances due to carbons 18, 14 and 16 were lost but they may have shifted and become merged with the nearby broad bands in each case. Carbons 50 and 2 were merged into a broad band between C25 and 37.

Region 4: 100-130ppm

In region four (Figure 3.21) the same observations apply regarding comparison with *cis*-Pt(II). Resonances 47, 44 and 44* were essentially not affected by addition of $Pt(NH_3)_2$(ETMAL). Resonance 9 was so broad as to be only just detectable. At the r = 0.5 level, the degenerate resonance due to carbons 15/20 was split into four bands spaced over some 2.5ppm.

Region 5: 130-160ppm

In region five (Figure 3.22) there are six main resonances. Peaks 45, 48, 48* and 26* remained unchanged by addition of $Pt(NH_3)_2$(ETMAL). Resonances due to carbons 27, 29 and 10 were classified as lost although at r = 0.5 some residual bands were barely detectable. Resonance 26 was broadened.

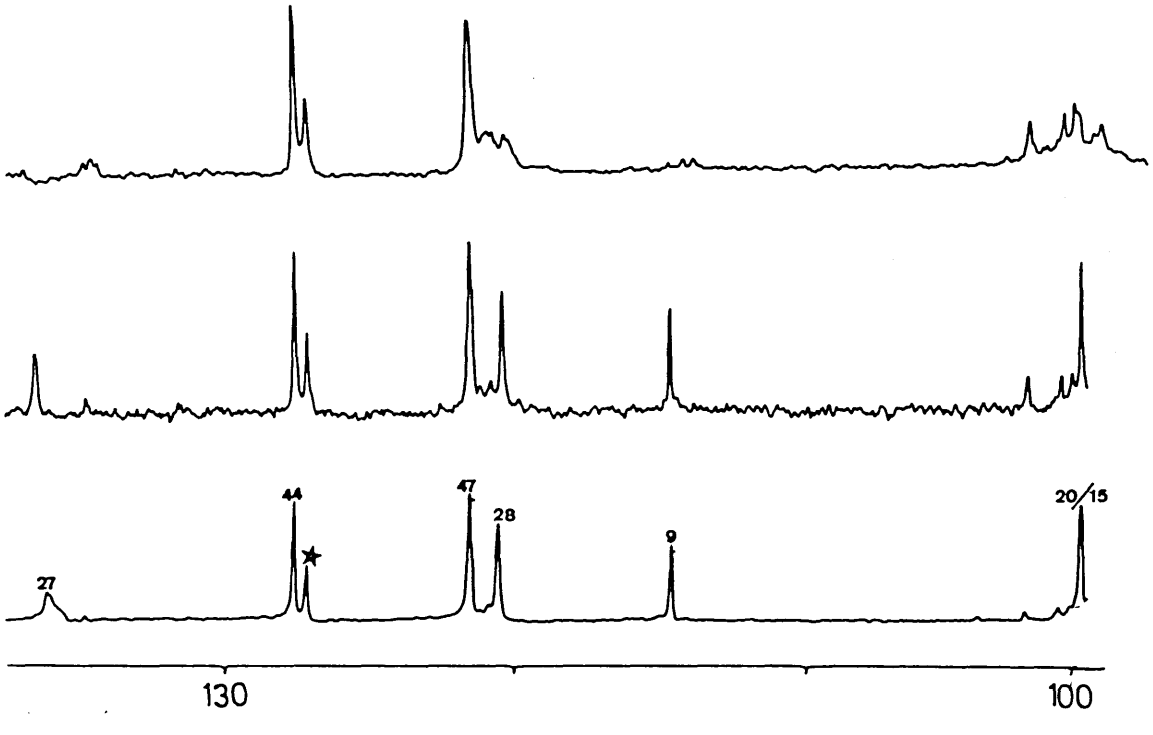


Fig. 3.21: Region 4 (90-130 ppm). ^{13}C-NMR spectra of Pt $(NH_3)_2$ (ETMAL) interaction with blenoxane (r = 0.1, 0.3 and 0.5).

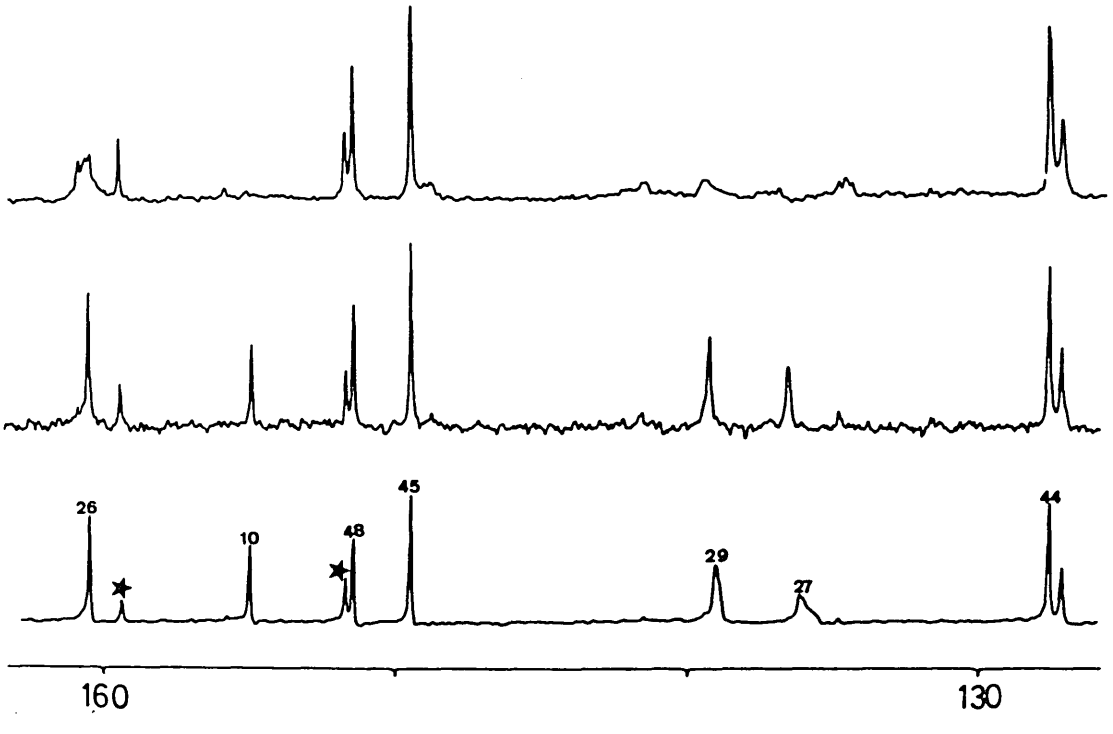


Fig. 3. 22: Region 5 (130-160 ppm). ^{13}C-NMR spectra of $Pt(NH_3)_2$ (ETMAL) interaction with blenoxane (r = 0.1, 0.3 and 0.5).

Region 6: 160-180ppm

In region six (Figure 3.23), apart from the resonances due to bleomycin, the carbonyl group of ethylmalonic acid was detectable at the 0.3 and 0.5 levels of $Pt(NH_3)_2$(ETMAL). At the r = 0.3 stage two peaks were observed at 180.91 and 183.40ppm due to the carbonyl of free (cf. 182.69) and complexed (cf. 183.67ppm) acid. These two peaks were of equal intensity which indicates that only half of the complex had interacted with BLM at this stage. Again this shows that the reaction has not proceeded as far in this case compared to *cis*-Pt(II). At r = 0.5 there was one peak due to the carbonyl, at 181.72ppm, assigned to free acid. The rest of the r = 0.5 spectrum was similar to the *cis*-Pt(II) case and the same comments apply. Resonances 36, 40, 49, 46 and 43 were broadened but essentially unshifted. The rest of the resonances 4, 1, 30, 12, 7 and 8 were all lost or only just detectable in the noise as broad bands.

In conclusion, at r = 0.5 the spectrum is extremely similar to that obtained with *cis*-$Pt(II)_{aq}$ in all regions. Therefore the interpretation of these data, as outlined in Figure 3.13 and the associated discussion on pages 75-80 apply here also.

This is reassuring as it indicates that the broad lines and lost resonances (i.e. resonances that have become so broad as to merge into the base line noise) are not caused by a *stray* paramagnetic entity in the *cis*-Pt(II) system. In both of these systems it is assumed that the "*cis*-$Pt(NH_3)_2$" unit remains intact. This leaves only two co-ordination sites on the Pt for interaction

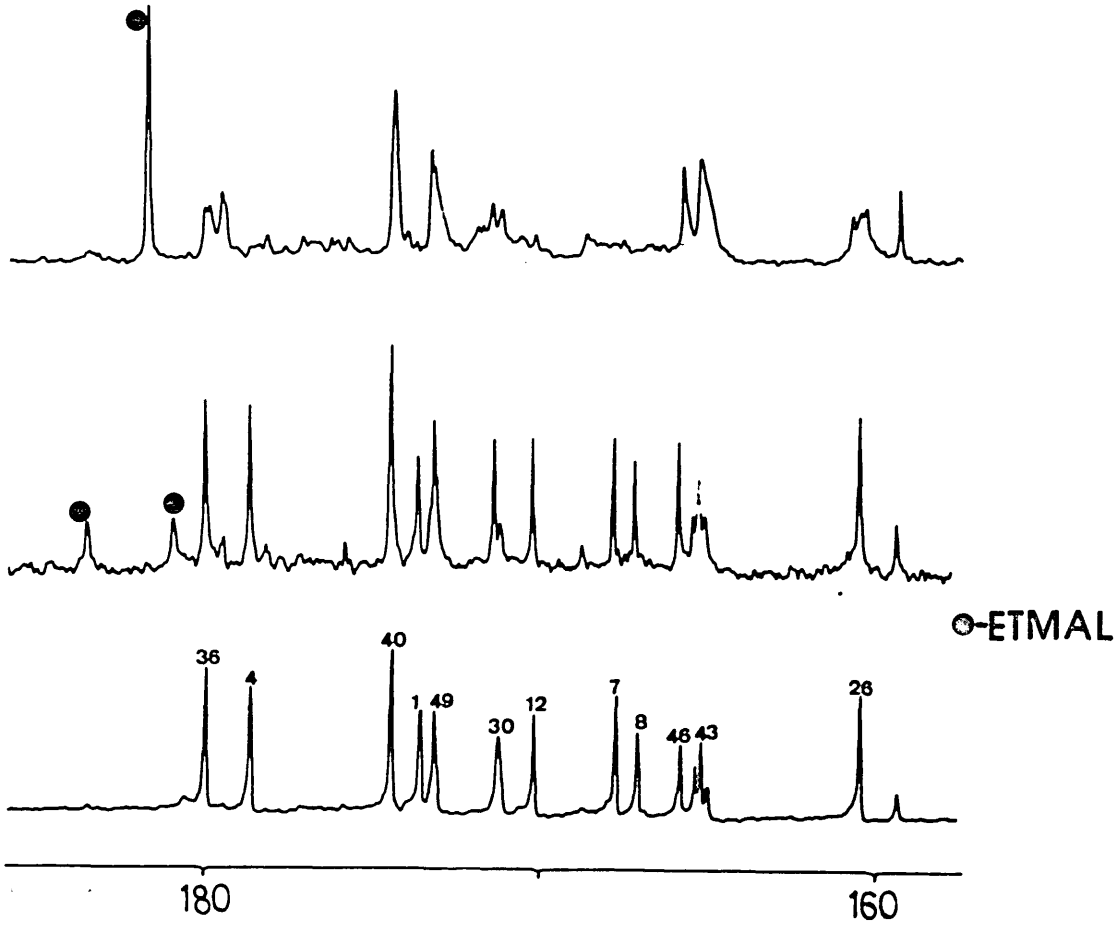


Fig. 3.23: Region 6 (160-180 ppm). ^{13}C-NMR spectra of $Pt(NH_3)_2$ (ETMAL) interaction with blenoxane (r = 0.1, 0.3 and 0.5).

with bleomycin. Obviously there are more than two potential sites on the bleomycin molecule and the data presented support this. In order to saturate all the sites an r-level of as high as 3 may have to be employed.

3:6iv Discussion of 3:6ii and iii

However, the argument presented so far does not adequately explain why the *cis*-Pt(II) interaction with BLN at the r = 1 ratio results in sharp resonances for all regions of the BLN molecule.

Firstly, it is prudent to consider the analogous *cis*-Pt(II) and $Pt(NH_3)_2$(ETMAL), r = 0.1 to 0.5 levels. Although the essentially identical results removed the probability of a *stray* paramagnetic species having been introduced into each system there is the possibility that on interaction with BLN a "Pt-blue" type of paramagnetic entity may be formed from the *cis*-$Pt(NH_3)_2^{2+}$ unit. If this is the case, then collapse of the carbon peaks in the vicinity of such a species would be expected. Indeed these so-called "lost" resonances may have been shifted outside the conventional spectral range (cf. the effect of the usual Lanthanide shift reagents).

It is desirable to consider the loss in intensity of each carbon as a function of concentration of *cis*-$Pt(NH_3)_2^{2+}$. This gives an indication of the proximity of the paramagnetic centre. The closer the more dramatic will be the loss in intensity. This analysis of the data (Figures 3.7-3.12) will be discussed in terms of regions of the skeletal framework of BLM.

In the C1 to C6 region, or "legs" of the molecule, carbon resonances C6 and C5 are completely lost at the 0.5 level of *cis*-Pt(II) and the carbonyl C4 is very weak. On the opposite "leg", C1 and C2 are both weakened but not to the same extent as C6 and C5, but the corresponding carbonyl C1 is completely lost at the 0.5 level.

On working down the molecule into the pyrimidine ring region the most dramatic effects are observed. At a level of Pt of only 0.3 complete loss of carbons 7 and 9 occurs. On the opposite side of this ring C9 and C10 are not lost until the 0.5 level. Indeed the methyl (C11) attached to the ring at C9 is only halved in relative intensity by the 0.5 stage. Moving away from the ring along the peptide backbone attached at C10 the first carbonyl, C12 is considerably broadened by the 0.3 stage as to be virtually classified as lost. We then arrive at the "king pin" of the molecule, C13. First let us follow the route which leads to the imidazole and sugar regions. C13 and C14 again are dramatically affected and are lost at the 0.3 stage. The first carbon of the imidazole ring C27 and C29 are also lost by the 0.3 stage, whereas C28 of the ring is still detectable at the 0.5 stage, though considerably weakened and broadened. The sugar residue will not be considered in detail apart from noting that the effects are probably mainly due to conformational effects. Returning to the "king pin" C13 and tracing along the peptide backbone towards the thiazole units we find, as expected, that the rate of decrease in intensity with respect to increasing r levels of "*cis* $Pt(NH_3)_2^{2+}$" falls off from carbon C30 (which is lost at 0.5) to C36.

This analysis allows the determination of the primary binding sites to be postulated. They are the N of the pyrimidine ring between C7 and C8 and, of equal importance, the N of the imidazole ring between C27 and C29. Presumably the "*cis*-$Pt(NH_3)_2^{2+}$" unit is binding across these two sites. This causes the molecule to fold around the C13-C14 bond. Hence, it is apparent why the intensity of the resonances due to carbons in the immediate vicinity are substantially affected and why this phenomenon decreases as the distance from this site increases.

It is interesting to note that out of the four drugs investigated in this chapter it is speculated that three form paramagnetic "Pt-blue" type species. They are all electron rich i.e. contain aromatic systems.

A very recent publication [18] points out that there is no acceptable reason as to why *cis*-Pt(II) is an active antitumour complex whereas the *trans* analog is not.

The "*cis*-$Pt(NH_3)_2^{2+}$" readily forms a notorious class of compounds the platinum blues. In the X-ray structure of α-pyridone blue [74] it is immediately apparent that *trans*-$Pt(NH_3)_2^{2+}$ could not form such a structure.

The alternative modes of action of *cis*-Pt(II) discussed in the literature (cf. Chapter 1) all involve essentially geometric considerations. That is to say that the presence of Pt is perturbing the physical structure of DNA.

Bleomycin itself acts via a free radical mechanism involving superoxide in a catalytic cycle (cf. page **66**). Indeed, the simple salt Na_2PtCl_4 has been shown [75] to be both an efficient stabilizer

of $^{\bullet}O_2^-$ or a stimulator of $^{\bullet}O_2^-$ production from isolated guinea-pig macrophages. It should be noted that in cells there exists an enzyme, superoxide dismutase, which has the specific capability of fast disproportionation of $^{\bullet}O_2^-$ radicals. This enzyme [76] contains two metal cofactors, Zn and Cu, and operates via a catalytic cycle involving Cu^{I} and Cu^{II} oxidation states.

Perhaps the paramagnetic platinum blues may in part be exerting their cell killing potential via a similar electronic mechanism involving superoxide radicals. This could be a further explanation why the *cis*- system is an essential feature of the platinum antitumour agents as the *trans* analogs cannot form "blues".

Furthermore, the generation of such "blues" reported in this work with common components of clinical regimes may explain the synergic effect observed in such treatments.

The formation of "blues" is usually considered to involve oxygen. In the system when *cis*-Pt(II) was interacted with BLN at an r = 1 there are two factors to be taken into consideration. First, only in this case was the solution de-oxygenated and second the ^{13}C NMR was obtained as quickly as possible. Indeed, the spectrum of the same solution was obtained a week later and the resolution was found to have degraded to a small extent. In the r = 0.1, 0.3 and 0.5 cases due to the small supply of the expensive drug appropriate aliquots were subsequently added over a period of weeks. No attempt was made to exclude O_2 and in these two cases and hence a "blue" species was obtained.

A recent publication [77] has shown that *cis*-Pt(II) alters the sequence-specific cleavage of DNA by bleomycin. In the systems studied an Fe(II)-BLM was employed. It would have been interesting to see the effect of starting with metal free-BLM and generating the Pt "blue" species found in this work. Moreover the testing of such solutions for antitumour activity should be considered.

3.6v Interaction of K_2PtCl_4 and blenoxane

A further study was made on the coordination sites of bleomycin with $PtCl_4^{2-}$ as the probe. This investigation was undertaken as a preliminary exercise with the idea in mind of producing a platinated bleomycin species with the accepted antitumour structure *cis*-$Pt(BLN)Cl_2$ for potential screening. Once again the ^{13}C NMR data will be presented region by region.

Region 1: 0-30ppm

In region 1 (Figure 3.24) at the r = 0.1 stage the spectrum was identical to that of blenoxane apart from a small peak to the lowfield of 54/55. This was not evident at later stages. Resonances 54/55 and 52 were not affected by addition of K_2PtCl_4. Resonance 39 exhibits a shoulder at the 0.7 level. Lines 35 and 32 were both broadened and shifted downfield by about 0.3ppm. The resonance due to carbon 11 was more interesting as, at the r = 0.3 level, two distinct peaks can be observed 11 and 11 (meaning complexed bleomycin) separated by 0.36ppm. At the 0.7 level 11

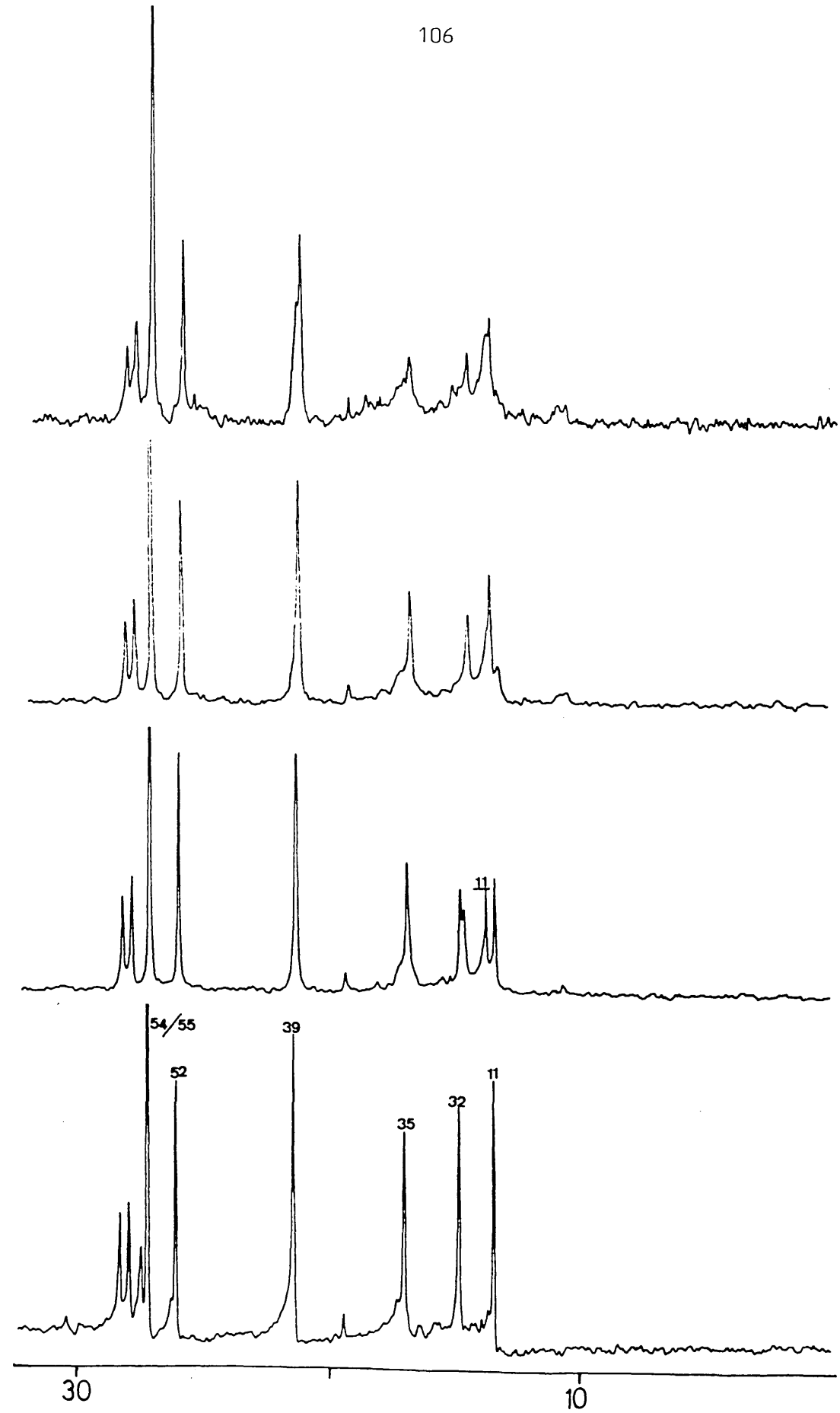


Fig. 3.24: Region 1 (0-30 ppm). ^{13}C-NMR spectra of K_2PtCl_4 interaction with blenoxane (r = 0.1, 0.3, 0.5 and 0.7).

was dominant. These observations do not correspond to either of the previous systems, but they are similar to the results reported [73] for the Zn(II) system.

Region 2: 30-60ppm

In region 2 (Figure 3.25) there are very pronounced differences as the concentration of $PtCl_4^{2-}$ was increased. Resonances 51, 41, 53 and 42 were not shifted. 31 and 34 were diminished in intensity and broadened. The resonance due to carbon 6 was shifted upfield by 1.09ppm on increasing the level of $PtCl_4^{2-}$ from r = 0.1 to 0.3, but by r = 0.5 it was no longer detectable. Resonance 3 was significantly diminished by r = 0.3 and only just observable at r = 0.7. However the new or complexed resonance 3 may be merged with the nearby broad band assigned to 31. Resonance 5 had vanished by the 0.3 level. There were several small peaks which can tentatively be assigned to complexed 5, the most prominent of which was at 36.94ppm (to the lowfield of 42). Resonance 13 at the 0.3 stage showed five separate lines which converged into two major wide peaks on a broad hump by the r = 0.7 stage.

Region 3: 60-90ppm

In region 3 (Figure 3.26) the resonances were very close together which makes assignment of shifted or "new" peaks a little difficult. Starting with those which were essentially unchanged, these are attributed to carbons 22/33, 19, 17, 21, 14, 25 and 50, although some were broadened to varying degrees. The two initially separate resonances 2 and 37 converged into a broad band by r = 0.7

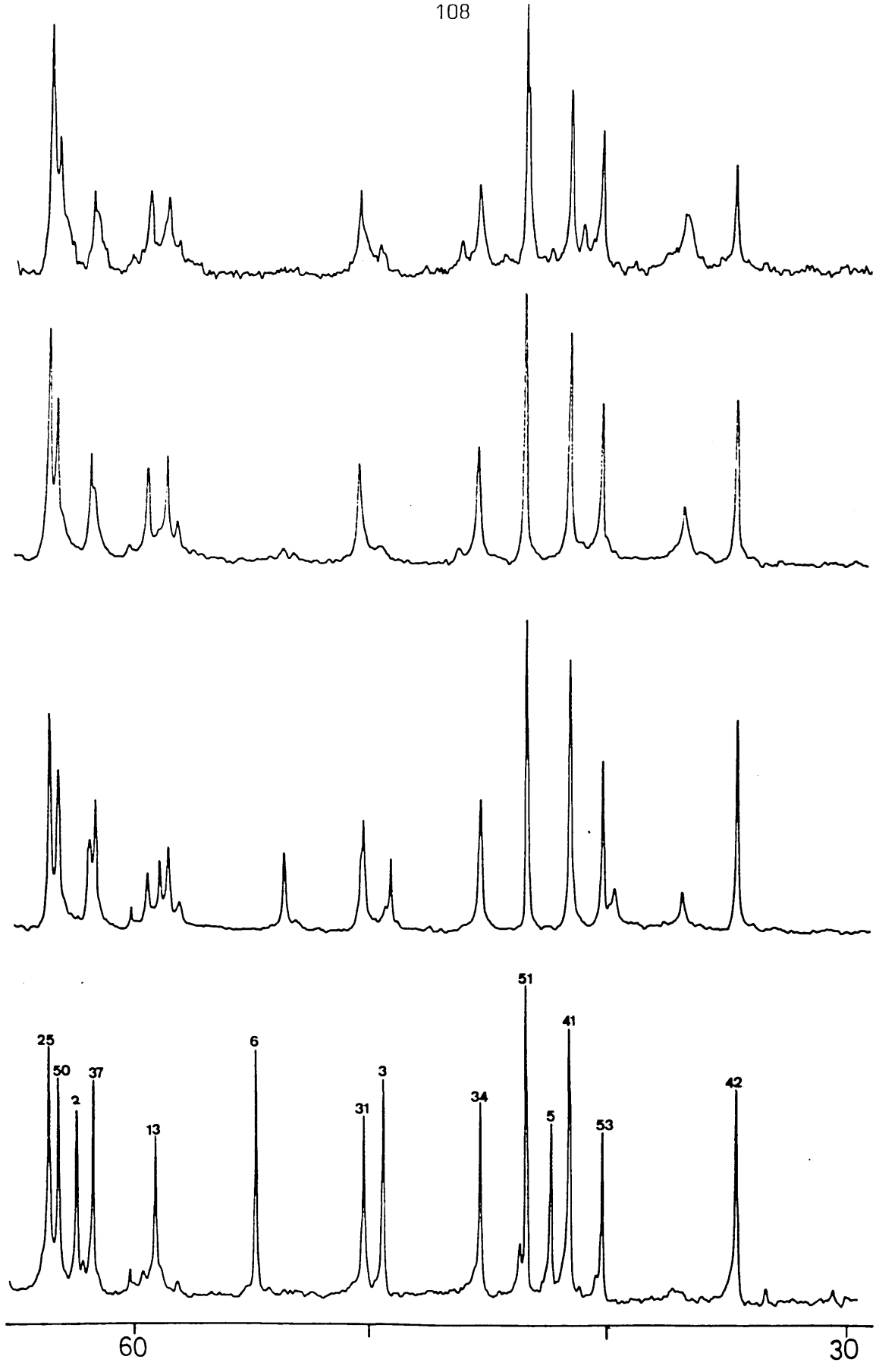


Fig. 3.25: Region 2 (30-60 ppm). ^{13}C-NMR spectra of K_2PtCl_4 interaction with blenoxane (r = 0.1, 0.3, 0.5 and 0.7).

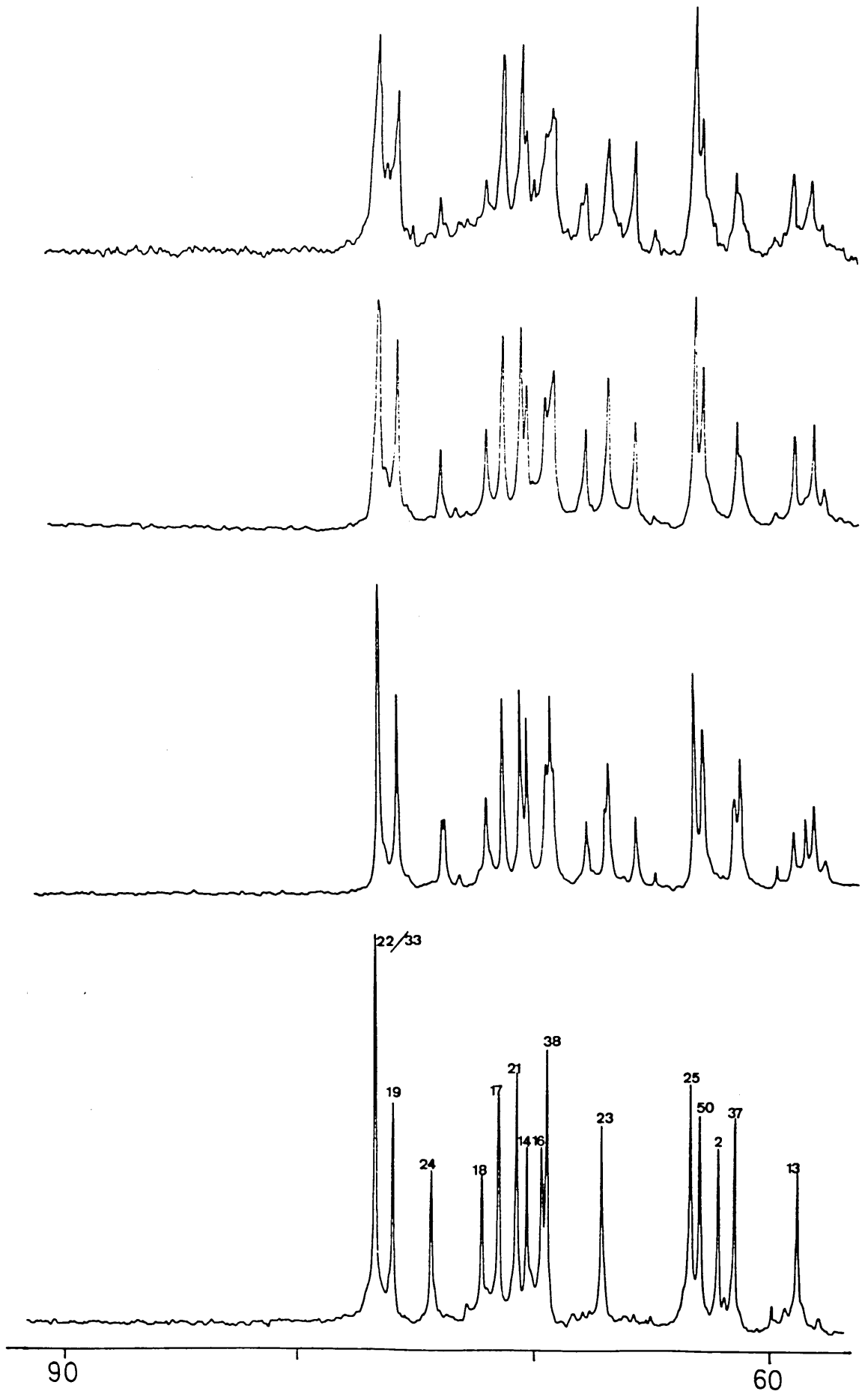


Fig. 3.26: Region 3 (60-90 ppm). ^{13}C-NMR spectra of K_2PtCl_4 interaction with blenoxane (r = 0.1, 0.3, 0.5 and 0.7).

and the same applies to 16 and 38. Resonance 23 was flanked by two new resonances by r = 0.3 which still persisted at r = 0.7.

Region 4: 100-130ppm

In region 4 (Figure 3.27) resonances assigned to carbons 15, 20, 47 and 28 were not affected by increasing concentration of $PtCl_4^{2-}$. It should be noted that in this case alone 15 and 20 now give rise to separate lines, whereas in the previous two systems they were degenerate. Resonance 44 and 44*, up to the r = 0.5 level, were essentially similar, but by the 0.7 stage had become a broad hump, with one prominant peak still in the same position (within 0.2ppm). Resonance 9 was at 114.48ppm at r = 0.1 which compares well to metal free BNX (114.68ppm) and there was a small blip to the left of it at about 119ppm. As the level of K_2PtCl_4 was increased this "blip" grew in intensity to the detriment of the original resonance 9. In the previous two similar cases 9 has simply been classified as lost.

Region 5: 130-160ppm

In region 5 (Figure 3.28) resonances 27, 29 and 45 remained unperturbed on addition of K_2PtCl_4. Resonance 48 (48*) at the 0.3 and 0.5 levels exhibited a new peak growing between them. This new resonance is assigned to complexed 10 as it increased in intensity as the original resonance 10 decreased. However, at the 0.7 level the new group assigned to 48, 48* and 10 had become rather broadened.

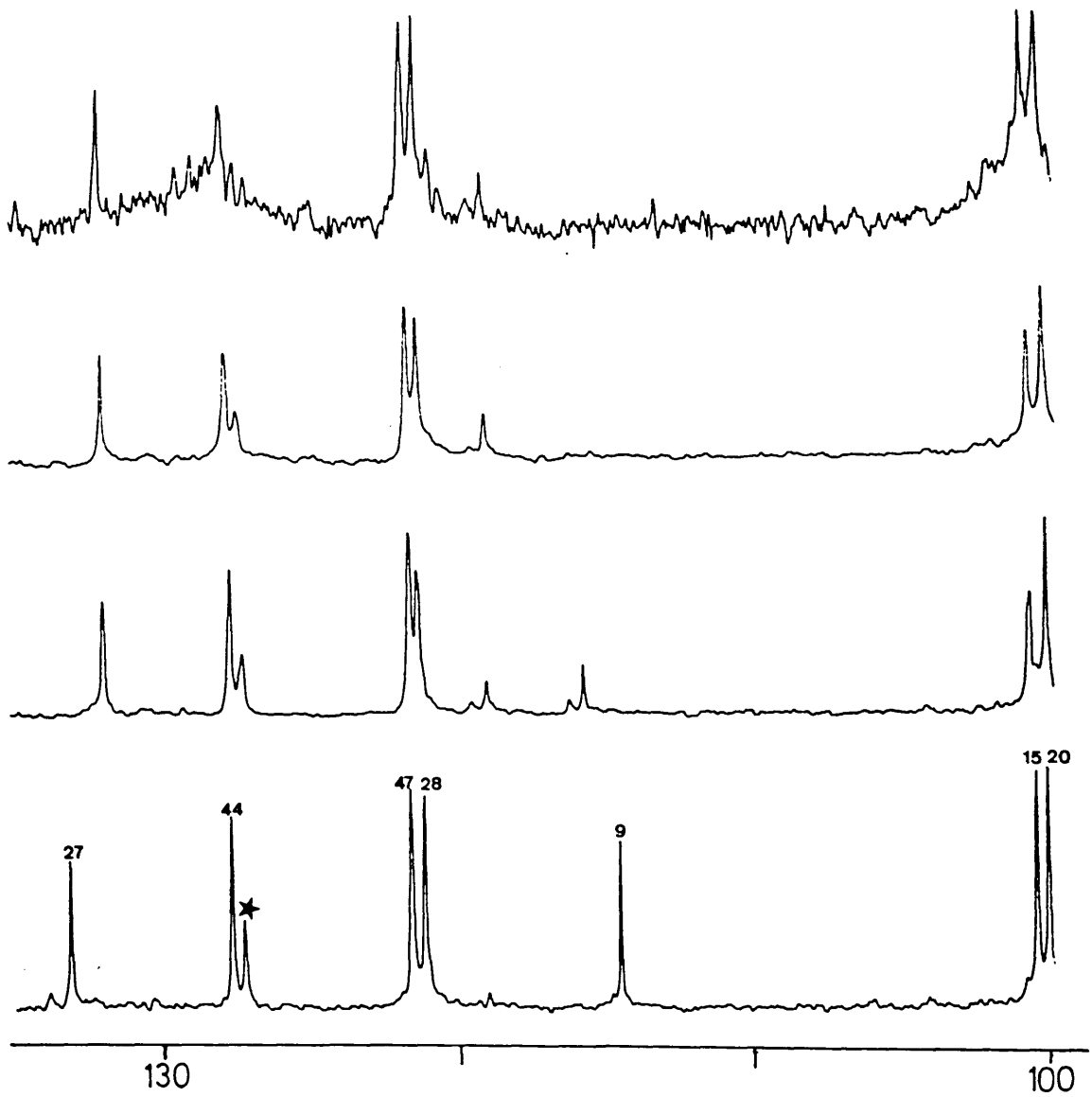


Fig. 3.27: Region 4 (90-130 ppm). ^{13}C-NMR spectra of K_2PtCl_4 interaction with blenoxane (r = 0.1, 0.3, 0.5 and 0.7).

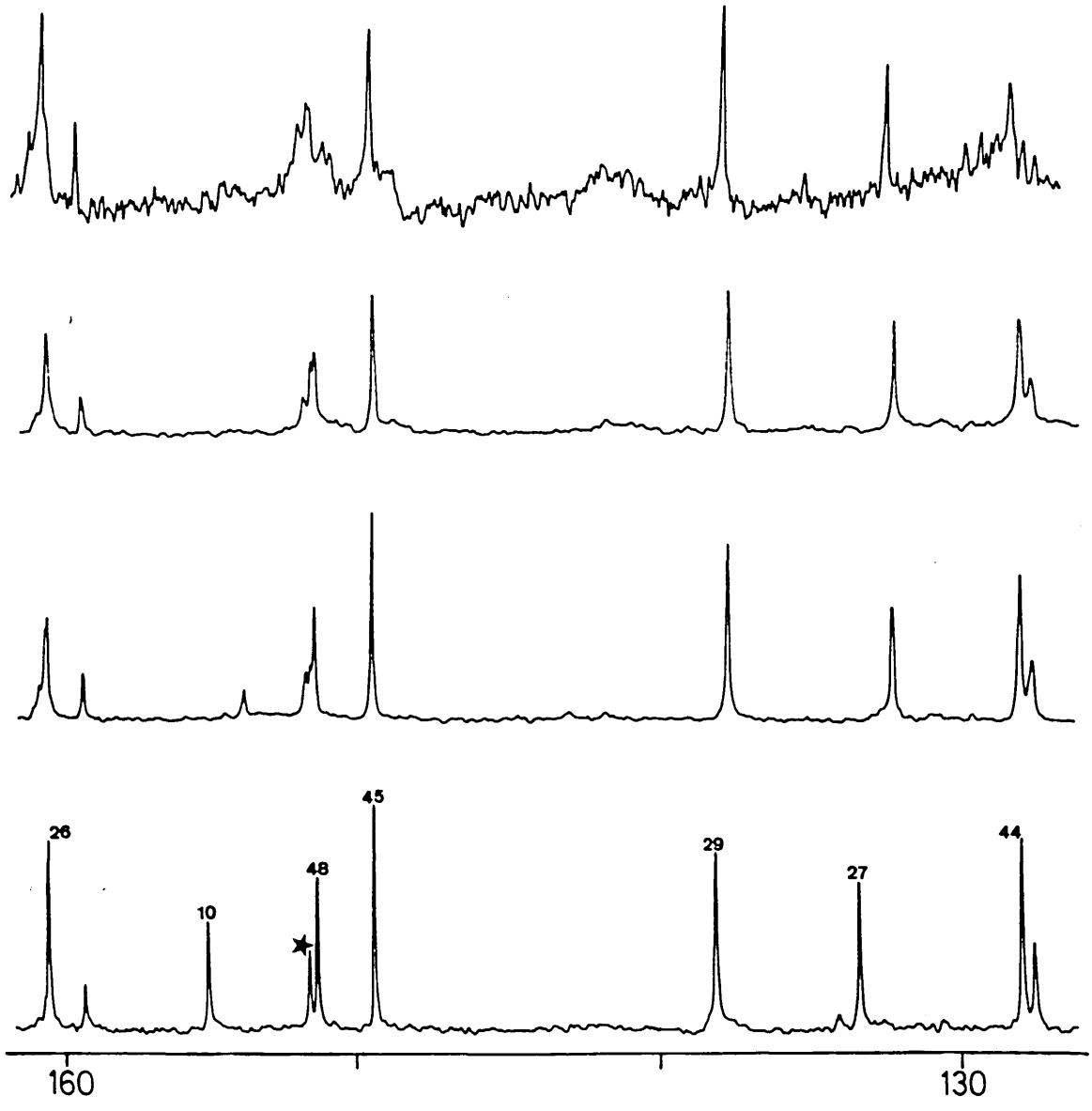


Fig. 3.28: Region 5 (130-160 ppm). ^{13}C-NMR spectra of K_2PtCl_4 interaction with blenoxane (r = 0.1, 0.3, 0.5 and 0.7).

Region 6: 160-180ppm

In region 6 (Figure 3.29) the results are difficult to analyse with any degree of certainty. Resonances 26 and 40 are the only members of the eleven peak set to be considered which remain unchanged. Resonance 4 was shifted upfield by 1.5ppm from the r = 0.3 level upwards. Resonances 46 and 43, although broadened, were not significantly affected. However, the remaining peaks produce a complicated and closely spaced pattern. At the r = 0.3 level two new peaks which are tentatively assigned to 12 and 7 at 168.2ppm persist to the 0.7 stage. A speculative assignment is shown on Figure 3.29 for the remaining peaks at the 0.5 stage which can be extrapolated to the rather broader bands at the r = 0.7 step.

These results will now be discussed in terms of specific areas of the bleomycin molecule. In the "legs", or amide groups, region the two carbonyl carbons, C4 and C1 both exhibited an upfield shift of $\Delta\delta$ + 1.5ppm. In both cases this had occurred by the r = 0.3 level of K_2PtCl_4. By the r = 0.3 level C5 at 42.32ppm had completely disappeared, but there was a new peak at 36.91ppm, which increased with the level of K_2PtCl_4. This is assigned to C5, giving a $\Delta\delta$ of 5.4ppm. Resonance C2 at 62.2ppm presumably undergoes a small upfield shift of $\Delta\delta \sim$ 0.3ppm and merges with C37. On increasing the Pt content from r = 0.1 to r = 0.3 C3 and C6, at 66.23 and 68.28ppm respectively initially, exhibited a small upfield shift, but by the r = 0.5 and 0.7 stages they were no longer detectable to the upfield side of their original positions. However

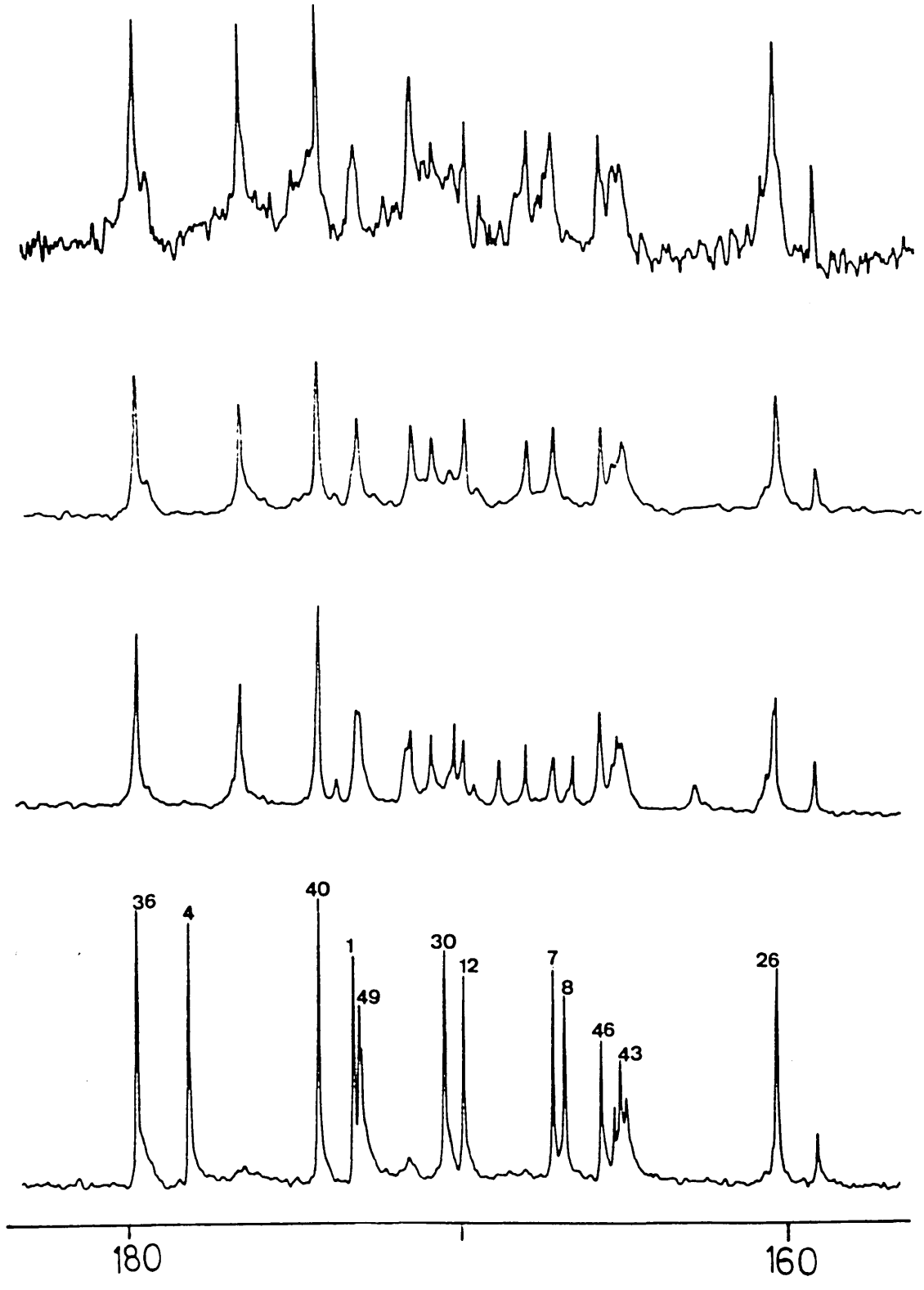


Fig. 3.29: Region 6 (160-180 ppm). ^{13}C-NMR spectra of K_2PtCl_4 interaction with blenoxane (r = 0.1, 0.3, 0.5 and 0.7).

to lowfield there were two new resonances adjacent to C23 which increased with increasing r. These are tentatively assigned to C3 and C6, with $\Delta\delta$ shifts of -16.83 and -13.55ppm respectively.

In the adjacent area, the pyrimidine ring C7 and C8 at the 0.3 level gives rise to a complex region of the spectrum (in combination with nearby resonances) but a tentative assignment at the 0.5 level gives rise to complexation shifts of $\Delta\delta$ -0.94 and -0.53ppm respectively. C9 of the ring exhibited a shift downfield of $\Delta\delta$ -4.62ppm and C10 appears to display the opposite effect with a shift upfield merging into a nearby resonance of $\Delta\delta$ +3.27ppm. The exocyclic methyl group, C11 had a small shift of $\Delta\delta$ -0.29ppm.

Moving away from the ring and tracing the peptide backbone of the molecule, the first carbonyl, C12, was not significantly shifted. Indeed, along the whole of the backbone the associated resonances showed little effect, apart from some broadening, which may be attributed to conformational aspects. Those which were broadened are the methyl groups C32 and C35.

C14, 27, 28 and 29 of the imidazole ring showed no broadening or shifts on increasing levels of K_2PtCl_4. The resonances associated with the sugar and thiazole regions also remained non-perturbed with increasing r.

In conclusion, the prime site of binding of the $PtCl_4^{2-}$ unit would appear to be the ring N of the pyrimidine unit. This causes significant shifts of the attached carbons C3, 6 and 5. It is surprising that the imidazole is not involved in bonding at this level of Pt concentration. However at a larger ratio (r value) it may become involved and this also applies to other potential

co-ordination sites on the bleomycin system.

3:7 Conclusion

In order to produce a new active antitumour drug the interaction of *cis*-Pt(II)with drugs used in combination therapy may be considered to be a naive conception. On co-ordination to the drug the two active sites on *cis*-Pt(II) would become blocked destroying its ability to interact with DNA. Furthermore the accepted mode of action of such a drug would be destroyed; for example the base antimetabolite 5-fluorouracil would not be able to mimic uracil with a platinum unit coordinated to it.

However this work has shown that with three of the drugs studied, 5-fluorouracil, cytosine arabinoside and bleomycin a paramagnetic blue complex was produced. Indeed the platinum blues are a class of antitumour compounds [59] in their own right. With cyclophosphamide no interaction with several platinum complexes was found.

A mechanism was proposed to account for the synergic effect observed in the drug combinations involving *cis*-Pt(II). With the aromatic drugs the formation of a blue may lead to an electronic mechanism involving superoxide radicals (cf. mode of action of bleomycin).

Further work would involve extending the studies with the bleomycin system particularly relating ^{13}C NMR measurements with epr studies. It would be interesting to extend this work to include other commonly used combination drugs particularly those involving aromatic systems.

CHAPTER FOUR

THE SYNTHESIS OF POTENTIAL PLATINUM ANTITUMOUR COMPLEXES

4.1 Introduction

In the years that followed the discovery of the antitumour agent [1] *cis*-Pt(II) many platinum complexes were screened for such activity. This resulted in the development of some useful structure/activity correlations [8] as discussed in Chapter One. A large number of workers exploited these ideas by simply varying A and X in the now classical structure *cis*-$Pt(A)_2(X)_2$. Indeed several new complexes, viz. the second generation drugs came to light through this rather hit or miss approach.

In this work a different tactic was employed. Ligands of biological significance were investigated.

4.2 Caffeine and related alkaloids

Caffeine has been shown to inhibit the postreplication repair mechanism of both UV and chemically induced damage in DNA [78,79]. Roberts and co-workers have shown that caffeine is particularly effective in enhancing the effects of the DNA lesions caused by *cis*-Pt(II). This led us to consider the hypothesis, in July 1979, that a platinum caffeine complex may have antitumour activity. It is a matter of interest to note that caffeine (and related alkaloids viz. theophylline and theobromine) are found in coffee and tea.

Indeed caffeine is used as a respiratory/heart stimulant in veterinary science.

This work produced the complex *cis*-$Pt(caffeine)_2Cl_2$ and, more interestingly, the salt $K[Pt(caffeine)Cl_3]$. In 1979, neither of these compounds was accepted for antitumour screening, the first because of its low aqueous solubility, the second because of its charged nature.

In 1981 Cramer et al. reported [80] the synthesis and structure of the analogous complex $[P(C_6H_5)_3(CH_3)]$ $[Pt(caffeine)Cl_3]$ and also the fact that the potassium salt had some antitumour activity. The salt, $K[PtCl_3(caffeine)]$ was found to have substantial anticancer activity against at least one type of cancer in mice. They proposed that this compound represents a new class of platinum antitumour drugs as it does not have the established *cis*-PtL_2X_2 stoichiometry. The preparative techniques of $K[Pt(caffeine)Cl_3]$ and *cis*-$PtCl_2(caffeine)_2$ developed prior to the publication of Cramer et al.[80] and also some of their physical and chemical properties will now be discussed. Analogous complexes with theophylline and theobromine will also be covered.

4.2i *cis*-$[Pt(caffeine)_2Cl_2].0.4H_2O$

This compound was obtained by the following synthetic route. A solution of K_2PtCl_4 (0.420g, 1mM) in water (10ml) after stirring, and filtering with charcoal to remove K_2PtCl_6 impurity, was added slowly to one of caffeine (0.390g,2mM) in water (20ml). The resulting orange-red solution was warmed (60°C, 1 hr.) and then left to stand for two days. The 2:1 complex separated as a pale yellow

microcrystalline solid and this was filtered off, washed with water, and dried in vacuo at 40°C overnight. Yield = 0.027g, 4.1% ν(Pt-Cl) 340cm^{-1}(br). [Anal. Found C, 28.94; H, 3.02; N, 16.47% Calc. for [Pt(caffeine)$_2$Cl$_2$].0.4H$_2$O; C, 29.04; H, 3.17; N, 16.94%].

The *cis*-arrangement of ligands was considered the more likely geometry taking into account the *trans*-effect and method of preparation, even though in the IR there is only one distinct band at 340cm^{-1} with a shoulder at 335cm^{-1}. For a *cis* arrangement of ligands in a square planar complex group theory calculations predict two distinct metal-halide IR active vibrations. Conversely for *trans* only one band would be expected. Thermogravimetric analysis of the complex confirmed the presence of the water of hydration. The crystal structure of this complex has recently been reported by Goodgame et al. [81]. The *cis*- arrangement is confirmed with the Pt-N(9) and Pt-Cl bonds of 2.029(5)Å and 2.271(2)Å respectively.

4.2ii K[PtCl$_3$(caffeine)]

The orange yellow filtrate remaining after separation of the 2:1 complex was evaporated to dryness and the residue recrystallised twice from refluxing methanol to give orange yellow crystals of K[PtCl$_3$(caffeine)].CH$_3$OH. Yield = 0.48g, 84.6%. ν(Pt-Cl) 320sh and 330cm^{-1}. [Anal. Found: C, 19.06; H, 2.39; N, 10.20%; Cl, 18.47; O, 8.15; Pt, 34.50% Calc. for K[Pt(caffeine)Cl$_3$)].CH$_3$OH: C, 19.07; H, 2.49; N, 9.89; Cl, 18.76; O, 8.49; Pt, 34.42%].

A quicker more direct route to $K[Pt(caffeine)Cl_3].CH_3OH$ was then devised. A mixture of K_2PtCl_4 (4.20g, 10mM) and caffeine (1.94g, 10mM) was slurried in methanol (100ml) and HCl (20ml of 1N) and gently refluxed for 4-5 hours. The black solution obtained was treated with charcoal and filtered hot through a pre-heated no.4 sinter. The orange yellow complex separated in 59% yield on cooling the filtrate in a fridge overnight. It was obtained as orange crystals on recrystallization from a hot methanol/dil. HCl mixture [Anal. Found: C, 18.82; H, 2.40; N, 9.85; Cl, 18.86%]. The IR was identical to the previous preparation.

The presence of methanol of solvation was confirmed by thermogravimetric analysis. The MeOH is lost at 160°C. At 510°C a plateau begins corresponding to 47.5% and is probably due to residual KCl and Pt(47.6%). By 900°C there is further weight loss; finally at 1300°C Pt(34.5%) remains.

The ^1H NMR of a saturated solution of $K[PtCl_3(caffeine)]$ in D_2O confirms coordination of Pt at the N9 position. The H8 resonance of free caffeine is shifted to lower field by some 0.57ppm to δ8.42 on coordination of platinum. At 60MHz in the ^1H NMR the H(8) resonance is flanked by two well-defined platinum satellites with J_{Pt-H} = 18Hz. However, at 250MHz these platinum satellites are not observed - even at 90MHz they are only barely detectable. This is an example of chemical anisotropy relaxation [82]. At higher applied fields ^{195}Pt couplings are not generally visible due to this mechanism.

The ^{13}C-NMR spectrum confirms the presence of MeOH, with a resonance at 48.91ppm from external TMS. Three resonances attributable to the methyl groups are observed at 34.36ppm, 32.40ppm and 29.06ppm and the carbonyl and other quaternary centres are all grouped together

centred on 145ppm downfield from external TMS.

The ^{195}Pt-NMR spectrum exhibits a broad resonance centred at 122.5ppm downfield from an external reference of K_2PtCl_4. Interestingly there is a further resonance of approximately one quarter of the intensity of the first centred at 245.6ppm. During the collection of the data for this spectrum the originally orange solution had turned darker and the smaller resonance is thought to be due to a hydrolysis product.

4.2iii Reactions of $[PtCl_3(caffeine)]^-$ with other ligands

The formation of the species $[PtL_3X]^-$ raised the interesting possibility of utilising it for the synthesis of mixed ligand complexes viz. *cis*-$PtLL'X_2$. Due to our general interest on the interaction of platinum complexes with DNA and DNA fragments nucleoside and nucleotide species were chosen as L'. Only with cytidine was an analytically pure complex isolated.

A sample of $K[Pt(caffeine)Cl_3].CH_3OH$ (0.2mM, 0.102g) was refluxed with cytidine (0.2mM, 0.049g) in a water/methanol mixture (10ml) for 6 hours. On cooling, a pale yellow powder was obtained. Yield 0.036g, 26%. ν(Pt-Cl) 326 and 338cm^{-1}. [Anal. Found: C, 28.75; H, 3.29; N, 13.66; Cl, 9.84%. Calc. for $PtCl_2$(caffeine)(cytidine): C, 29.03; H, 3.30; N, 13.94; Cl, 10.08%]. The complex has a very low solubility in common solvents.

Reaction of $[PtCl_3(caffeine)]^-$ with 5'-CMP, 5'-GMP, guanosine, uracil or uridine gave extensive or partial reduction to platinum. In the case of guanosine, treatment of the reaction mixture with charcoal followed by filtration afforded an impure solid which contained

both caffeine and guanosine. The formation of a blue was observed with 5'-UMP.

Reaction of $[PtCl_3(caffeine)]^-$ with an aqueous solution of ammonia produced the complex *cis*-$PtCl_2(caffeine)(NH_3)$. [Anal. Found: C, 20.43; H, 2.79; N, 14.64; Cl, 14.58%. Calc. for $PtCl_2(NH_3)(caffeine)$: C, 20.13; H, 2.75; N, 14.67; Cl, 14.86%] ν(Pt-Cl) 321 and 338cm^{-1}.

Within the last 12 months the three complexes *cis*-$PtCl_2(caffeine)_2$, $K[PtCl_3(caffeine)]$ and *cis*-$PtCl_2(caffeine)(NH_3)$ have been screened for antitumour activity in mice. Whilst they showed some activity the results were deemed to be not promising enough for further evaluation studies.

4.2iv Analogous alkaloid complexes

By employing the direct methanol route (4.2ii) the salts $K[PtCl_3(theophylline)]$ and $K[PtCl_3(theobromine)]$ were also prepared.

$K[PtCl_3(theophylline)]$. [Anal. Found: C, 15.53; H, 1.56; N, 10.19; Cl, 19.97%. Calc. for $K[PtCl_3(theophylline)]$: C, 16.14; H, 1.55; N, 10.75; Cl, 20.42%]. ν(Pt-Cl) 330cm^{-1}. H(8) δ8.24ppm. J_{Pt-H} = 18Hz.

$K[PtCl_3(theobromine)]$. [Anal. Found: C, 16.18; H, 1.51; N, 10.51%. Calc. as for theophylline]. ν(Pt-Cl) 335cm^{-1}. H(8) δ8.49ppm. J_{Pt-H} = 18Hz.

4.3 Krebs cycle acids

Two of the second generation drugs contain dicarboxylic acids as the leaving, or "X_2" group. In view of the success of $Pt(NH_3)_2$(CBDCA) and $Pt(NH_3)_2$(ETMAL) in the clinical trials [27] (as known to us at that time) it was decided to investigate the formation of similar complexes involving Krebs Cycle and closely related, acids with the simplest ammine system "*cis*-$Pt(NH_3)_2$".

4.3i Succinic and related acids

The complex *cis*-$Pt(NH_3)_2(O_2C(CH_2)_2\ CO_2)$ was prepared as the monohydrate. The efficient synthetic route developed by Harrison et al. [83] was employed.

Cis-$Pt(NH_3)_2I_2$ (4.83g, 10mM) was slurried with a 2% deficiency of Ag_2SO_4 (3.05g, 9.8mM) in water (80ml) in the dark overnight. The AgI precipitate was filtered off. Succinic acid (1.18g, 10mM) and $Ba(OH)_2.6H_2O$ (3.09g, 9.8mM) were dissolved in water (50ml). To this solution the freshly prepared *cis*-$Pt(II)_{aq}$ was added with rapid stirring. Immediately a fine white precipitate of $BaSO_4$ formed. After half an hour the $BaSO_4$ was filtered off with the aid of celite.

The clear pale yellow filtrate (negative Ba^{2+} test with saturated Na_2SO_4) was warmed at about 60°C for three hours. A fine white precipitate formed and the mixture was left in the fridge overnight.

The white amorphous precipitate was filtered off, washed with water, ethanol and ether and finally dried in vacuo over silica gel. (Yield = 1.5g, 41%). All attempts at recrystallization failed due to the complex having very low solubility. [Anal. Found: C, 13.46; H, 3.26; N, 7.52%. Calc. for $PtC_4H_{12}N_2O_{15}$: C, 13.32; H, 3.33;

N, 7.71%]. The IR and possible structure of this complex will be discussed later.

A similar preparation was carried out with glutaric acid. However, in this case the crude white amorphous product (Yield = 1.2g, 30.3%), was successfully recrystallised from hot (70°C) water (400ml) to give white crystals of stoichiometry $Pt(NH_3)(O_2C(CH_2)_3CO_2).2H_2O$. [Anal. Found: C, 15.11; H, 3.98; N, 6.89. Calc. for $PtC_5H_{16}N_2O_6$: C, 13.23; H, 3.33; N 7.71%].

With adipic and pimelic acid no product was isolated. 2-ketoglutaric acid gave an orange amorphous powder of variable composition and with citric acid a blue was formed. Fumaric acid yielded a red/brown solid and mucic acid gave a brown/yellow product.

The complexes formed with malonic acid derivatives are fairly water soluble. This raises questions about the structures of the essentially insoluble succinate and poorly soluble glutarate complexes. The complex $Pt(NH_3)_2(CBDCA)$ is known [28] to be monomeric. However, during the large scale preparation of this complex an insoluble product [84] is also isolated. In view of these anomalies the structure of the glutarate system was determined [85] by X-ray crystallography. The result was somewhat surprising.

The $[Pt_2(NH_3)_4(glutarate)_2]$ molecule (Fig. 4.1) is a centro-symmetric dimer in which the two *cis*-square-planar arrays about each platinum atom are bridged by the glutarate ligands to give a 16-atom ring system. The coordination about platinum is planar with the Pt atom ca: 0.06Å out of the coordination plane. Of the two independent carboxylate groups, one is almost normal to the coordination plane (87.8°) while the other makes an angle of 58.8° to this plane.

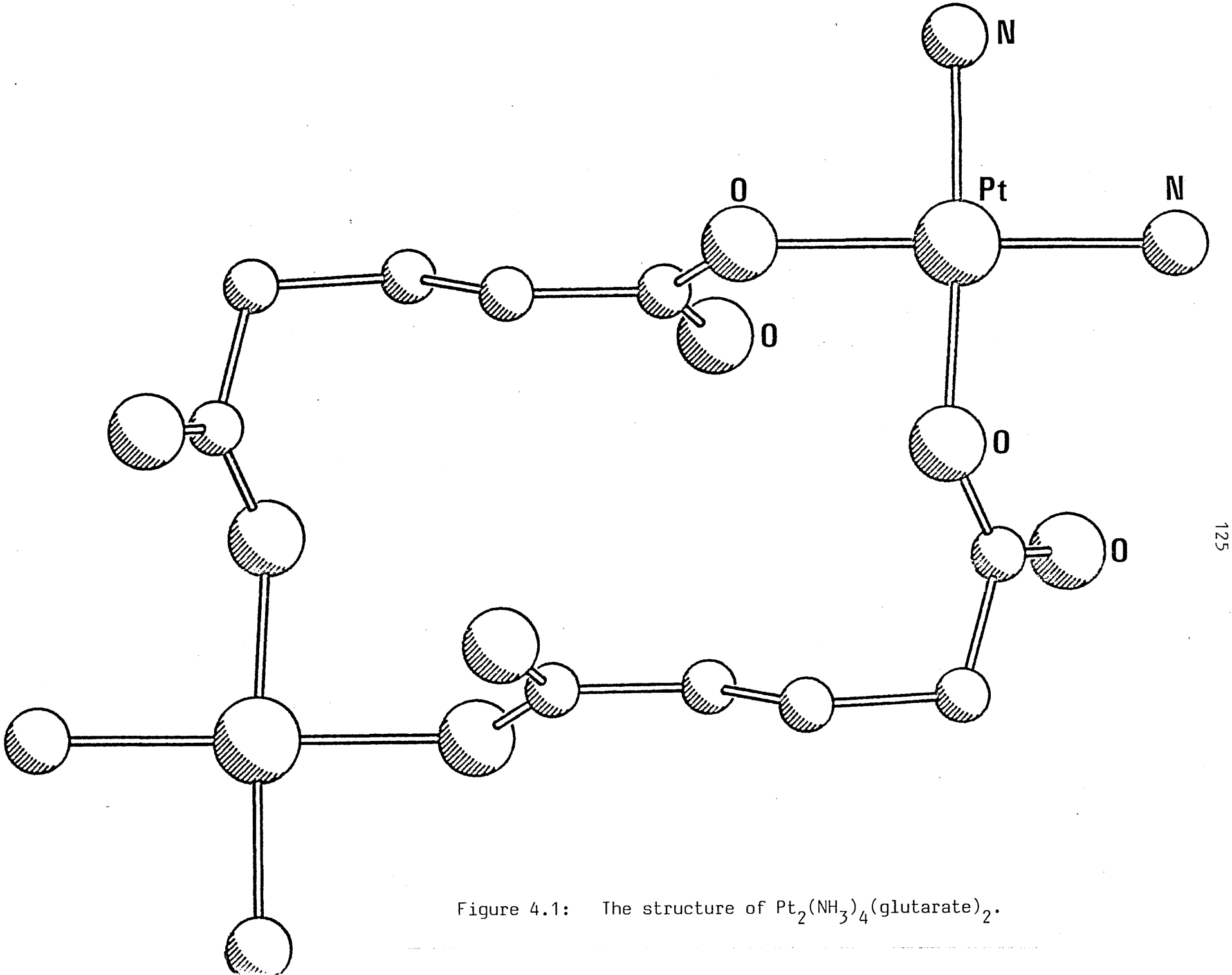


Figure 4.1: The structure of $Pt_2(NH_3)_4(glutarate)_2$.

The mean Pt-N distance is 2.032Å while the Pt-O is 2.023Å. These agree favourably with similar complexes [29,86].

The solution of the glutarate structure together with that known for $Pt(NH_3)_2(CBDCA)$ led to the possibility that an IR and Raman study may be able to solve the structures of the succinate and the insoluble [84] Johnson Matthey material. Previous workers have shown [87] that a study of the ν(CO) region does not lead to an unambiguous distinction between bridging, (as in a polymeric or binuclear complex) chelating or indeed monomeric dicarboxylic acid forms. In view of this, whilst we observed some differences in the ν(CO) and ν(C-H) regions, a detailed analysis of the low wavenumber region (200-600cm^{-1}) was undertaken (Table 4.1).

In the infrared $Pt(NH_3)_2(CBDCA)$ exhibits two bands at 574cm^{-1} and 550cm^{-1} which are medium and very weak in intensity respectively. However, in the Raman the bands at 576cm^{-1} and 551cm^{-1} have reversed their relative intensity, weak and strong, allowing them to be assigned as the ν(Pt-N) asymmetric and symmetric stretching modes respectively. ν(Pt-O) is assigned to a strong band in both the IR and Raman at 476 and 477cm^{-1} respectively. A strong band in the IR at 350cm^{-1} is countered by a weak Raman band at 356cm^{-1}(there is also a weak band in the Raman at 299cm^{-1}). This could be assigned to asymmetric ν(Pt-O). This strong IR active band at 350cm^{-1} is not observed in the other complexes studied. It may be indicative of the DCA acting as a chelate i.e. a deformation mode of the six membered chelate ring. If this is the case ν(Pt-O) symmetric and asymmetric bands are assumed to be degenerate.

The spectra of the insoluble $[Pt(NH_3)_2(CBDCA)]_n$ product exhibit two sets of ν(Pt-N) asymmetric (593 and 610cm^{-1})and one (but broad in the Raman) ν(Pt-N) symmetric (552cm^{-1})which were assigned by applying

TABLE 4.1: IR and Raman data (600-200cm^{-1}) of dicarboxylic acid complexes

COMPLEX	ν(Pt-N)asymm.	ν(Pt-N)sym.	ν(Pt-O)	not assigned
$Pt(NH_3)_2(CBDCA)$	576*(w) 574(m)	551*(s) 550(vw)	477*(s) 476(s)	299*(w) 356*(w) 350(s)
$[Pt(NH_3)_2)glutarate)]_2$	583*(w) 582(mw)	539*(s) 552*(m) 545(w)	435*(vw) 436(mw)	335*(w)
$[Pt(NH_3)_2(succinate)]_n$	~600(br. mw)		410(mw)	290(br.mw)
$[Pt(NH_3)_2(CBDCA)]_n$	593*(mw) 610*(mw)	552*(br.s)	439*(w)	313*(s)
	591(m) 611(m)	550(vw)	440(mw)	310(mw) 362(mw)

* Data from Raman spectra

the same intensity selection rules. In this case ν(Pt-O) is observed at 439cm^{-1} as a weak band in the Raman and concurrently at 440cm^{-1} in the IR. In this case a strong Raman active mode at 313cm^{-1} is paired with a medium weak IR mode at 310cm^{-1}. There is also a medium weak IR band at 362cm^{-1}.

To summarise, the insoluble product has no strong ν(Pt-O), or chelate ring deformation mode but does exhibit a strong new band in the Raman at 313cm^{-1}. These results suggest that the insoluble product has a polymeric structure which would also tie in with the observation of two sets of ν(Pt-N) bands. This conclusion is supported by the data for the slightly soluble dimeric glutarate system. Apart from the ν(Pt-N) bands the remaining low energy bands are weak in intensity with ν(Pt-O) in the IR at 436cm^{-1}, 435cm^{-1}Raman - very weak and only one other detectable band in the Raman at 335cm^{-1} - weak. The Raman active strong band at 313cm^{-1} observed for the CBDCA polymer may be associated with a skeletal mode of the polymeric structure. For the succinate complex only IR data are available. However, due to its similarity to the CBDCA polymer and taking into account its low solubility a similar polymeric structure may be considered as a strong possibility.

4.3ii Some reactions of $[Pt(NH_3)_2(glutarate)]_2$

In view of the structure of the glutarate complex and the antitumour activity of the malonate derivatives the possibility of cleaving the bridge with nucleic acid components was investigated.

When the solid complex was stirred with inosine or Na_2 5'-GMP

in water at room temperature there was no apparent reaction. However, when the solid compound was warmed with an aqueous solution of inosine to ca. 45°C, after 2 days a clear solution was obtained. Evaporation of this to dryness gave a solid, which, in contrast to the original dimer, was very soluble in water. ^{1}H-NMR studies of such a solution in D_2O showed the presence of coordinated inosine (δH(8) 8.72 and H(2) 8.22ppm) and methylene resonances identical to those of sodium glutarate. Similar results were obtained when the dimer was warmed (ca. 45°C) with $Na_2$5'-GMP, (δH(8) 8.64ppm).

With the sodium salt of β-D-thioglucose, however there was a reaction at even room temperature, with the formation of Pt(thioglucose)$_2$ in solution, though this reaction occurred much more slowly than with related monomeric platinum DCA complexes. This raises the interesting possibility that such a bridged complex could undergo selective bridge cleavage under biological conditions, with the slow release of active platinum species.

In this work we have surveyed two sets of biological ligands - alkaloids and Krebs Cycle acids. Some interesting and unusual complexes have been prepared and studied. Obviously the scope for enlarging upon this work is considerable.

CHAPTER FIVE

EXPERIMENTAL TECHNIQUES

5.1 Physical Methods

Microanalysis

All microanalyses were performed by the Imperial College Microanalytical Laboratory.

Infrared Spectra

Infrared spectra were obtained on Perkin Elmer 683 and 325 ($4000-200cm^{-1}$) spectrometers. Samples were made as nujol mulls and run between caesium iodide plates. In each case the spectrometer was calibrated with reference to a polystyrene film.

Raman Spectra

Raman spectra were measured by D.N. Campbell on a Spex Ramalog 5 instrument with a DPC-2 detector, using a krypton-ion laser.

UV and Visible Solution Spectra

UV/Visible solution spectra were recorded on a Perkin Elmer 551 spectrometer using 0.5cm path length, quartz cells.

EPR

EPR measurements were made at room temperature using powdered solid samples on a Varian 4 X-band (ca. 9GHz) spectrometer.

Steve Gunn is gratefully acknowledged for his assistance.

X-ray Crystallography

Data for the $[Pt(NH_3)_2(glutarate)]_2$ system were collected on a Nicolet R3m Diffractometer. This was performed by Dr M.V. Capparelli and Dr A.C. Skapski. Least squares refinement reached R = 0.0266.

Thermogravimetric Analysis

A 760-TG Stanton-Redcroft thermo-balance was utilised. Samples, (ca. 1mg), were heated from room temperature to 1300°C, at a heating rate of 5°C/min. The final mass afforded a reliable platinum analysis.

NMR

^{1}H-NMR were obtained on Perkin-Elmer R12 (60MHz) and R32 (90MHz) spectrometers. 250MHz spectra were run on a Fourier transform Bruker W.M. machine. The Bruker spectrometer was also used for ^{13}C (62.9MHz) and ^{195}Pt (98.2MHz) work. The help of the operators Dick Shepherd and Sue Johnson, is gratefully acknowledged. 400MHz ^{1}H spectra were obtained on the Bruker spectrometer at Queen Mary College under the ULIRS service.

5.2 Ligands

Adenosine, cytidine, inosine and the sodium salts of the nucleotides GMP, IMP, AMP and CMP were obtained commercially (usually from Sigma but in some cases from Aldrich or Koch Light) and were used without further purification.

Blenoxane was kindly donated by Bristol-Myers. Cyclophosphamide, 5-fluoruracil and cytosine arabinoside were all purchased from Sigma and used without further purification.

The acids and alkaloids used in Chapter Four were obtained from Sigma or Aldrich. In all the above cases purity checks by NMR and IR were satisfactory. However, with both the dicarboxylic acids - ethylmalonic and cyclobutanedicarboxylic acids difficulties were encountered. ETMAL (Aldrich) was supplied as a pale blue, wet solid. Treatment with charcoal and recrystallisation resulted in white crystals of good analytical purity. CBDCA (Aldrich) was found to contain substantial amounts of an aromatic species on inspection of the ^{1}H-NMR spectrum of the free acid. Attempts to purify the acid by recrystallisation from several solvents failed. By following a published method (Vogel Edn. 1, 797) a fresh sample of CBDCA was synthesised from diethylmalonate and 1,3-dibromopropane [Anal.: Calc. for $C_6H_8O_4$: C, 50.00; H, 5.60%. Found: C, 50.02; H, 5.63%].

5.3 Platinum antitumour agents

cis-Pt(II)

Cis-Pt(II) was kindly loaned by Johnson Matthey PLC.

cis-Pt(II)$_{aq}$

cis-Pt(II)$_{aq}$ was prepared from *cis*-$Pt(NH_3)_2(I)_2$ by treatment with a 2% deficiency of $AgNO_3$ in water, in diffuse light. Removal of the AgI precipitate by careful filtration gave an aqueous solution of diammineaquahydroxy-platinum(II).

A supply of *cis*-$Pt(NH_3)_2(I)_2$ was prepared by a modified Dhara's

method [88]. To K_2PtCl_4 (20.75g, 50mM) in water (200ml) - charcoaled and filtered to remove K_2PtCl_6 impurity - was added a solution of KI(33.45g, 0.2M) in water (100ml). After rapid stirring for ca. 45s, ammonia (15ml of 1:1, aqueous : 0.88NH_4OH) was slowly added. After ca. 4 hours the resultant yellow precipitate was isolated in 95% (22.98g) yield.

$\underline{Pt(NH_3)_2(DCA)}$

$Pt(NH_3)_2$(ETMAL) and $Pt(NH_3)_2$(CBDCA) were prepared via the $BaSO_4$ route [83] (section 4.3i).

Analysis for $Pt(NH_3)_2$(ETMAL): Calc. C, 16.72; H, 3.37; N, 7.80%. Found: C, 16.70; H, 3.51; N, 7.33%.

Analysis for $Pt(NH_3)_2$(CBDCA): Calc. C, 19.41; H, 3.26; N, 7.54%. Found: C, 19.29; H, 3.28; N, 7.50%.

REFERENCES

(1) B. Rosenberg, L. VanCamp, J.E. Trosko and V.H. Mansour. Nature 222, 385 (1969).

(2) B. Rosenberg, L. VanCamp and T. Krigas. Nature 205, 698 (1965).

(3) B. Rosenberg and L. VanCamp. Cancer Res., 30(6), 1799 (1970).

(4) E. Wiltshaw. Platinum Metals Review 23, 90 (1979).

(5) M.H. Cleare. Coord. Chem. Revs., 12, 349 (1974).

(6) M.J. Cleare, P.C. Hydes, B.W. Malerbi and D.M. Watkins. Biochimie 60, 835 (1978).

(7) M.J. Cleare, P.C. Hydes, D.R. Hepburn and B.W. Malerbi. "Cisplatin", Current Status and New Development. Ed. by A.W. Prestayko, S.T. Crooke and S.K. Carter, Academic Press (NY) 149 (1980).

(8) B. Rosenberg. "Cisplatin", 9 (1980).

(9) R. Wilkinson, P.J. Cox, M. Jones and K.R. Harrap. Biochimie 60, 851 (1978).

(10) R.H. Earhart. Cancer Treat Reports 63 231 (1979).

(11) B. Rosenberg. Biochimie 60 859 (1978).

(12) C.J. Boreham, J.A. Broomhead and D.P. Fairlie. Aust. J. Chem., 34, 659 (1981).

(13) B. Rosenberg. A.C.S. Symp. Ser-Eng., 140, 143 (1980).

(14) J.J. Roberts and A.J. Thomson. Progress Nucleic Acid Res. and Mol. Biol., 22, 71 (1979).

(15) D.M.L. Goodgame, I. Jeeves, F.L. Phillips and A.C. Skapski. Biochim. et Biophys. Acta. 378, 153 (1975).

(16) J.N. Davidson. "The Biochem. of the Nucleic Acids". 7th edition. Chapman & Hall, London, 1972.

(17) J-P Macquet and T. Theophanides. Bioinorganic Chem., 5, 59 (1975).

(18) R.M. Wing, P. Pjura, H.R. Drew and R.E. Dickerson. The EMBO J. 3, 1201 (1984).

(19) J.R. Rubin, M. Sabat and M. Sundaralingam. Nucleic Acid Res., 11, 6571 (1983).

(20) R. Rawls. Science, 35 (Jan. 21, 1980).

(21) J.P. Caradonna, S.J. Lippard, M.J. Gait and M. Singh. J. Amer. Chem. Soc., 104, 5793 (1982).

(22) J-P Girault, J-C Chottard, E.R. Guittet, J-Y Lallemand, T. Huyh-Dinh and J. Igolen. Biochem. Biophys. Res. Comm., 109, 1157 (1982).

(23) A.T.M. Marcelis, J.H.J. den Hartog, G.A. van der Marel, G. Wilde and J. Reedijk. Eur. J. Biochem., 135, 343, (1983).

(24) T.D. Tullius and S.J. Lippard. J. Amer. Chem. Soc., 103, 4620 (1981).

(25) R. Faggiani, C.J.L. Lock and B. Lippert. J. Amer. Chem. Soc., 102, 5419 (1980).

(26) B. Lippert. J. Amer. Chem. Soc., 103, 5691 (1981).

(27) Johnson-Matthey Cancer Research Group Meeting - 26th February 1981.

(28) S. Neidle, I.M. Ismail and P.J. Sadler. J. Inorg. Biochem., 13, 205 (1980).

(29) F.A. Cotton and G.Wilkinson. "Advanced Inorg. Chem.". Wiley, London.

(30) C. Barnard. Personal Communication.

(31) P.J. Stones, A.D. Kelman and F.M. Sinex. Nature 251, 736 (1974).

(32) R.E. Cramer, P.L. Dahlstrom, M.J.T. Seu, T. Norton and M. Kashiwagi. Inorg. Chem., 19, 148 (1980).

(33) R.W. Gellert and R. Bau. J. Amer. Chem. Soc., 97, 7379 (1975).

(34) R. Melanson and F.D. Rochon. Can. J. Chem., 57, 57 (1979).

(35) M.J. Cleare and J.D. Hoeschele. Bioinorg. Chem., 2, 187 (1973).

(36) P.C. Kong and T. Theophanides. Bioinorg. Chem., 5, 51 (1975).

(37) P.C. Kong and T. Theophanides. Inorg. Chem., 13, 1167 (1974).

(38) G.H.Y. Chu, S. Mansy, R.E. Duncan and R.S. Tobias. J. Amer. Chem. Soc., 100, 593 (1978).

(39) A.T.M. Marcelis, C.G. van Kralingen and J. Reedijk. J. Inorg. Biochem., 13, 213 (1980).

(40) P.C. Kong and F.D. Rochon. J.C.S. Chem. Comm., 599 (1977).

(41) L.G. Marzilli, P. Chalilpoyl, C.C. Chiang and T.J. Kistenmacher. J. Amer. Chem. soc., 102, 2480 (1980).

(42) G.V.H. Chu and R.S. Tobias. J. Amer. Chem. Soc., 98, 2641 (1976).

(43) I. Sovago and R.B. Martin. Inorg. Chem., 19, 2868 (1980).

(44) T.J. Kistenmacher, C.C. Chiang, P. Chalilpoyil and L.G. Marzilli. J. Amer. Chem. Soc., 101, 1143 (1979).

(45) R. Bau, R.W. Gellert, S.M. Lehovec and S. Louie. J. Clin. Hematol. Oncol., 7, 51 (1977).

(46) T.J. Kistenmacher, C.C. Chiang, P. Chalilpoyil and L.G. Marzilli. Biochem. Biophys. Res. Commn., 84, 70 (1978).

(47) R. Melanson and F.D. Rochon, Acta Crystallogr., B34, 3594 (1978).

(48) K.H. Scheller, V. Scheller-Krattiger and R.B. Martin. J. Amer. Chem. Soc., 103, 6833 (1981).

(49) J.C. Chottard, J.P. Girault, G. Chottard, J.Y. Lallemand and D. Mansuy. J. Amer. Chem.Soc., 102, 5565 (1980).

(50) M.C. Lim and R.B. Martin. J. Inorg. Nucl. Chem., 38, 1915 (1976).

(51) A. Terzis, Inorg. Chem., 15, 793 (1976).

(52) R.E. Cramer and P.L. Dahlstrom. J. Amer. Chem. Soc., 101, 3679 (1979).

(53) A.T.M. Marcelis, J.L. van der Verr, J.C.M. Zwetsloot and J. Reedijk. Inorg. Chim. Acta, 78, 195 (1983).

(54) A.D. Newman, H. Ridgway, R.J. Spear and J.M. Hill. J. Clin. Hem. and Onc., 9, 208 (1979).

(55) B.T. Hill. Biochem. Biophys. Acta, 516, 389 (1978).

(56) S. Neidle, G.L. Taylor and A.B. Robbins. Acta Cryst., B34, 1838 (1981).

(57) R. Ettore. Inorg. Chim. Acta, 46, 27 (1980).

(58) B. Lippert, J. Clin. Hem. and Oncol., 7, 26 (1977).

(59) J.P. Davidson, P.J. Faber, R.G. Fischer Jr., S. Mansy, H.J. Peresie, B. Rosenberg and L. VanCamp. Cancer Chem. Rep., 59, 287 (1975).

(60) S. Hecht. Ed. "Bleomycin: Chemical, Biochemical and Biological Aspects". Springer-Verlag, New York, 1979.

(61) D.C. Ash, J. Clin. Hem. and Onc., 10, 55 (1980).

(62) Y. Itaka, H. Nakamura, T. Nakatina, Y. Muraoka, A. Fukii, T. Takita and H. Umezawa. J. Antibiot., 30, 789 (1977).

(63) J.C. Dabrowiak. J. of Inorg. Biochem., 13, 317 (1980).

(64) Y. Itaka, H. Nakamura, T. Natatani, Y. Muraoka, A. Fujii, T. Takita, and H. Umezawa. J. Antibiot., 31, 1070 (1978).

(65) M. Takeshita, A.P. Grollman, E. Ohtsubo and H. Ohtsubo. Proc. Natl. Acad. Sci., 75, 5983 (1978).

(66) J.C. Dabrowiak, F.T. Greenway, F.S. Santillo and S.T. Crooke. Biochem. Biophys.Res. Commun., 91, 721 (1979).

(67) H. Kuranoochi, K. Takahaski, T. Takita and H. Umezawa. J. Antibiot., 34, 576 (1981).

(68) L. Giloni, M. Takeshita, F. Johnson, C. Iden and A.P. Grollman. J. Biol. Chem., 256, 8608 (1981).

(69) D. Solaiman, E.A. Rao, and D.H. Petering. Int. J. Rad. Onc. (Biol-Phys)., 5, 1519 (1979).

(70) W.J. Caspary, D.A. Lanzo and C. Niziak, Biochem., 70, 3868 (1981).

(71) W.E. Antholine and D.H. Petering. Biochem. Biophys. Res. Commun., 90, 384 (1979).

(72) F.K.V. Leh and W. Wolf. Int. J. of Pharmaceutics, 1, 41 (1978).

(73) J.C. Dabrowiak, F.T. Greenaway and R. Grulick. Biochem., 17, 4090 (1978).

(74) J.K. Barton, C. Caravana and S.J. Lippard. J. Amer. Chem. Soc., 101, 7269 (1979).

(75) Y. Oyanagui, Biochem. Pharmacol., 26, 473 (1977).

(76) I. Fridovich. Annu. Rev. Biochem., 44, 147 (1975).

(77) P.K. Mascharak, Y. Sugiura, J. Kuwahara, T. Suzuki and S.J. Lippard. Proc. Natl. Acad. Sci., 80, 6795 (1983).

(78) J.J. Roberts. Adv. Rad. Biol., 7, 211 (1978) and refs. therein.

(79) J.J. Roberts, Adv. Inorg. Biochem., 3, 273 (1981).

(80) R.E. Cramer, D.M. Ho, W.V. Doorne, J.A. Ibers, T.Norton and M. Kashiwagi. Inorg. Chem., 20, 2457 (1981).

(81). D.M.L. Goodgame, P.B. Hayman, R.T. Riley and D.J. Williams. Inorg. Chim. Acta, 91, 89 (1984).

(82) J-Y Lallemand, J. Soulie and J.C. Chottard. J.C.S. Chem. Comm., 436 (1980).

(83) R.C. Harrison, C.A. McAuliffe and A.M. Zak. Inorg. Chim. Acta, 46, L15 (1980).

(84) C. Barnard. Personal Communication.

(85) M.V. Capparelli, D.M.L. Goodgame, R.T. Riley and A.C. Skapski. Inorg. Chim. Acta. 67, L9 (1982).

(86) C.G. van Kralingen, J. Reedijk and A.L. Speck. Inorg. Chem., 19, 1481 (1980).

(87) J. Catterick and P. Thornton. Adv. Inorg. Radiochem., 20, 291 (1977).

(88) S.G. Dhara. Indian J. Chem., 8, 193 (1970).

ACKNOWLEDGEMENTS

First and foremost, I should like to express my thanks to my supervisor, Dr D.M.L. Goodgame for his advice and guidance throughout the years of research work.

I wish to thank Professor Steve Ley for his invaluable advice and encouragement, all of my colleagues for helpful discussions, in particular Steven Gunn, Doug Armstrong, Bob Rollins, Michael Augenstein and Dave Hollinshead.

The CASE award in conjunction with Johnson Matthey PLC is gratefully acknowledged.